

COM-02-041-1
Revision 0
May 1983
64.305.1100

DRESDEN NUCLEAR POWER STATION
UNITS 2 AND 3
PLANT UNIQUE ANALYSIS REPORT
VOLUME 1
GENERAL CRITERIA AND
LOADS METHODOLOGY

Prepared for:
Commonwealth Edison Company

Prepared by:
NUTECH Engineers, Inc.
San Jose, California

Approved by:

RE Wise
R. E. Wise
Project Leader

John V Massey
Dr. J. V. Massey
Engineering Manager

Edmond Kost
Dr. E. G. Kost, P.E.
Engineering Director

Issued by:

A G Brnilovich
A. G. Brnilovich
Project Manager

R H Buchholz
R. H. Buchholz
Project Director

8307070181 830627
PDR ADOCK 05000237
P PDR

REGULATORY DOCKET FILE COPY

nutech
ENGINEERS

REVISION CONTROL SHEET

TITLE Dresden Nuclear Power Station
Units 2 and 3 Plant Unique
Analysis Report, Volume 1

REPORT NUMBER: COM-02-041-1
Revision 0

L. D. Marble
Senior Specialist

LSM
INITIALS

R. E. Wise
Specialist

REW
INITIALS

D. C. Talbott
Consultant

DCT
INITIALS

C. F. Villanueva
Technician II

CKV
INITIALS

J. G. Hwang, P.E.
Principal Engineer

JGH
INITIALS

A. S. Herlekar, P.E.
Principal Engineer

ASH
INITIALS

R. A. Sanchez, P.E.
Principal Engineer

RAS
INITIALS

C. T. Shyy, P.E.
Senior Engineer

CTS
INITIALS

EFFEC-TIVE PAGE (S)	REV	PRE-PARED	ACCURACY CHECK	CRITERIA CHECK	EFFEC-TIVE PAGE (S)	REV	PRE-PARED	ACCURACY CHECK	CRITERIA CHECK
1-ii- 1-xvii-	0	N/A	N/A	N/A	1-2.4- 1-2.6	0	DCT	REW	N/A
1-1.1- 1-1.4	↓	REW	RAS	RAS	1-2.7- 1-2.8	↓	REW	DCT	CTS
1-1.5		REW	DCT	N/A	1-2.9- 1-2.10		DCT	REW	N/A
1-1.6- 1-1.22		REW	RAS	RAS	1-2.11- 1-2.12		REW	DCT	CTS
1-2.1- 1-2.3	↓	REW	RAS	RAS	1-2.13- 1-2.19	↓	DCT	REW	N/A
					1-2.20		REW	DCT	CTS

QEP-001.4-00

REVISION CONTROL SHEET
(Continuation)

TITLE: Dresden Nuclear Power Station
Units 2 and 3, Plant Unique
Analysis Report, Volume 1

REPORT NUMBER: COM-02-041-1
Revision 0

EFFECTIVE PAGE (S)	REV	PRE-PARED	ACCURACY CHECK	CRITERIA CHECK	EFFECTIVE PAGE (S)	REV	PRE-PARED	ACCURACY CHECK	CRITERIA CHECK
1-2.21- 1-2.23	0	DCT	REW	N/A	1-4.23- 1-4.24	0	DCT	REW	N/A
1-2.24- 1-2.25		REW	RAS	RAS	1-4.25- 1-4.31		REW	RAS	RAS
1-2.26- 1-2.29		DCT	REW	N/A	1-4.32- 1-4.33		CFV	REW	N/A
1-2.30- 1-2.32		REW	ASH	ASH	1-4.34- 1-4.35		DCT	REW	N/A
1-2.33- 1-2.34		REW	ASH	N/A	1-4.36- 1-4.38		REW	RAS	RAS
1-2.35		REW	RAS	RAS	1-4.39		CFV	REW	N/A
1-2.36- 1-2.37		CFV	REW	N/A	1-4.40- 1-4.41		DCT	REW	N/A
1-3.1- 1-3.8		REW	RAS	RAS	1-4.42 1-4.46		REW	RAS	RAS
1-3.9- 1-3.11		REW	CTS	CTS	1-4.47- 1-4.48		CFV	REW	N/A
1-3.12- 1-3.13		CFV	DCT	DCT	1-4.49		CFV	CTS	N/A
1-3.14- 1-3.15		CFV	ASH	ASH	1-4.50		CFV	REW	N/A
1-3.16		REW	CTS	CTS	1-4.51- 1-4.53		DCT	REW	N/A
1-4.1		REW	RAS	RAS	1-4.54- 1-4.57		REW	RAS	RAS
1-4.2		CFV	REW	N/A	1-4.58- 1-4.62		CFV	REW	N/A
1-4.3- 1-4.12		REW	RAS	RAS	1-4.63- 1-4.67		DCT	REW	N/A
1-4.13- 1-4.14		DCT	REW	N/A	1-4.68- 1-4.70		REW	RAS	RAS
1-4.15- 1-4.16		REW	RAS	RAS	1-4.71		CFV	REW	N/A
1-4.17- 1-4.18		DCT	REW	N/A	1-4.72		REW	RAS	RAS
1-4.19- 1-4.22		REW	RAS	RAS	1-4.73		DCT	REW	N/A

REVISION CONTROL SHEET
(Continuation)

TITLE: Dresden Nuclear Power Station
Units 2 and 3, Plant Unique
Analysis Report, Volume I

REPORT NUMBER: COM-02-041-1
Revision 0

EFFECTIVE PAGE (S)	REV	PRE-PARED	ACCURACY CHECK	CRITERIA CHECK	EFFECTIVE PAGE (S)	REV	PRE-PARED	ACCURACY CHECK	CRITERIA CHECK
1-4.74-1-4.76	0	REW	RAS	RAS	1-4.115-1-4.116	0	REW	RAS	RAS
1-4.77-1-4.78		CKV	REW	N/A	1-4.117		CKV	REW	N/A
1-4.79-1-4.81		DOCT	REW	N/A	1-4.118		REW	RAS	RAS
1-4.82-1-4.84		REW	RAS	RAS	1-4.119-1-4.120		CKV	REW	N/A
1-4.85		DOCT	REW	N/A	1-4.121-1-4.123		DOCT	REW	N/A
1-4.86-1-4.87		REW	RAS	RAS	1-4.124		REW	RAS	RAS
1-4.88-1-4.89		CKV	REW	N/A	1-4.125		DOCT	REW	N/A
1-4.90-1-4.91		REW	RAS	RAS	1-4.126		REW	RAS	RAS
1-4.92-1-4.93		DOCT	REW	N/A	1-4.127		DOCT	REW	N/A
1-4.94-1-4.98		REW	RAS	RAS	1-5.1-1-5.4		REW	JGH	RAS
1-4.99		CKV	REW	N/A	1-5.5-1-5.7		CKV	REW	N/A
1-4.100-1-3.102		REW	RAS	RAS	1-5.8		DOCT	REW	N/A
1-4.103-1-4.104		CKV	REW	N/A	1-5.9-1-5.12		JGH	REW	REW
1-4.105-1-4.107		REW	RAS	RAS	1-6.1-1-6.3		REW	LSM	LSM
1-4.108		CKV	REW	N/A					
1-4.109		DOCT	REW	N/A					
1-4.110		DOCT	REW	N/A					
1-4.111-1-4.113		REW	RAS	RAS					
1-4.114		DOCT	REW	N/A					

ABSTRACT

The primary containments for the Dresden Nuclear Power Station Units 2 and 3 were designed, erected, pressure-tested, and N-stamped in accordance with the ASME Boiler and Pressure Vessel Code, Section III, 1965 Edition with addenda up to and including Summer 1965 for the Commonwealth Edison Company (CECo) by the Chicago Bridge and Iron Company. Since then, new requirements have been established. These requirements affect the design and operation of the primary containment system and are defined in the Nuclear Regulatory Commission's (NRC) Safety Evaluation Report, NUREG-0661. This report provides an assessment of containment design loads postulated to occur during a loss-of-coolant accident or a safety relief valve discharge event. In addition, it provides an assessment of the effects that the postulated events have on containment systems operation.

This plant unique analysis report (PUAR) documents the efforts undertaken to address and resolve each of the applicable NUREG-0661 requirements. It demonstrates that the design of the primary containment system is adequate and that original design safety margins have been restored in accordance with NUREG-0661 acceptance criteria. The Dresden Units 2 and 3 PUAR is composed of the following seven volumes:

- o Volume 1 - GENERAL CRITERIA AND LOADS METHODOLOGY
- o Volume 2 - SUPPRESSION CHAMBER ANALYSIS
- o Volume 3 - VENT SYSTEM ANALYSIS
- o Volume 4 - INTERNAL STRUCTURES ANALYSIS
- o Volume 5 - SAFETY RELIEF VALVE DISCHARGE LINE PIPING ANALYSIS
- o Volume 6 - TORUS ATTACHED PIPING AND SUPPRESSION CHAMBER PENETRATION ANALYSES (DRESDEN UNIT 2)

o Volume 7 - TORUS ATTACHED PIPING AND SUPPRESSION
CHAMBER PENETRATION ANALYSES (DRESDEN
UNIT 3)

Volumes 1 through 4 and 6 and 7 have been prepared by NUTECH Engineers, Incorporated (NUTECH), acting as an agent to the Commonwealth Edison Company. Volume 5 has been prepared by Sargent and Lundy (also acting as an agent to the Commonwealth Edison Company), who performed the safety relief valve discharge line (SRVDL) piping analysis. Volume 5 describes the methods of analysis and procedures used in the SRVDL piping analysis.

This volume provides introductory and background information regarding the reevaluation of the primary containment system and torus attached piping. It includes a description of the Dresden Units 2 and 3 pressure suppression containment system, a description of the structural and mechanical acceptance criteria, and the hydrodynamic loads methodology used in the analyses presented in Volumes 2, 3, 4, 6, and 7.

NOTE: Identification of the volume number precedes pages, sections, subsections, tables, and figures for each volume.

TABLE OF CONTENTS

	<u>Page</u>
ABSTRACT	1-v
LIST OF ACRONYMS	1-x
LIST OF TABLES	1-xii
LIST OF FIGURES	1-xiv
1-1.0 INTRODUCTION	1-1.1
1-1.1 Scope of Analysis	1-1.6
1-1.2 General Description of the Containment System	1-1.9
1-1.3 Review of Phenomena	1-1.11
1-1.3.1 LOCA-Related Phenomena	1-1.12
1-1.3.2 SRV Discharge Phenomena	1-1.14
1-1.4 Evaluation Philosophy	1-1.16
1-2.0 PLANT UNIQUE CHARACTERISTICS	1-2.1
1-2.1 Plant Configuration	1-2.2
1-2.1.1 Suppression Chamber	1-2.7
1-2.1.2 Vent System	1-2.11
1-2.1.3 Internal Structures	1-2.20
1-2.1.4 SRV Discharge Piping	1-2.24
1-2.1.5 Torus Attached Piping and Penetrations	1-2.30
1-2.2 Operating Parameters	1-2.35
1-3.0 PLANT UNIQUE ANALYSIS CRITERIA	1-3.1
1-3.1 Hydrodynamic Loads: NRC Acceptance Criteria	1-3.2
1-3.1.1 LOCA-Related Load Applications	1-3.4
1-3.1.2 SRV Discharge Load Applications	1-3.6
1-3.1.3 Other Considerations	1-3.8

TABLE OF CONTENTS

(Continued)

	<u>Page</u>
1-3.2 Component Analysis: Structural Acceptance Criteria	1-3.9
1-3.2.1 Classification of Components	1-3.10
1-3.2.2 Service Level Assignments	1-3.11
1-3.2.3 Other Considerations	1-3.16
1-4.0 HYDRODYNAMIC LOADS METHODOLOGY AND EVENT SEQUENCE SUMMARY	1-4.1
1-4.1 LOCA-Related Loads	1-4.3
1-4.1.1 Containment Pressure and Temperature Response	1-4.5
1-4.1.2 Vent System Discharge Loads	1-4.6
1-4.1.3 Pool Swell Loads on the Torus Shell	1-4.8
1-4.1.4 Pool Swell Loads on Elevated Structures	1-4.10
1-4.1.4.1 Impact and Drag Loads on the Vent System	1-4.11
1-4.1.4.2 Impact and Drag Loads on Other Structures	1-4.15
1-4.1.4.3 Pool Swell Froth Impingement Loads	1-4.19
1-4.1.4.4 Pool Fallback Loads	1-4.25
1-4.1.5 LOCA Water Jet Loads on Submerged Structures	1-4.28
1-4.1.6 LOCA Bubble-Induced Loads on Submerged Structures	1-4.36
1-4.1.7 Condensation Oscillation Loads	1-4.42
1-4.1.7.1 CO Loads on the Torus Shell	1-4.43
1-4.1.7.2 CO Loads on the Downcomers and Vent System	1-4.54
1-4.1.7.3 CO Loads on Submerged Structures	1-4.68
1-4.1.8 Chugging Loads	1-4.72
1-4.1.8.1 Chugging Loads on the Torus Shell	1-4.74
1-4.1.8.2 Chugging Downcomer Lateral Loads	1-4.82
1-4.1.8.3 Chugging Loads on Submerged Structures	1-4.86

TABLE OF CONTENTS
(Concluded)

	<u>Page</u>
1-4.2 Safety Relief Valve Discharge Loads	1-4.90
1-4.2.1 SRV Actuation Cases	1-4.94
1-4.2.2 SRV Discharge Line Clearing Loads	1-4.100
1-4.2.3 SRV Loads on the Torus Shell	1-4.105
1-4.2.4 SRV Loads on Submerged Structures	1-4.111
1-4.3 Event Sequence	1-4.115
1-4.3.1 Design Basis Accident	1-4.118
1-4.3.2 Intermediate Break Accident	1-4.124
1-4.3.3 Small Break Accident	1-4.126
1-5.0 SUPPRESSION POOL TEMPERATURE MONITORING SYSTEM	1-5.1
1-5.1 Suppression Pool Temperature Response to SRV Transients	1-5.2
1-5.2 Suppression Pool Temperature Monitoring System Design	1-5.9
1-6.0 LIST OF REFERENCES	1-6.1

LIST OF ACRONYMS

ADS	Automatic Depressurization System
ASME	American Society of Mechanical Engineers
ATWS	Anticipated Transients Without Scram
BDC	Bottom Dead Center
BWR	Boiling Water Reactor
CECo	Commonwealth Edison Company
CDF	Cumulative Distribution Function
CO	Condensation Oscillation
DBA	Design Basis Accident
DC/VH	Downcomer/Vent Header
ECCS	Emergency Core Cooling System
FSI	Fluid-Structure Interaction
FSTF	Full-Scale Test Facility
HPCI	High Pressure Coolant Injection
IBA	Intermediate Break Accident
I&C	Instrumentation & Control
ID	Inside Diameter
IR	Inside Radius
LDR	Load Definition Report (Mark I Containment Program)
LOCA	Loss-of-Coolant Accident
LPCI	Low Pressure Coolant Injection
LTP	Long-Term Program
MCF	Modal Correction Factor
NEP	Non-Exceedance Probability

LIST OF ACRONYMS

(Concluded)

NOC	Normal Operating Conditions
NRC	Nuclear Regulatory Commission
NSSS	Nuclear Steam Supply System
OD	Outside Diameter
PUAAG	Plant Unique Analysis Application Guide
PUA	Plant Unique Analysis
PUAR	Plant Unique Analysis Report
QSTF	Quarter-Scale Test Facility
RCIC	Reactor Core Isolation Cooling
RPV	Reactor Pressure Vessel
RSEL	Resultant Static-Equivalent Load
SAR	Safety Analysis Report
SBA	Small Break Accident
SORV	Stuck-Open Safety Relief Valve
SPTMS	Suppression Pool Temperature Monitoring System
SRSS	Square Root of the Sum of the Squares
SRV	Safety Relief Valve
SRVDL	Safety Relief Valve Discharge Line
STP	Short-Term Program
TAP	Torus Attached Piping

LIST OF TABLES

<u>Number</u>	<u>Title</u>	<u>Page</u>
1-1.0-1	Dresden Units 2 and 3 Containment Modification Status	1-1.5
1-2.2-1	Primary Containment Operating Parameters	1-2.36
1-3.2-1	Event Combinations and Service Levels for Class MC Components and Internal Structures	1-3.12
1-3.2-2	Event Combinations and Service Levels for Class 2 and 3 Piping	1-3.14
1-4.0-1	Plant Unique Analysis/NUREG-0661 Load Sections Cross-Reference	1-4.2
1-4.1-1	Hydrodynamic Mass and Acceleration Drag Volumes for Two-Dimensional Structural Components (Length L For All Structures)	1-4.32
1-4.1-2	Plant Unique Parameters for LOCA Bubble Drag Load Development - Zero and Operating Drywell-to-Wetwell Pressure Differential	1-4.39
1-4.1-3	DBA Condensation Oscillation Torus Shell Pressure Amplitudes	1-4.47
1-4.1-4	FSTF Response to Condensation Oscillation	1-4.49
1-4.1-5	Condensation Oscillation Onset and Duration	1-4.50
1-4.1-6	Downcomer Internal Pressure Loads for DBA Condensation Oscillation	1-4.58
1-4.1-7	Downcomer Differential Pressure Loads for DBA Condensation Oscillation	1-4.59
1-4.1-8	Downcomer Internal Pressure Loads For IBA Condensation Oscillation	1-4.60
1-4.1-9	Downcomer Differential Pressure Loads For IBA Condensation Oscillation	1-4.61
1-4.1-10	Condensation Oscillation Loads on the Vent System	1-4.62
1-4.1-11	Amplitudes at Various Frequencies for Condensation Oscillation Source Function for Loads on Submerged Structures	1-4.71

LIST OF TABLES
(Concluded)

<u>Number</u>	<u>Title</u>	<u>Page</u>
1-4.1-12	Chugging Onset and Duration	1-4.77
1-4.1-13	Post-Chug Rigid Wall Pressure Amplitudes on Torus Shell Bottom Dead Center	1-4.78
1-4.1-14	Amplitudes at Various Frequencies for Chugging Source Function for Loads on Submerged Structures	1-4.88
1-4.2-1	SRV Load Case/Initial Conditions	1-4.99
1-4.2-2	Plant Unique Initial Conditions for Actuation Cases Used for SRVDL Clearing Transient Load Development	1-4.103
1-4.2-3	SRVDL Analysis Parameters	1-4.104
1-4.2-4	Comparison of Analysis and Monticello Test Results	1-4.108
1-4.3-1	SRV and LOCA Structural Loads	1-4.117
1-4.3-2	Event Timing Nomenclature	1-4.119
1-4.3-3	SRV Discharge Load Cases for Mark I Structural Analysis	1-4.120
1-5.1-1	Summary of Dresden Units 2 and 3 Pool Temperature Response to SRV Transients	1-5.5

LIST OF FIGURES

<u>Number</u>	<u>Title</u>	<u>Page</u>
1-2.1-1	General Arrangement of Mark I Containment	1-2.4
1-2.1-2	Elevation View of Containment	1-2.5
1-2.1-3	Plan View of Containment	1-2.6
1-2.1-4	Suppression Chamber Section - Midbay Vent Line Bay	1-2.9
1-2.1-5	Suppression Chamber Section - Miter Joint	1-2.10
1-2.1-6	Plan View of Vent Header	1-2.13
1-2.1-7	Vent Line-Vent Header Spherical Junction	1-2.14
1-2.1-8	Typical View of Downcomer Longitudinal Bracing System	1-2.15
1-2.1-9	Downcomer-to-Vent Header Intersection	1-2.16
1-2.1-10	Vacuum Breaker Header Penetration Details	1-2.17
1-2.1-11	Vacuum Breaker Locations	1-2.18
1-2.1-12	SRV Penetration in Vent Line	1-2.19
1-2.1-13	Plan View of Suppression Chamber Internal Catwalk	1-2.21
1-2.1-14	Suppression Chamber Internal Catwalk - Typical Support at Miter Joint	1-2.22
1-2.1-15	Suppression Chamber Internal Catwalk - Typical Support Between Miter Joints	1-2.23
1-2.1-16	T-quencher and T-quencher Supports	1-2.26
1-2.1-17	T-quencher and Downcomer Longitudinal Bracing Locations - Dresden Unit 2	1-2.27
1-2.1-18	T-quencher and Downcomer Longitudinal Bracing Locations - Dresden Unit 3	1-2.28
1-2.1-19	Plan View of SRV Pipe Routing in Suppression Chamber	1-2.29
1-2.1-20	Essential TAP Penetration Locations on Suppression Chamber-Plan View (Dresden Unit 2)	1-2.33

LIST OF FIGURES
(Continued)

<u>Number</u>	<u>Title</u>	<u>Page</u>
1-2.1-21	Essential TAP Penetration Locations on Suppression Chamber-Plan View (Dresden Unit 3)	1-2.34
1-4.1-1	Downcomer Impact and Drag Pressure Transient	1-4.13
1-4.1-2	Application of Impact and Drag Pressure Transient to Downcomer	1-4.14
1-4.1-3	Pulse Shape for Water Impact on Cylindrical Targets	1-4.17
1-4.1-4	Pulse Shape for Water Impact on Flat Targets	1-4.18
1-4.1-5	Froth Impingement Zone - Region I	1-4.23
1-4.1-6	Froth Impingement Zone - Region II	1-4.24
1-4.1-7	Quarter-Scale Downcomer Water Slug Ejection, Dresden, Test 3 - Operating Differential Pressure	1-4.34
1-4.1-8	Quarter-Scale Downcomer Water Slug Ejection, Dresden, Test 5 - Zero Differential Pressure	1-4.35
1-4.1-9	Quarter-Scale Drywell Pressure Time-History - Operating Differential Pressure	1-4.40
1-4.1-10	Quarter-Scale Drywell Pressure Time-History - Zero Differential Pressure	1-4.41
1-4.1-11	Condensation Oscillation Baseline Rigid Wall Pressure Amplitudes on Torus Shell Bottom Dead Center	1-4.51
1-4.1-12	Mark I Condensation Oscillation - Torus Vertical Cross-Sectional Distribution for Pressure Oscillation Amplitude	1-4.52
1-4.1-13	Mark I Condensation Oscillation - Multiplication Factor to Account for the Effect of the Pool-to-Vent Area Ratio	1-4.53
1-4.1-14	Downcomer Dynamic Load	1-4.63
1-4.1-15	Downcomer Pair Internal Pressure Loading for DBA CO	1-4.64

LIST OF FIGURES
(Continued)

<u>Number</u>	<u>Title</u>	<u>Page</u>
1-4.1-16	Downcomer Pair Differential Pressure Loading for DBA CO	1-4.65
1-4.1-17	Downcomer CO Dynamic Load Application	1-4.66
1-4.1-18	Downcomer Internal Pressure Loading for IBA CO	1-4.67
1-4.1-19	Typical Chug Average Pressure Trace on the Torus Shell	1-4.73
1-4.1-20	Mark I Chugging - Torus Asymmetric Longitudinal Distribution for Pressure Amplitude	1-4.79
1-4.1-21	Mark I Chugging - Torus Vertical Cross-Sectional Distribution for Pressure Amplitude	1-4.80
1-4.1-22	Post-Chug Rigid Wall Pressure Amplitudes on Torus Shell Bottom Dead Center	1-4.81
1-4.1-23	Probability of Exceeding a Given Force Per Downcomer for Different Numbers of Downcomers	1-4.85
1-4.2-1	T-quencher and SRV Line	1-4.92
1-4.2-2	Elevation and Section Views of T-quencher Arm Hole Patterns	1-4.93
1-4.2-3	Comparison of Predicted and Measured Shell Pressure Time-Histories for Monticello Test 801	1-4.109
1-4.2-4	Modal Correction Factors for Analysis of SRV Discharge Torus Shell Loads	1-4.110
1-4.2-5	Plan View of Dresden Units 2 and 3 T-quencher Arm Jet Sections	1-4.114
1-4.3-1	Loading Condition Combinations for the Vent Header, Main Vents, Downcomers, and Torus Shell During a DBA	1-4.121
1-4.3-2	Loading Condition Combinations for Submerged Structures During a DBA	1-4.122

LIST OF FIGURES
(Concluded)

<u>Number</u>	<u>Title</u>	<u>Page</u>
1-4.3-3	Loading Condition Combinations for Small Structures Above Suppression Pool During a DBA	1-4.123
1-4.3-4	Loading Condition Combinations for the Vent Header, Main Vents, Downcomers, Torus Shell, and Submerged Structures During an IBA	1-4.125
1-4.3-5	Loading Condition Combinations for the Vent Header, Main Vents, Downcomers, Torus Shell, and Submerged Structures During a SBA	1-4.127
1-5.1-1	Local Pool Temperature Limit for Dresden Units 2 and 3	1-5.8
1-5.2-1	Suppression Pool Temperature Monitor Locations for Dresden Units 2 and 3	1-5.12

The primary containments for the Dresden Nuclear Power Station Units 2 and 3 were designed, erected, pressure-tested, and N-stamped in accordance with the ASME Code, Section III, 1965 Edition and with addenda up to and including Summer 1965. Subsequently, while performing large-scale testing for the Mark III containment system and in-plant testing for Mark I primary containment systems, new suppression chamber hydrodynamic loads were identified. The new loads are related to the postulated loss-of-coolant accident (LOCA) and safety relief valve (SRV) operation.

The new loads were identified by the NRC as a generic open item for utilities with Mark I containments. To determine the magnitude, time characteristics, etc., of the dynamic loads in a timely manner and to identify courses of action needed to resolve any outstanding concerns, the utilities with Mark I containments formed the Mark I Owners Group. The Mark I Owners Group established a two-part program consisting of: (1) a short-term program (STP) which was completed in 1976, and (2) a

long-term program (LTP). The LTP was completed with submittal of the "Mark I Containment Program Load Definition Report" (LDR) (Reference 1), the "Mark I Containment Program Structural Acceptance Criteria Plant Unique Analysis Application Guide" (PUAAG) (Reference 2), and supporting reports on experimental and analytical tasks of the long-term program. The NRC reviewed the LTP generic documents and issued acceptance criteria to be used during the implementation of the Mark I plant unique analyses. The NRC acceptance criteria are described in Appendix A of NUREG-0661 (Reference 3).

The objective of the LTP was to establish the final design loads and load combinations, and to verify that existing or modified containment systems are capable of withstanding these loads with acceptable design margins. To meet the objectives of the LTP, CECO implemented a containment study program that provided analysis, design, and modification, if required, in a timely manner.

Table 1-1.0-1 provides a listing of the containment modification status. All major modifications have

now been installed in accordance with the NRC order dates. These modifications insure the design margins required by NUREG-0661 for the Mark I containment loads. The containments and the Nuclear Steam Supply Systems (NSSS) are identical for Dresden Units 2 and 3. Differences between Dresden Units 2 and 3 exist primarily in the torus attached piping (TAP) systems and their corresponding branch connections.

This report documents the results of the evaluation of the Dresden Units 2 and 3 suppression chamber and internals, and of the safety relief valve discharge line (SRVDL) and torus attached piping. The evaluation was performed in accordance with the requirements of NUREG-0661. The alternate criteria allowed by NUREG-0661, Appendix A, Article 2.13.9 were used in the evaluation of SRV discharge loads. A series of in-plant tests were performed to confirm that the computed loadings and predicted structural responses for SRV discharges are conservative (Reference 4).

Accordingly, with the submittal of this PUAR, Commonwealth Edison Company believes that their

containment modification program has addressed the requirements of NUREG-0661 for Dresden Units 2 and 3.

COM-02-041-1
Revision 0

1-1.4

Table 1-1.0-1

DRESDEN UNITS 2 AND 3 CONTAINMENT MODIFICATION STATUS

COMPONENT	MODIFICATION DESCRIPTION	DR 2 DATE (2)	DR 3 DATE
TORUS	ADDITIONAL RING GIRDER REINFORCEMENT	3/83	12/83 ⁽¹⁾
	MITER JOINT SADDLES	3/80	3/80
	ADDITIONAL RING GIRDER-TO-TORUS WELD	3/83	4/82
	THERMOWELLS	4/81	4/82
	SADDLE EXTENSION PLATES	9/83	12/83
VENT SYSTEM	DOWNCOMER/VENT HEADER STIFFENERS	4/81	4/82
	DOWNCOMER LATERAL BRACING	4/81	3/80
	DOWNCOMER LONGITUDINAL BRACING	3/83	4/82
	VENT HEADER DEFLECTOR	4/81	3/80
	VENT LINE DRAIN REINFORCEMENT	4/81	4/82
	DW/WV VACUUM BREAKERS	1979	1979
	VACUUM BREAKER HEADER SUPPORTS	9/83 ⁽¹⁾	12/83 ⁽¹⁾
INTERNAL STRUCTURES	CATWALK MIDDAY SUPPORTS	3/83	4/82
	CATWALK LATERAL BRACING	3/83	4/82
	CATWALK SUPPORTS AT RING GIRDERS	4/81	4/82
	CONDUIT REROUTED	3/83	4/82
WETWELL PIPING MODIFICATIONS (INTERNAL)	HPCI TURBINE EXHAUST LINE SUPPORT	3/83	4/82
	HPCI POT DRAIN LINE SUPPORT	3/83	4/82
	ECCS SUCTION STRAINER REINFORCEMENT	3/83	4/82
	SPRAY HEADER SUPPORTS	3/83	4/82
	LPCI FULL FLOW TEST LINE SUPPORTS	3/83	4/82
SRV/L PIPING	REINFORCED VENT LINE PENETRATION ⁽³⁾	3/83	12/83
	ADDED T-QUENCHERS	4/81	3/80
	ADDED T-QUENCHER SUPPORTS	4/81	3/80
	ADDED SRV LINE SUPPORT	4/81	3/80
	SRV/L VACUUM BREAKERS	3/83	12/83 ⁽¹⁾
SYSTEM MODIFICATIONS	DW/WV ΔP	1976	1976
	SRV LOGIC	3/83	12/83 ⁽¹⁾
	SUPPRESSION POOL TEMPERATURE MONITORING SYSTEM (SPTMS)	3/83	4/82
TORUS ATTACHED PIPING MODIFICATIONS (EXTERNAL)	ECCS SUCTION HEADER PENETRATION AND TEE REINFORCEMENT	4/83 ⁽¹⁾	12/83 ⁽¹⁾
	ECCS SUCTION HEADER SNUBBERS	9/83 ⁽¹⁾	12/83 ⁽¹⁾
	LPCI PENETRATION REINFORCEMENT	7/83 ⁽¹⁾	12/83 ⁽¹⁾
	HPCI TURBINE EXHAUST PENETRATION REINFORCEMENT	7/83 ⁽¹⁾	12/83 ⁽¹⁾
	LARGE DIAMETER PIPING MODIFICATIONS	9/83 ⁽¹⁾	12/83 ⁽¹⁾
	SMALL DIAMETER PIPING MODIFICATIONS	6/83 ⁽¹⁾	12/83 ⁽¹⁾
	LPCI FULL FLOW TEST LINE TEE REPLACEMENT	3/83	4/82

- (1) SUBJECT TO REVISION IF MODIFICATION SCHEDULE CHANGES.
(2) THESE DATES REFLECT COMPLETION OF SCHEDULED MODIFICATIONS.
(3) FINAL CONFIGURATION OF SARGENT & LUNDY MODIFICATIONS.

The structural and mechanical elements addressed in the various volumes of this report include the following.

- o Containment Vessel
 - The torus shell with associated penetrations, reinforcing rings and support attachments
 - The torus supports
 - The vent lines between the drywell and the vent header, including SRV penetrations
 - The local region of the drywell at the vent line penetration
 - The bellows between the vent lines and the torus shell
 - The vent line-vent header spherical junctions
 - The vent header and attached downcomers
 - The vent header supports
 - The vacuum breaker penetrations at the vent line and the torus shell

- The downcomer rings and vent header support collars
- The suction header and attached suction lines
- o Internal Structures
 - The suppression chamber internal structural elements, including the catwalk and its supports
 - The vent header deflectors and their supports
- o The SRVDL piping and supports

(For Dresden Units 2 and 3, five valves are attached to the main steam lines. Only one of the five valves, the Target Rock valve, is capable of functioning in the safety mode. Thus, these units are equipped with one SRV and four relief valves (RV). However, references in this report to SRV's are to include both the one SRV and the four RV's.)

- o The internal and external TAP lines and their various branch connections
 - The drywell penetrations
 - The torus penetrations
 - Valve operability
 - Equipment operability

- o Miscellaneous
 - The instrumentation and control (I&C) conduit and tubing inside or attached to the torus
 - The suppression pool temperature monitoring system (SPTMS).

The Mark I containment is a pressure suppression system which houses the Boiling Water Reactor (BWR) pressure vessel, the reactor coolant recirculation loops, and other branch connections of the Nuclear Steam Supply System. The containment consists of a drywell, a pressure suppression chamber (wetwell or torus) approximately half-filled with water, and a vent system connecting the drywell to the suppression pool. The suppression chamber is toroidal in shape. It is located below and encircles the drywell. The drywell-to-wetwell vents are connected to a vent header contained within the airspace of the wetwell. Downcomers project downward from the vent header and terminate below the water surface of the suppression pool. The pressure suppression system is described in greater detail in Sections 1-2.1.1 and 1-2.1.2 and in Volumes 2 and 3.

BWR's utilize safety relief valves attached to the main steam lines as a means of primary system over-pressure protection. The outlet of each valve is connected to discharge piping which is routed to the suppression pool. The discharge lines end in

T-quencher discharge devices. The SRV discharge lines are described in detail in Section 1-2.1.4 and in Volume 5.

COM-02-041-1
Revision 0

1-1.10

nutech
ENGINEERS

1-1.3

Review of Phenomena

The following subsections provide a brief qualitative description of the various phenomena that could occur during a postulated LOCA and during SRV actuations. The LDR (Reference 1) provides a detailed description of the hydrodynamic loads which these phenomena could impose upon the suppression chamber and related structures. Section 1-4.0 presents the load definition procedures used to develop the Dresden Units 2 and 3 hydrodynamic loads.

COM-02-041-1
Revision 0

1-1.11

1-1.3.1 LOCA-Related Phenomena

Immediately following a postulated design basis accident (DBA) LOCA, the pressure and temperature of the drywell and vent system atmosphere rapidly increase. With the drywell pressure increase, the water initially present in the downcomers is accelerated into the suppression pool until the downcomers clear of water. Following downcomer water clearing, the downcomer air, which is at essentially drywell pressure, is exposed to the relatively low pressure in the wetwell, producing a downward reaction force on the torus. The consequent bubble expansion causes the pool water to swell in the torus (pool swell), compressing the airspace above the pool. This airspace compression results in an upward reaction force on the torus. Eventually, the bubbles "break through" to the torus airspace, equalizing the pressures. An air-water froth mixture continues upward due to the momentum previously imparted to the water, causing impingement loads on elevated structures. The transient associated with this rapid drywell air venting to the pool typically lasts for 3 to 5 seconds.

Following air carryover, there is a period of high steam flow through the vent system. The discharge of steam into the pool and its subsequent condensation causes pool pressure oscillations which are transmitted to submerged structures and the torus shell. This phenomenon is referred to as condensation oscillation (CO). As the reactor vessel depressurizes, the steam flowrate to the vent system decreases. Steam condensation during this period of reduced steam flow is characterized by up-and-down movement of the water-steam interface within the downcomer as the steam volumes are condensed and replaced by surrounding pool water. This phenomenon is referred to as chugging.

Postulated intermediate break accident (IBA) and small break accident (SBA) LOCA's produce drywell pressure transients which are sufficiently slow that the dynamic effects of vent clearing and pool swell are negligible. However, CO and chugging occur for an IBA and chugging occurs for a SBA.

1-1.3.2 SRV Discharge Phenomena

Dresden Units 2 and 3 are equipped with one SRV and four RV's per unit to control primary system pressure during transient conditions. The SRV's are mounted on the main steam lines inside the drywell, with the discharge piping routed down the main vents into the suppression pool. When a SRV is actuated, steam released from the primary system is discharged into the suppression pool, where it is condensed.

Prior to the initial actuation of a SRV, the SRVDL piping contains air at atmospheric pressure and suppression pool water in the submerged portion of the piping. Following SRV actuation, steam enters the SRVDL, compressing the air within the line and expelling the water slug into the suppression pool. During water clearing, the SRVDL undergoes a transient pressure loading.

Once the water has been cleared from the T-quencher discharge device, the compressed air enters the pool as high pressure bubbles. These bubbles expand, resulting in an outward acceleration of the surrounding pool water. The momentum of the accel-

erated water results in an overexpansion of the bubbles, causing the bubble pressure to become negative relative to the ambient pressure of the surrounding pool. This negative bubble pressure slows and reverses the motion of the water, leading to a compression of the bubbles and a positive pressure relative to that of the pool. The bubbles continue to oscillate in this manner as they rise to the pool surface. The positive and negative pressures developed due to this phenomenon attenuate with distance and result in an oscillatory pressure loading on the "wetted" portion of the torus shell and submerged structures.

Evaluation Philosophy

The development of event sequences, assumptions, load definitions, analysis techniques, and all the other facets comprising the Dresden Units 2 and 3 plant unique analysis are specifically formulated to provide a conservative evaluation. This section describes, in qualitative terms, some of the conservative elements inherent in the Dresden Units 2 and 3 plant unique analysis.

Event Sequences and Assumptions

Implicit in the analysis of a LOCA is the assumption that the event will occur, although the probability of such pipe breaks is low. No credit is taken for detection of leaks to prevent loss-of-coolant accidents. Furthermore, various sizes of pipe breaks are evaluated to consider various effects. The large, instantaneous pipe breaks are considered to evaluate the initial, rapidly occurring events such as vent system pressurization and pool swell. Smaller pipe breaks are analyzed to maximize prolonged effects such as CO and chugging.

The various LOCA's analyzed are assumed to occur coincident with plant conditions which maximize the parameter of interest. For example, the reactor is assumed to be at 102% of rated power; a single failure is assumed; and no credit is taken for normal auxiliary power. Operator action which can mitigate effects of a LOCA is assumed to be unavailable for a specified period. Other assumptions are also selected to maximize the parameter to be evaluated. This approach results in a conservative evaluation since the plant conditions are not likely to be in this worst case situation if a LOCA were to occur.

Test Results and Load Definitions

The load definitions utilized in the Dresden Units 2 and 3 plant unique analysis (PUA) are based on conservative test results and analyses. For example, the LOCA steam condensation loads (CO and chugging) are based on tests in the Mark I Full-Scale Test Facility (FSTF). The FSTF is a full-size 1/16 segment of a Mark I torus. To ensure that conservative results would be obtained on a generic basis, the FSTF was specifically designed

and constructed to promote rapid air and steam flow from the drywell to the wetwell. While this maximizes hydrodynamic loads, it does not take into account the features of actual plants which would mitigate the LOCA effects. Actual Mark I drywells have piping and equipment which would absorb some of the energy released during a loss-of-coolant accident. There are other features of the FSTF which are not typical of actual plant configurations, yet contribute to more conservative load definitions. Pre-heating of the drywell to minimize condensation and heat losses is an example of this feature. Additionally, the load definitions developed from FSTF data apply the maximum observed load over the entire period during which the load may occur. This conservative treatment takes no credit for the load variation observed in the tests.

The LOCA pool swell loads were developed from similarly conservative tests at the Quarter-Scale Test Facility (QSTF). These tests were performed with the driving medium consisting of 100% noncondensables. This maximizes the pool swell because this phenomenon would be driven by condensable steam if a LOCA were to occur in an actual plant. The QSTF tests also minimized the

loss coefficient and maximized the drywell pressurization rate, thus maximizing the pool swell loads. The drywell pressurization rate used in the tests was calculated using conservative analytical modeling and initial conditions. Structures above the pool are assumed to be rigid when analyzed for pool swell impact and drag loads. This assumption maximizes loads and is also used to evaluate loads on submerged structures.

The methodology used to develop SRV loads is based on conservative methods and assumptions. Safety relief valve loads are calculated using a minimum or manufacturer-specified SRV opening time, a maximum steam flow rate, and a maximum steam line pressure. Appropriate assumptions are also applied to conservatively predict SRV load frequency ranges. The SRV loads on submerged structures are similarly determined with the additional assumptions that maximize the pressure differential across the structure due to bubble pressure phasing. The conservatism in the SRV load definition approach has been demonstrated by in-plant tests performed at Dresden Unit 2 and at several other plants. All such tests have confirmed that actual plant responses are significantly less than predicted.

Load Combinations

Conservative assumptions have also been made in developing the combinations of loading phenomena to be evaluated. Many combinations of loading phenomena are investigated although it is very unlikely for such combinations of phenomena to occur. For example, mechanistic analysis has shown that a SRV cannot actuate during the pool swell phase of a design basis loss-of-coolant accident. However, that combination of loading phenomena is evaluated. Both the pool swell and SRV load phenomena involve pressurized air bubbles in the pool and the structural response to these two different bubbles is assumed to be additive, either by absolute sum or by the square root of the sum of the squares (SRSS) method. This rationale is also valid for other hydrodynamic phenomena in the pool such as CO and chugging, which are also combined with SRV discharge. Section 1-3.2.2 includes tables of the actual load combinations used in the analysis for both Class MC internal structures and Class 2 and 3 piping.

When evaluating the structural response to combinations of loading phenomena, the peak responses due

to the various loading phenomena are assumed to occur at the same time. While this is not an impossible occurrence, the probability that the actual responses will combine in that fashion is very remote. Furthermore, the initiating events themselves (e.g., LOCA or safe shutdown earthquake) are of extremely low probability.

Analysis Techniques

The methodology used for analyzing LOCA and SRV loads also contributes to conservatism. These loads are assumed to be smooth curves of regular or periodic shape. This simplifies load definitions and analyses, but maximizes predicted responses. Data from Dresden's SRV test show actual forcing functions to be much less "pure" or "perfect" than those assumed for analysis.

The analyses generally treat a nonlinear problem as a linear, elastic problem with the load "tuned" to the structural frequencies which produce maximum response. The nonlinearities which exist in both the pool and structural dynamics would preclude the attainment of the elastic transient and steady-state responses that are predicted mathematically.

Inherent in the structural analyses are additional conservatisms. Damping is assumed to be low to maximize response, but in reality, damping is likely to be much higher. Allowable stress levels are low compared to the expected material capabilities. Conservative boundary conditions are also used in the analyses.

Conclusion

The loads, methods, and results described above and elsewhere in this report demonstrate that the margins of safety which actually existed for the original design loads have not only been restored, but have been increased. The advancements in understanding the hydrodynamic phenomena and in the structural analyses and modeling techniques have substantially increased since the original design and analysis were completed. This increased understanding and analysis capability is applied to the original loads as well as to the newly defined loads. Thus, not only have the original safety margins been restored, but even greater margins now exist than in the original design.

1-2.0

PLANT UNIQUE CHARACTERISTICS

This section describes the general plant unique geometric and operating parameters pertinent to the reevaluation of the suppression chamber design. Specific details are provided in subsequent volumes, where the detailed analyses of individual components are described.

COM-02-041-1
Revision 0

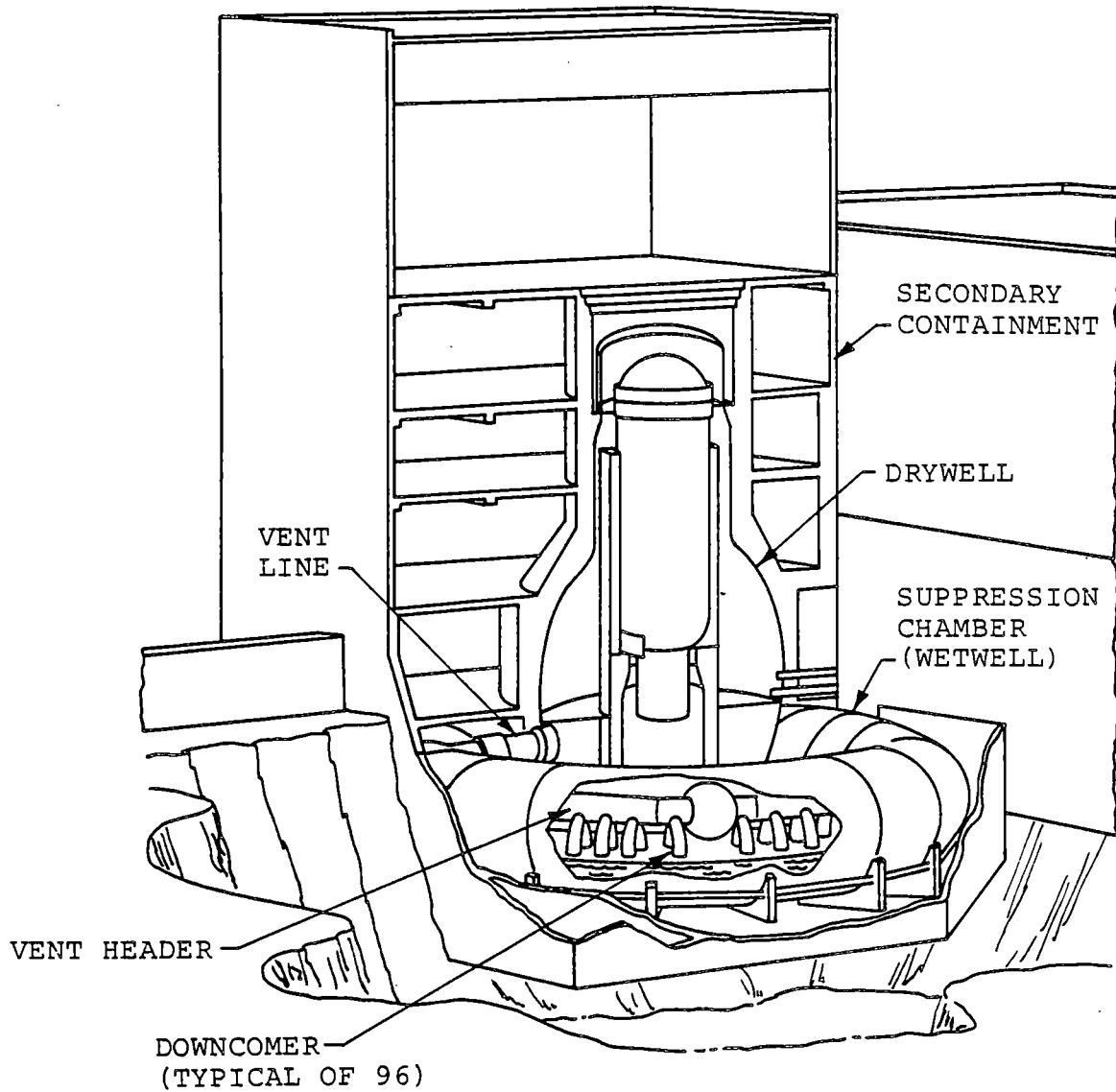
1-2.1

The containment vessel is a Mark I design with a drywell and toroidal-shaped suppression chamber (Figures 1-2.1-1 through 1-2.1-3). The structural components affected by the LOCA and SRV discharge loads include the suppression chamber and its column supports, the vent system and its supports, and the intersections of the vent lines with the drywell. Other items connected to the suppression chamber such as the catwalk, catwalk supports, and the horizontal seismic supports are also included in this plant unique analysis.

The suppression chamber is in the general form of a torus, but is actually constructed of 16 mitered cylindrical shell segments (Figure 1-2.1-3). A reinforcing ring with two supporting columns and a saddle is provided at each miter joint.

Eight vent lines connect the suppression chamber to the drywell. Within the suppression chamber, the vent lines are connected to a common vent header. Also connected to the vent header are downcomers which terminate below the water level of the suppression pool. A bellows assembly connecting the

suppression chamber to the vent line allows for differential movement between the drywell and the suppression chamber.



1. THE DRYWELL AND SUPPRESSION CHAMBER FORM THE PRIMARY CONTAINMENT.

Figure 1-2.1-1

GENERAL ARRANGEMENT OF MARK I CONTAINMENT

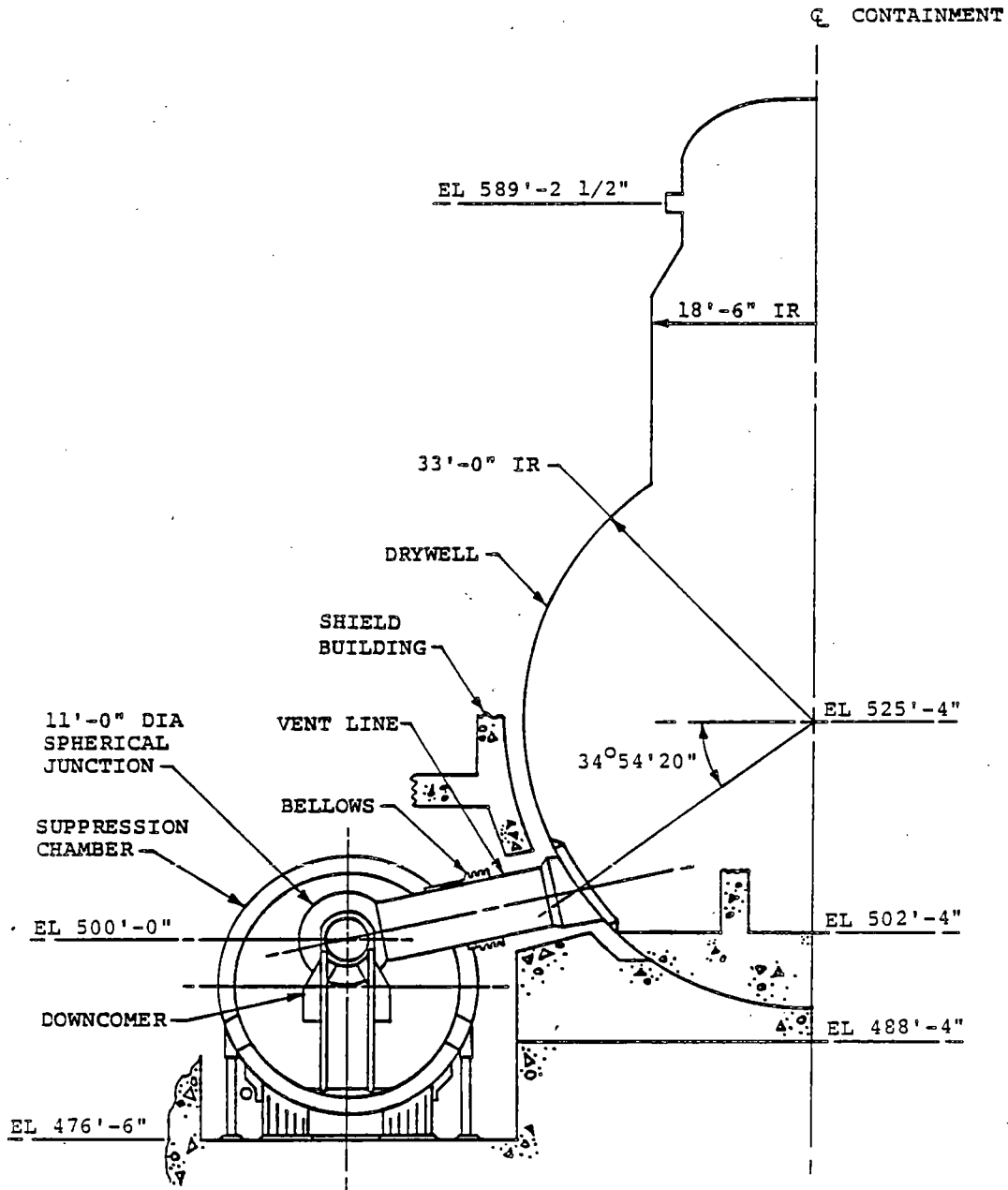


Figure 1-2.1-2

ELEVATION VIEW OF CONTAINMENT

COM-02-041-1
Revision 0

1-2.5

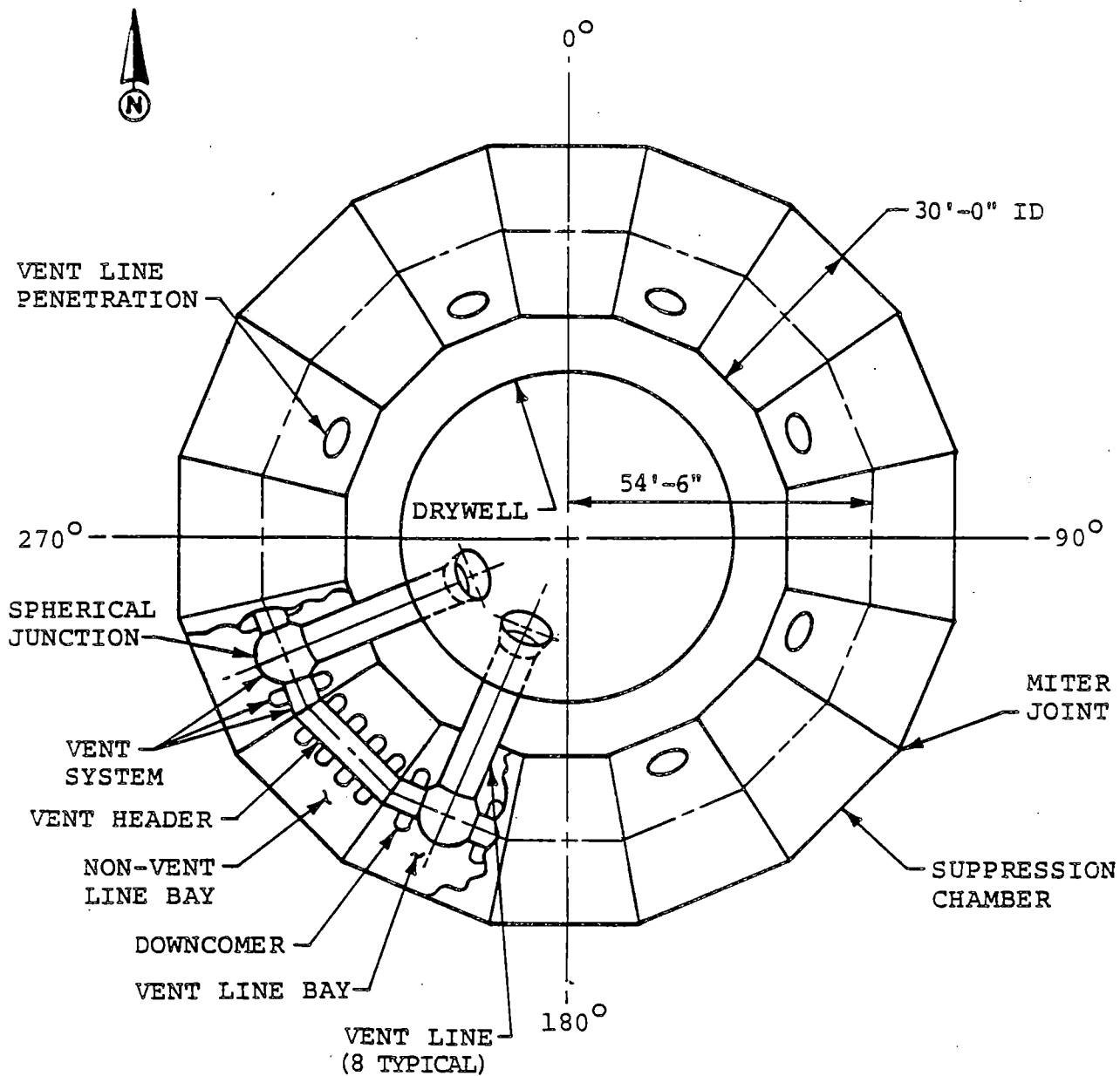


Figure 1-2.1-3
PLAN VIEW OF CONTAINMENT

COM-02-041-1
 Revision 0

1-2.6

1-2.1.1 Suppression Chamber

The inside diameter (ID) of the mitered cylinders which make up the suppression chamber is 30'0" (Figure 1-2.1-3). The suppression chamber shell thickness is typically 0.585" above the horizontal centerline and 0.653" below the horizontal centerline, except at penetration locations, where it is locally thicker (Figure 1-2.1-4).

The suppression chamber shell is reinforced at each miter joint location by a T-shaped ring girder (Figure 1-2.1-5). A typical ring girder is located in a plane parallel to and on the nonvent line bay side of each miter joint. The ring girder is braced laterally with stiffeners connecting the ring girder web to the suppression chamber shell.

The suppression chamber is supported vertically at each miter joint location by inside and outside columns and by a saddle support which spans the inside and the outside columns (Figure 1-2.1-5). The columns and associated column patch plates are located perpendicular to the torus centerline. The saddle supports are located parallel to the miter joint in the plane of the ring girder web.

The inside and outside column members are pipe members. The connection of the column members to the suppression chamber shell is achieved with column stubs, consisting of several plates joined together to form a "T", with stiffeners located on the web of the "T".

The anchorage of the suppression chamber to the basemat is achieved by a system of base plates, stiffeners, and anchor bolts located at two locations on each saddle support and at the base of the column connections. Eight epoxy-grouted anchor bolts are provided at each saddle base plate location. Four epoxy-grouted and two regular anchor bolts are provided at each outside column base plate location, and two epoxy-grouted anchor bolts and two regular anchor bolts are provided at each inside column location. A total of twenty-six anchor bolts at each miter joint location provides the principal mechanism for transfer of uplift loads to the basemat.

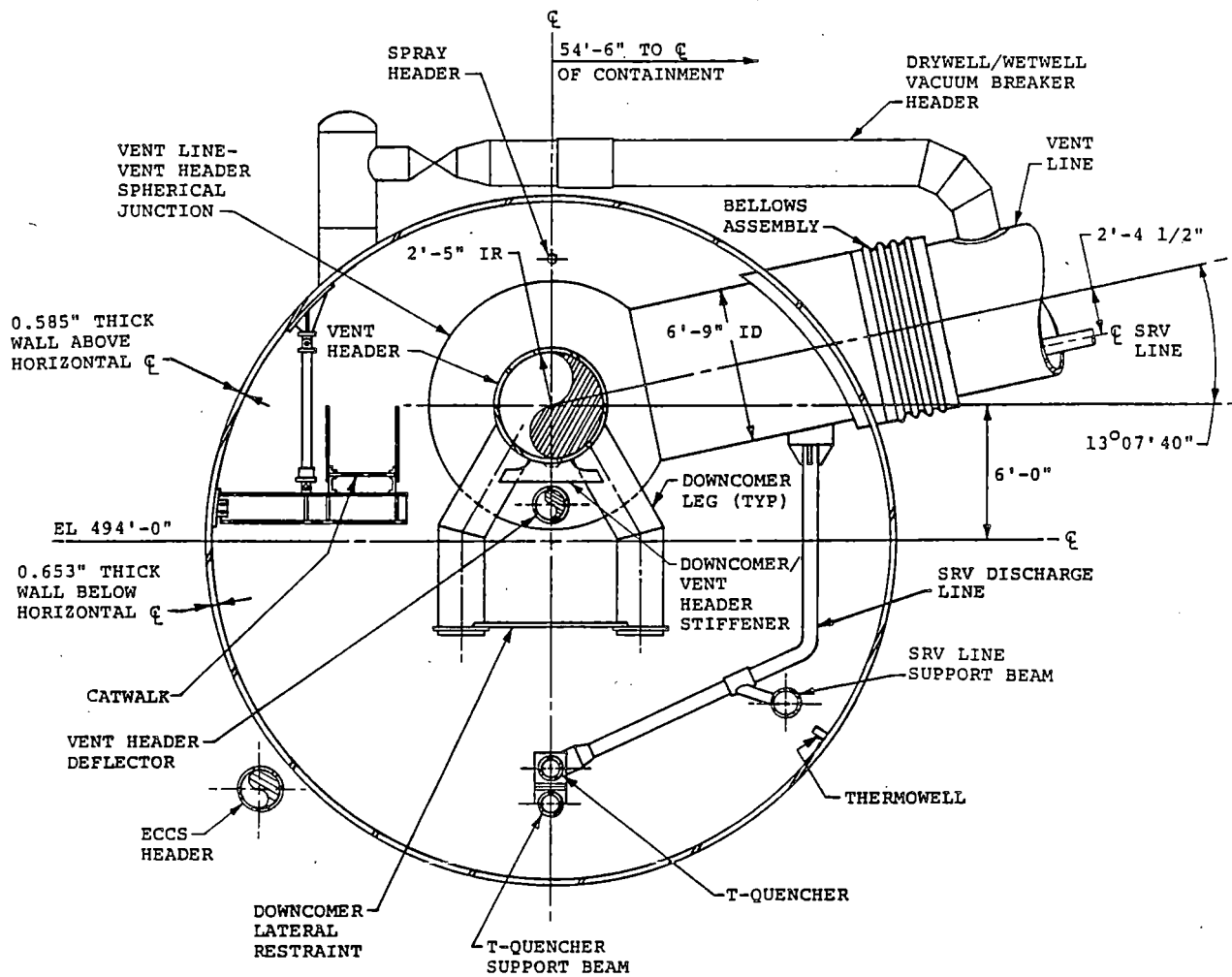


Figure 1-2.1-4
SUPPRESSION CHAMBER SECTION -
MIDBAY VENT LINE BAY

COM-02-041-1
 Revision 0

1-2.9

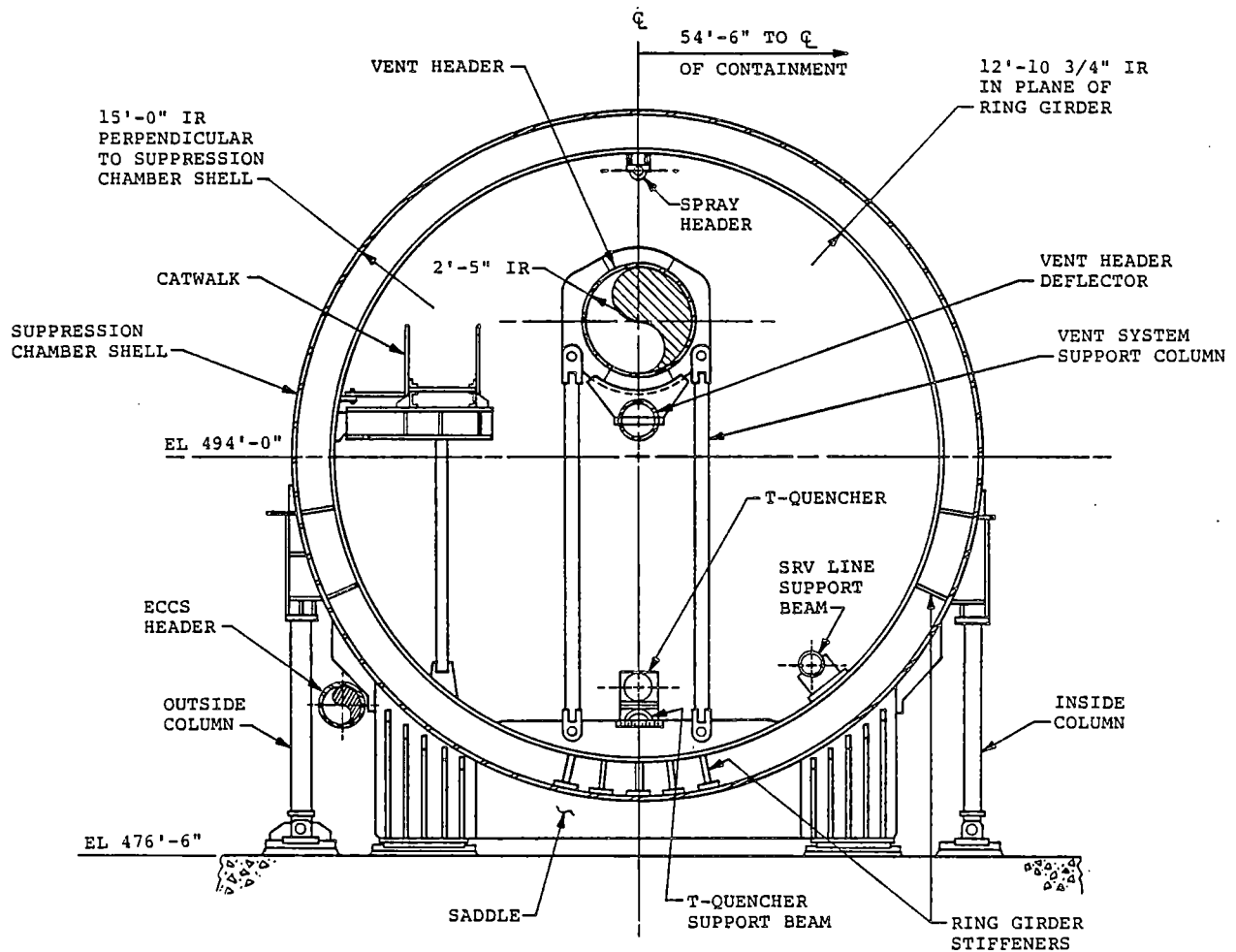


Figure 1-2.1-5

SUPPRESSION CHAMBER SECTION -
MITER JOINT

COM-02-041-1
Revision 0

1-2.10

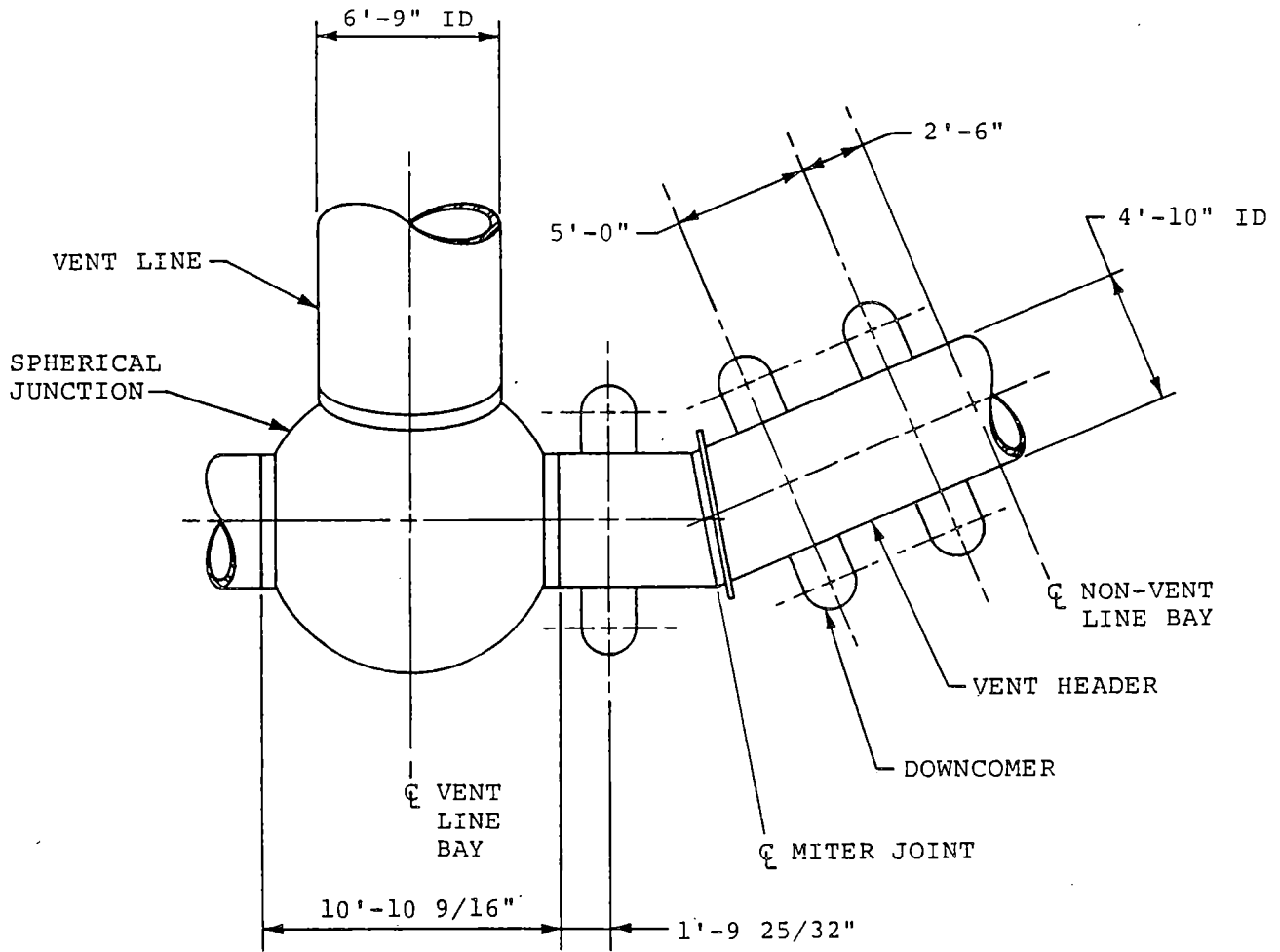
1-2.1.2 Vent System

The vent system is constructed from cylindrical segments joined together to form a manifold-like structure which connects the drywell to the suppression chamber. Figure 1-2.1-6 shows a partial plan view of the vent system. The spherical junction connected to the end of the vent line has an inside diameter of 11'0". Beyond the vent line spherical junction, the vent header inside diameter is 4'10". There are 96 downcomers which protrude from the vent header.

The vent system is supported by two column members at each miter joint location (Figure 1-2.1-5). Figure 1-2.1-7 shows the vent line-to-vent header intersection. A longitudinal bracing system stiffens the downcomer intersection in a direction parallel to the vent header longitudinal axis (Figure 1-2.1-8). For horizontal loadings in a direction perpendicular to the vent header longitudinal axis, the downcomer-to-vent header (DC/VH) intersection is stiffened by means of the DC/VH stiffener plates and lateral bracing members (Figure 1-2.1-9).

There are two external vacuum breakers on six of the eight vent lines. Figure 1-2.1-10 shows the locations of the vacuum breaker header penetrations on the vent line and the torus shell. Figure 1-2.1-11 shows details of the vacuum breaker lines and penetrations and indicates which vent lines have vacuum breaker penetrations.

The vent system also provides support for a portion of the SRV piping inside the vent line and suppression chamber (Figure 1-2.1-12). Loads which act on the SRV piping inside the vent line are transferred to the vent system by the penetration assembly on the vent line and by supports located inside the vent line.



1. DOWNCOMER BRACING NOT SHOWN FOR CLARITY.

Figure 1-2.1-6

PLAN VIEW OF VENT HEADER

COM-02-041-1
Revision 0

1-2.13

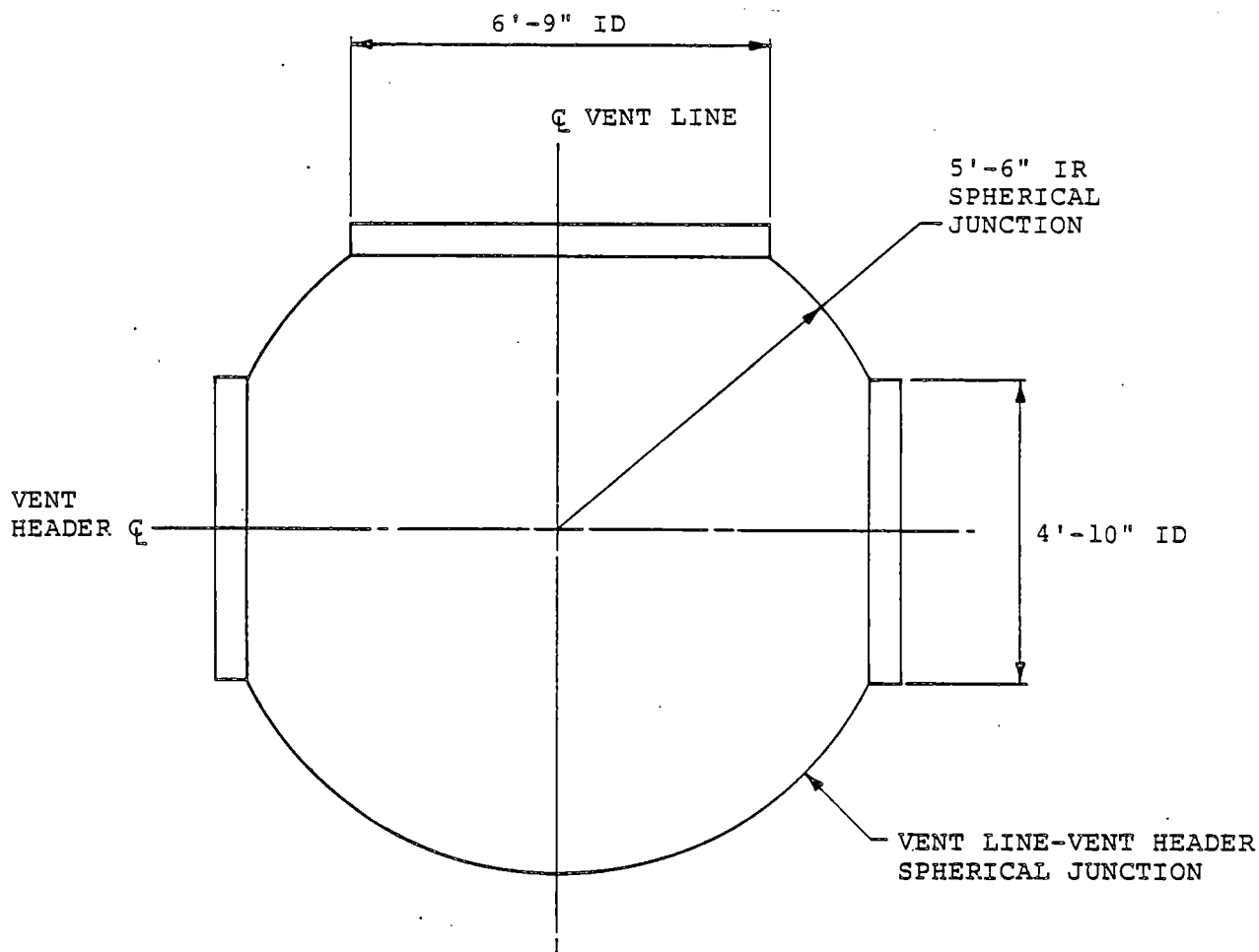
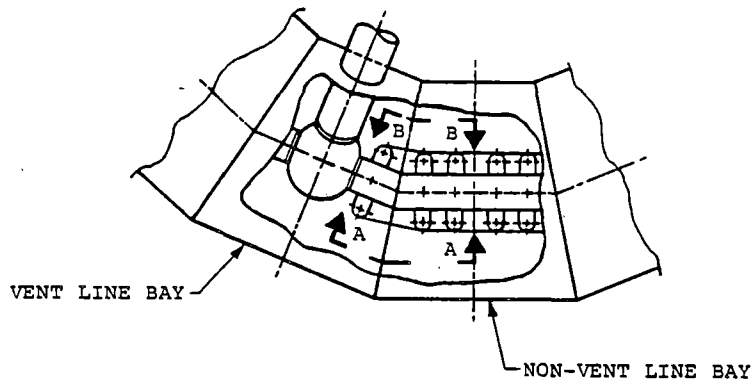


Figure 1-2.1-7

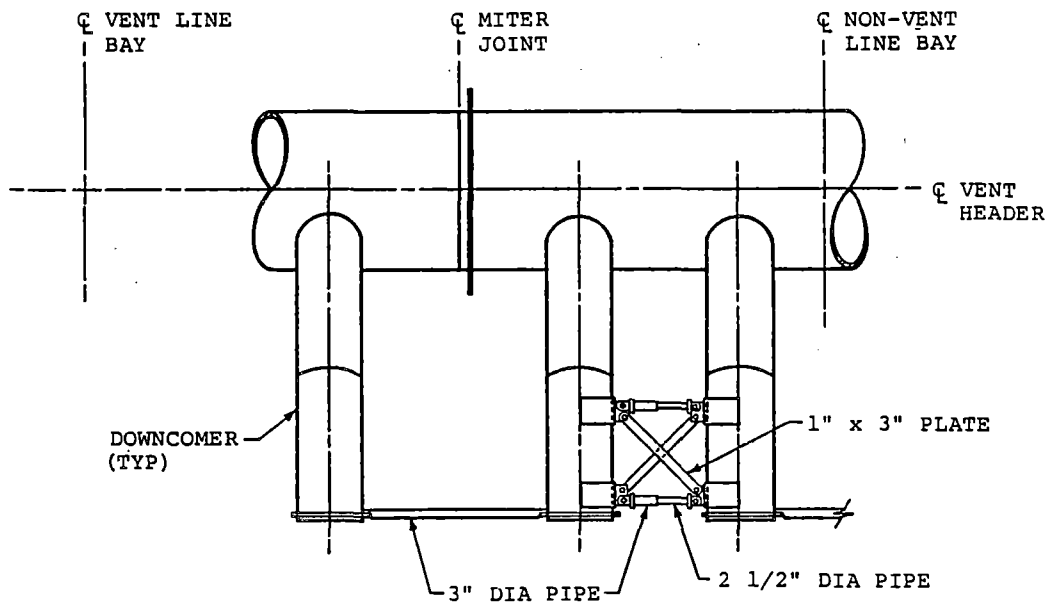
VENT LINE-VENT HEADER SPHERICAL JUNCTION

COM-02-041-1
Revision 0

1-2.14



PARTIAL PLAN VIEW OF SUPPRESSION CHAMBER



VIEW A-A
VIEW B-B (OPPOSITE HAND)

1.. VENT HEADER DEFLECTOR AND VENT HEADER COLUMNS NOT SHOWN FOR CLARITY.

Figure 1-2.1-8

TYPICAL VIEW OF DOWNCOMER LONGITUDINAL BRACING SYSTEM

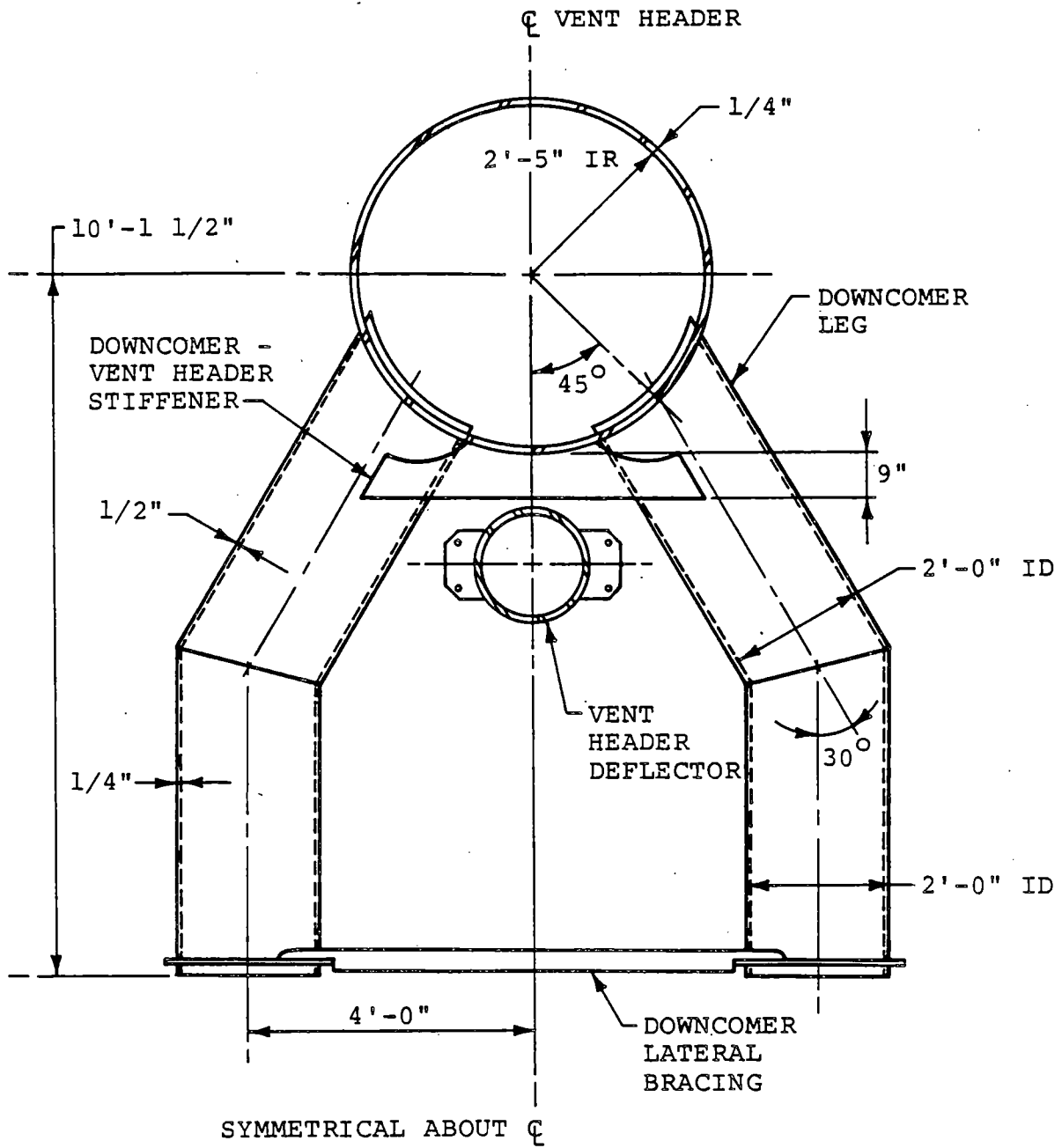
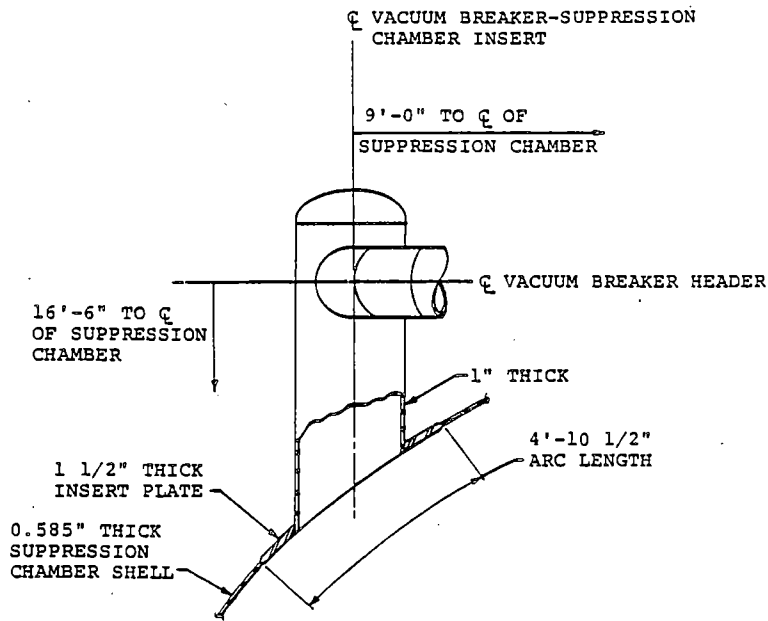


Figure 1-2.1-9

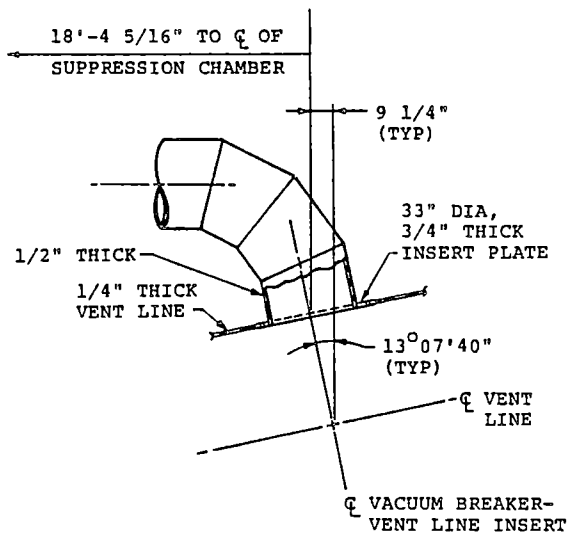
DOWNCOMER-TO-VENT HEADER INTERSECTION

COM-02-041-1
Revision 0

1-2.16



SUPPRESSION CHAMBER PENETRATION



VENT LINE PENETRATION

Figure 1-2.1-10

VACUUM BREAKER HEADER PENETRATION DETAILS

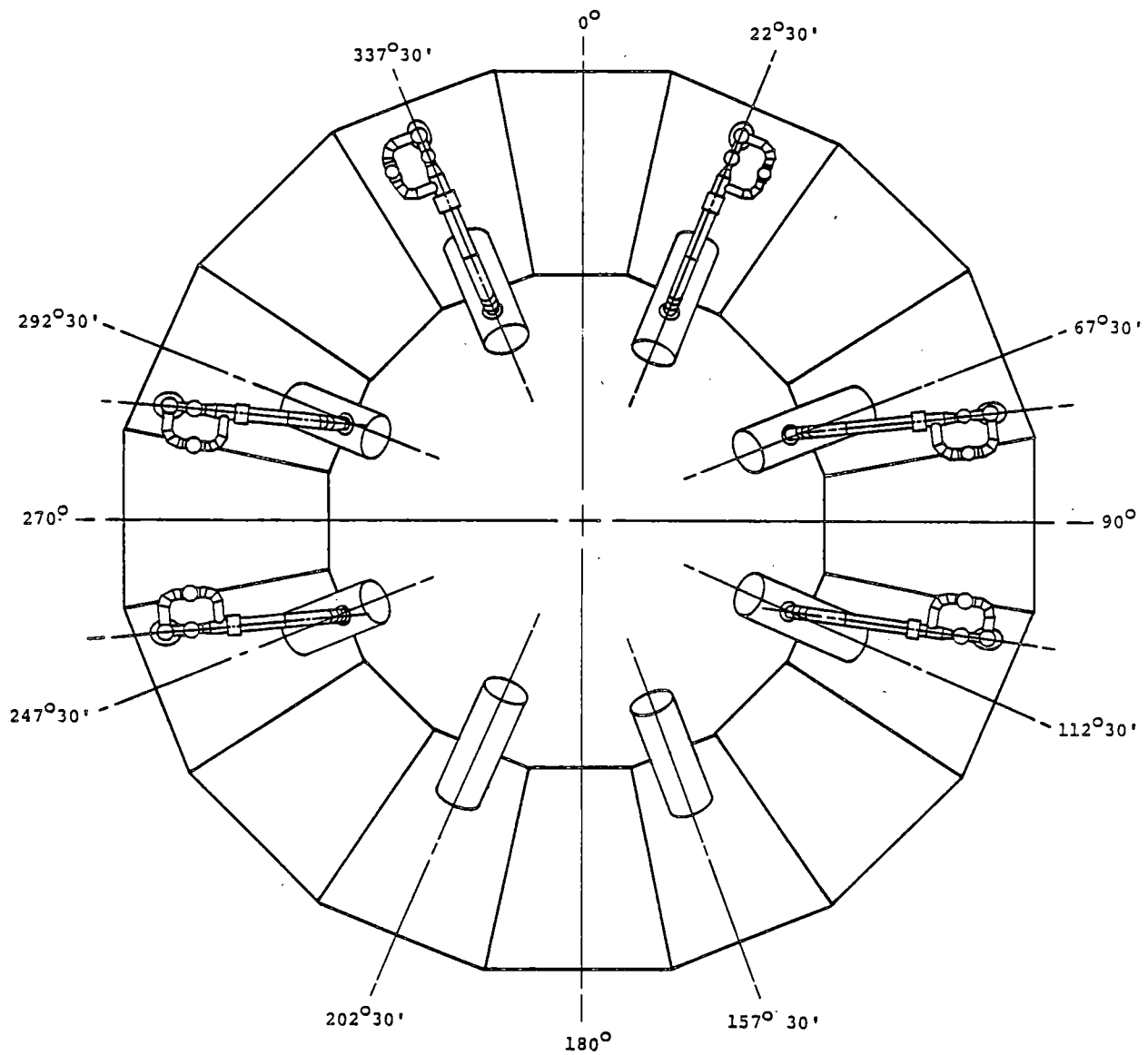
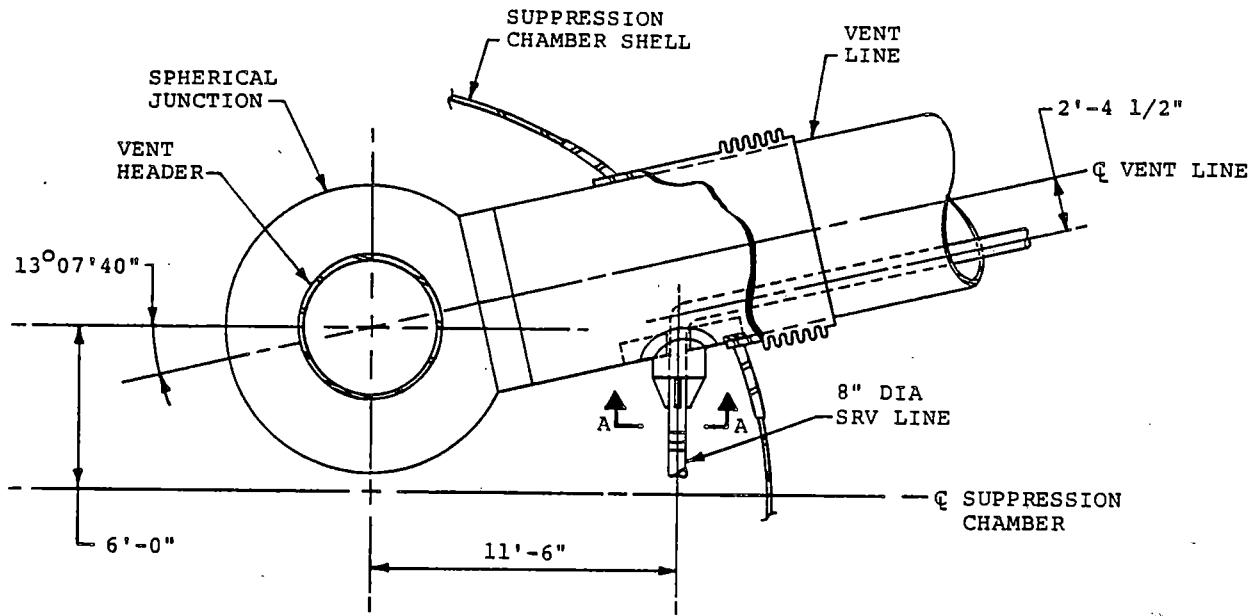


Figure 1-2.1-11

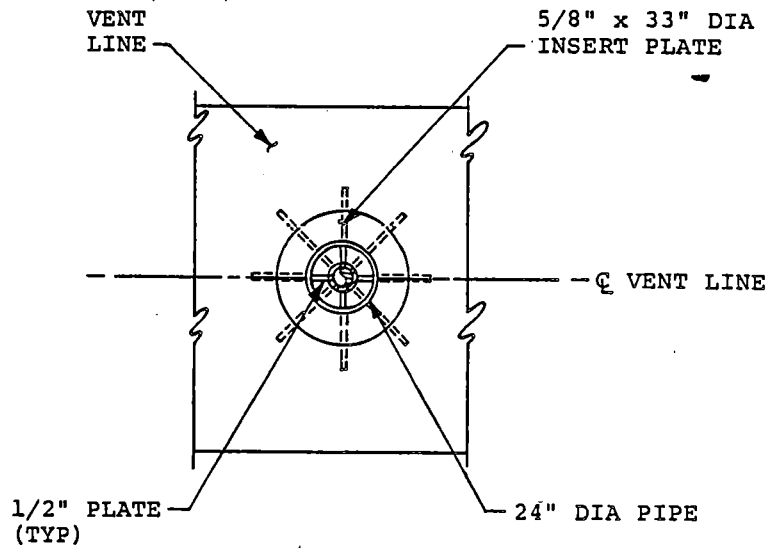
VACUUM BREAKER LOCATIONS

COM-02-041-1
Revision 0

1-2.18



VENT LINE ELEVATION VIEW



VIEW A-A

Figure 1-2.1-12

SRV PENETRATION IN VENT LINE

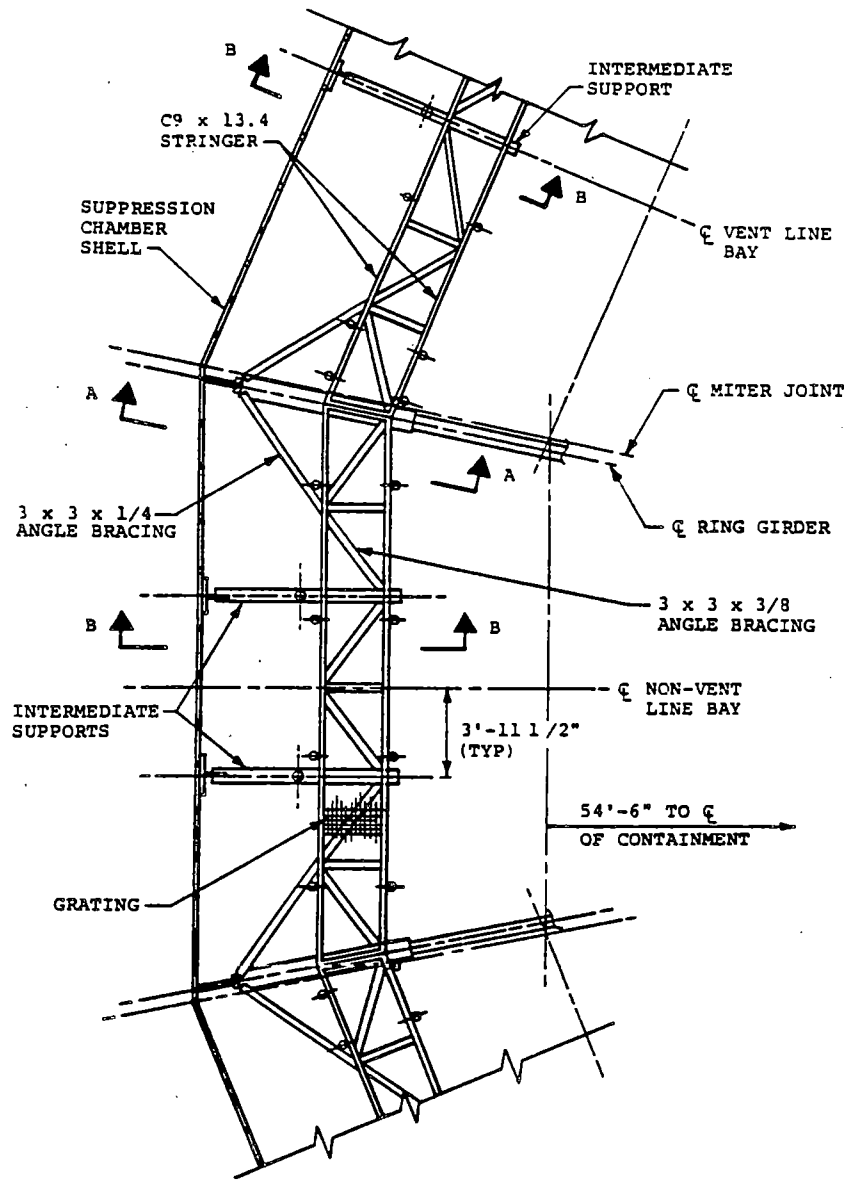
COM-02-041-1
Revision 0

1-2.19

1-2.1.3 Internal Structures

Figures 1-2.1-4 and 1-2.1-5 show the location of the catwalk relative to other major components within the suppression chamber. The catwalk is located parallel to the suppression chamber longitudinal axis. Figures 1-2.1-13 through 1-2.1-15 show that the catwalk is supported by columns at the miter joint ring girder and hangers between each miter joint. The support hangers consist of 4", Schedule 120 pipe which extends vertically upward from the catwalk support beam (Figure 1-2.1-15). The columns consist of 6", Schedule XXS pipe which extends vertically downward from the catwalk support beam to the ring girder (Figure 1-2.1-14).

The catwalk provides support for the electrical conduits. The loads which act on the conduit are transferred to the catwalk by channel sections, which connect the conduit to the catwalk.



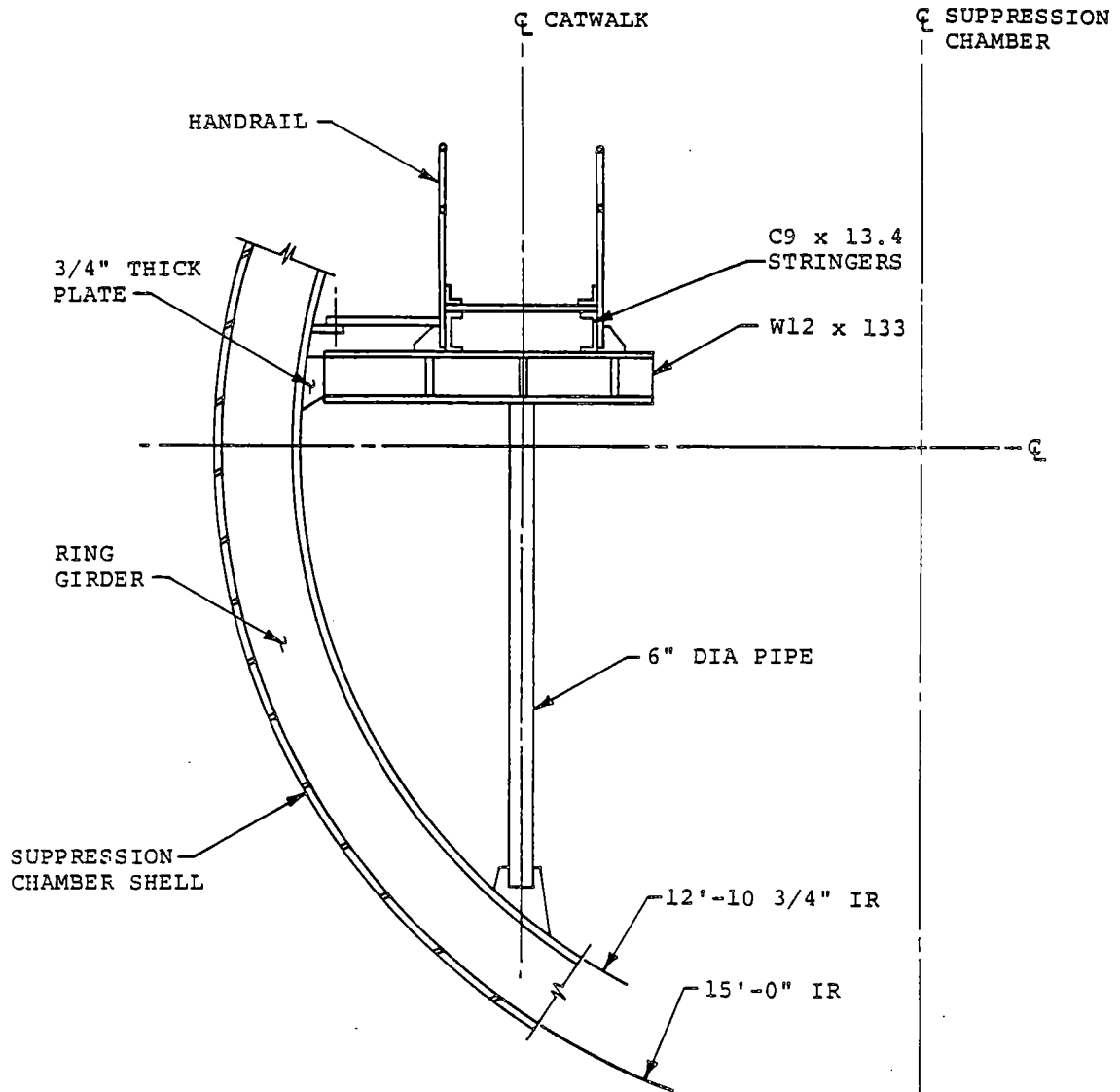
1. SEE FIGURE 1-2.1-14 FOR SECTION A-A.
2. SEE FIGURE 1-2.1-15 FOR SECTION B-B.

Figure 1-2.1-13

PLAN VIEW OF SUPPRESSION CHAMBER
INTERNAL CATWALK

COM-02-041-1
Revision 0

1-2.21

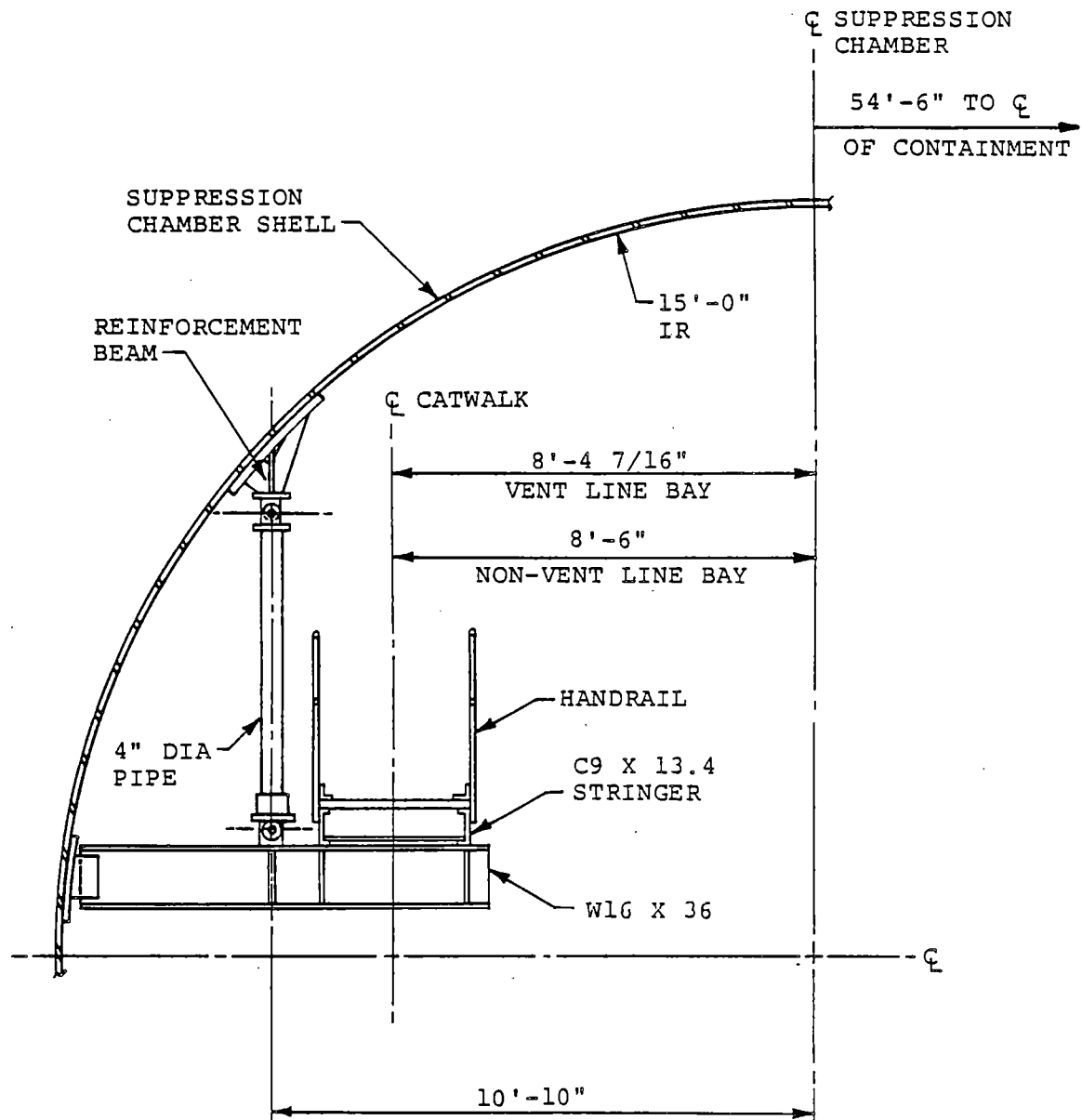


SECTION A-A
 (FROM FIGURE 1-2.1-13)

Figure 1-2.1-14
SUPPRESSION CHAMBER INTERNAL CATWALK -
TYPICAL SUPPORT AT MITER JOINT

COM-02-041-1
 Revision 0

1-2.22



VIEW B-B
 (FROM FIGURE 1-2.1-13)

Figure 1-2.1-15
SUPPRESSION CHAMBER INTERNAL CATWALK -
TYPICAL SUPPORT BETWEEN MITER JOINTS

1-2.1.4 SRV Discharge Piping

A total of five T-quenchers per unit are located midway between the miter joints, with the quencher arms located in the plane of the vertical centerline of the suppression chamber (Figures 1-2.1-16 through 1-2.1-18). Each quencher is supported by a T-quencher support pipe which is connected to the ring girder. Loads which act on the submerged portion of the SRVDL, the SRVDL support pipe, the quencher arms, and the quencher support pipe are transferred to the ring girders.

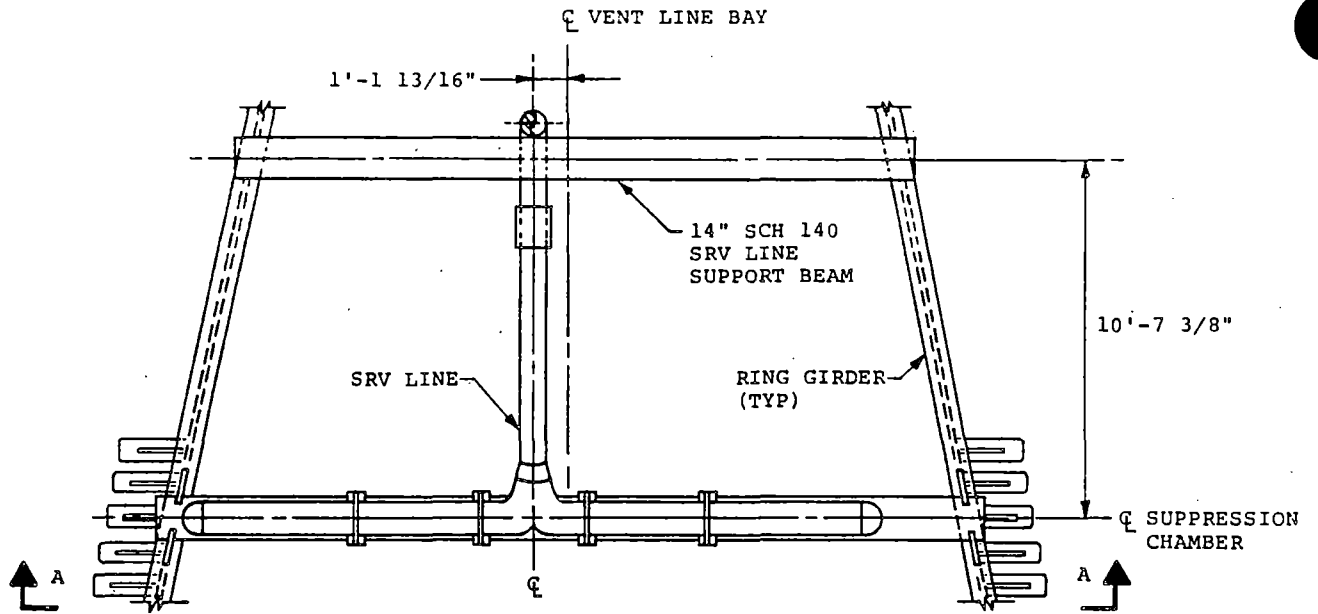
The outlet of each SRV is connected to discharge piping which is routed to the suppression pool. Routing of the SRV discharge piping is such that five of the vent lines are used, with only one SRVDL being routed through any one vent line. The SRV piping in the drywell is supported by hangers, struts, and snubbers connected to the back-up steel structures.

The SRV piping exits the vent line through a stiffened insert plate (Figure 1-2.1-12). Each line is then routed to the center of the bay, where the

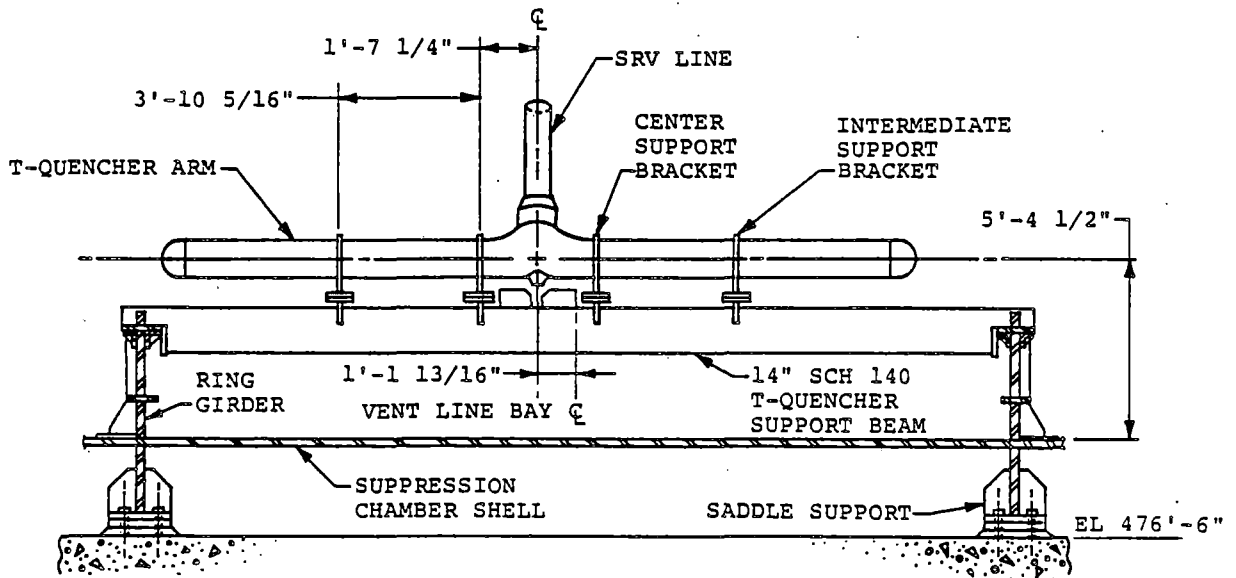
ramshead and T-quencher are attached to the T-quencher support beam. Figures 1-2.1-4 and 1-2.1-19 show typical SRV pipe routing in the wetwell.

COM-02-041-1
Revision 0

1-2.25



PLAN VIEW



VIEW A-A

Figure 1-2.1-16

T-QUENCHER AND T-QUENCHER SUPPORTS

COM-02-041-1
Revision 0

1-2.26

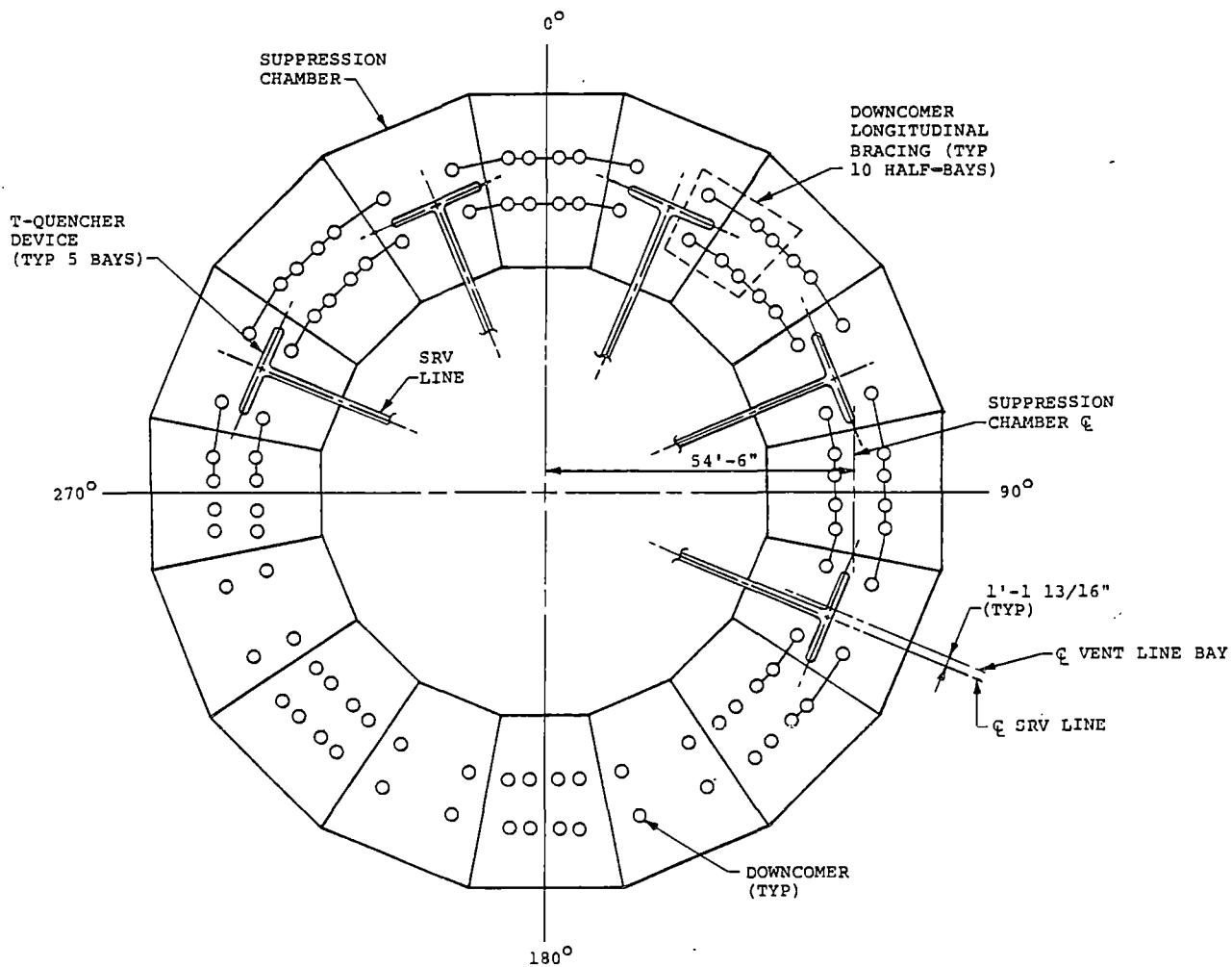


Figure 1-2.1-17

T-QUENCHER AND DOWNCOMER LONGITUDINAL BRACING LOCATIONS -
DRESDEN UNIT 2

COM-02-041-1
Revision 0

1-2.27

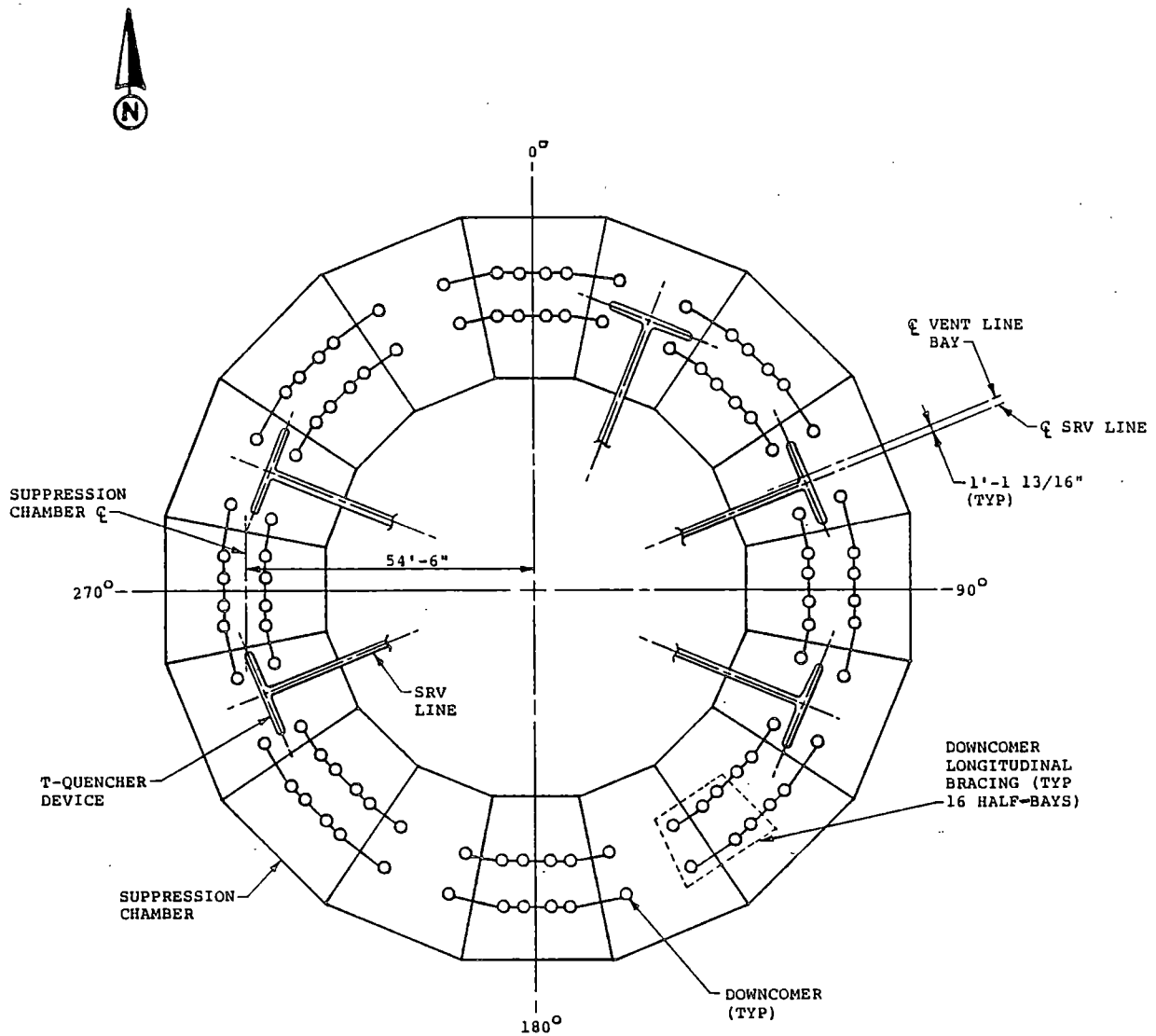
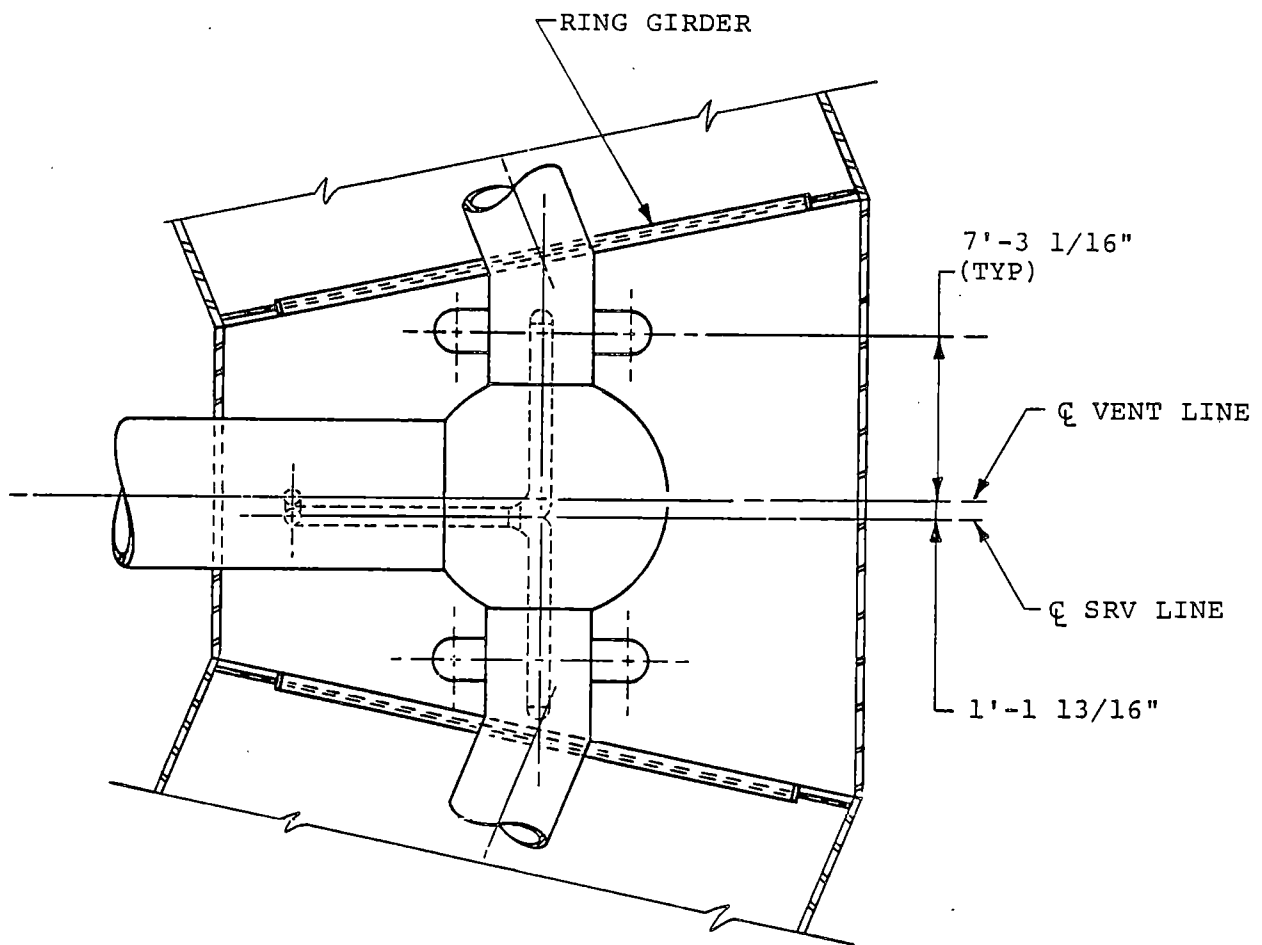


Figure 1-2.1-18

T-QUENCHER AND DOWNCOMER LONGITUDINAL BRACING LOCATIONS -
DRESDEN UNIT 3

COM-02-041-1
 Revision 0

1-2.28



1. VENT SYSTEM STIFFENING AND T-QUENCHER SUPPORTS NOT SHOWN FOR CLARITY.

Figure 1-2.1-19

PLAN VIEW OF SRV PIPE ROUTING
IN SUPPRESSION CHAMBER

1-2.1.5 Torus Attached Piping and Penetrations

The large bore TAP for Dresden Units 2 and 3 consists of 4" and larger nominal diameter piping, which penetrates or is directly attached to the suppression chamber. This section gives a general description of the large bore TAP systems and their associated components.

Large bore TAP lines range in size from 4" to 24" nominal diameter and have varying schedules, although most of the piping consists of ASTM A106, Grade B carbon steel material.

Large bore TAP may be grouped into two general categories: (1) torus external piping, and (2) torus internal piping. Examples of systems with only torus external piping are the low pressure coolant injection (LPCI) pump suction line and the emergency core cooling system (ECCS) suction header. Typical systems having both torus external and internal piping are the high pressure coolant injection (HPCI) turbine exhaust line and the low pressure coolant injection (LPCI) discharge line.

In addition to the large bore systems described above, one small diameter piping system for each unit, the HPCI pot drain line, is included in this report since they have been analyzed using the same methods applied to the large bore piping.

The small bore TAP for Dresden Units 2 and 3 consists of 4" and smaller nominal diameter piping, which is attached to the suppression chamber or to the large bore torus attached piping.

The small bore piping (SBP) lines may be grouped into the following system types:

- (1) Cantilevered Drains and Vents
- (2) Small bore piping with flex loops
- (3) Other small bore piping systems.

Volumes 6 and 7 of the PUAR provide the evaluation for the SBP lines.

Figures 1-2.1-20 and 1-2.1-21 show the numbers and locations of essential suppression chamber penetrations evaluated in Volumes 6 and 7 of the plant unique analysis report. The principal components of

the penetrations are the nozzles, the insert plates, and the "spider" reinforcements. The nozzle extends from the outer circumferential pipe weld through the insert plate to the inner circumferential pipe weld or flange. The insert plate and "spider" provide local reinforcement of the suppression chamber shell near the penetration.

Each penetration modification is designed to allow the penetrations to sustain TAP reaction loads produced by suppression chamber motions due to normal loads and hydrodynamic loads, while keeping component stress intensities below the specified allowable values.

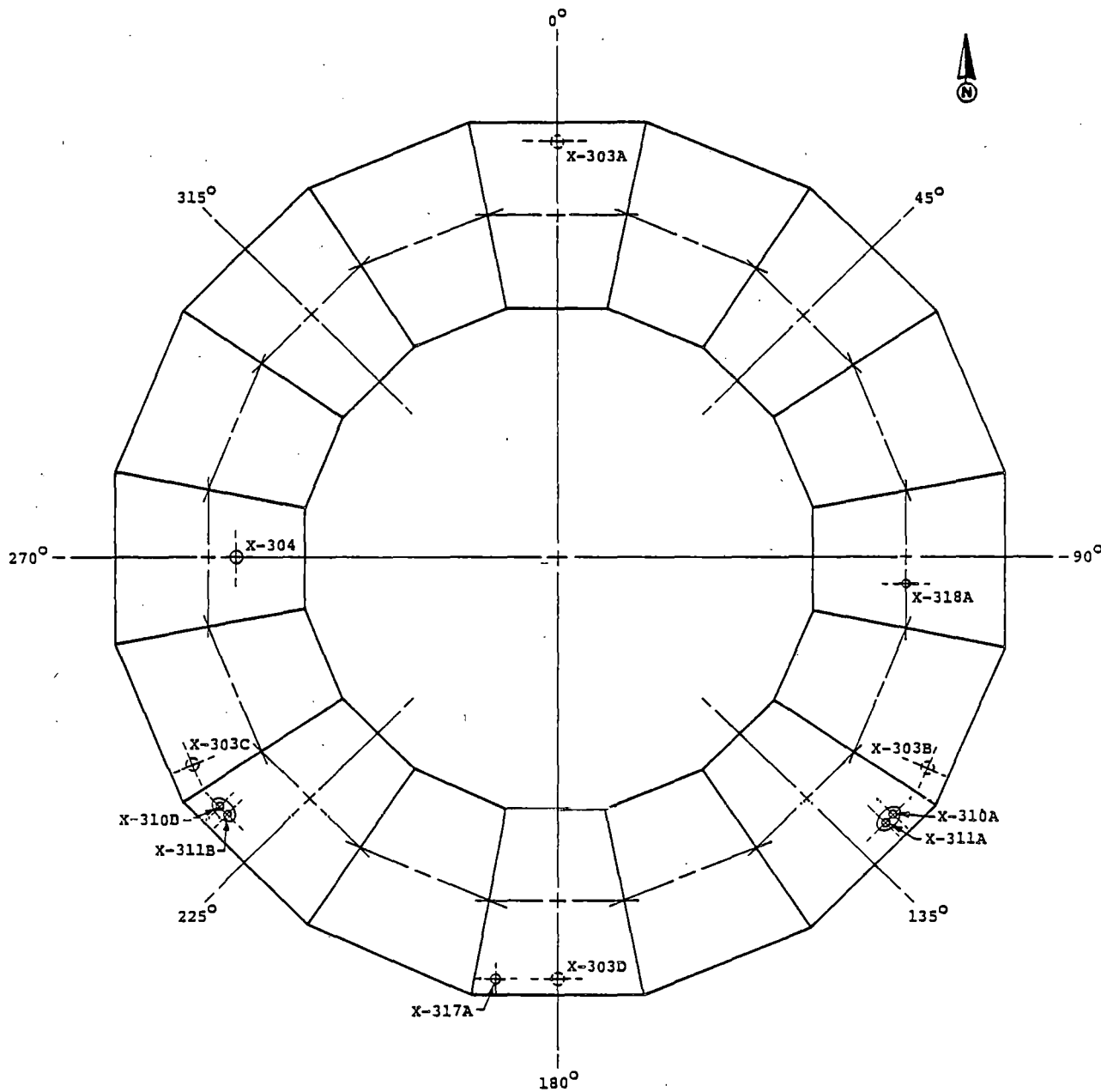


Figure 1-2.1-20

ESSENTIAL TAP PENETRATION LOCATIONS ON SUPPRESSION CHAMBER -
PLAN VIEW (DRESDEN UNIT 2)

COM-02-041-1
 Revision 0

1-2.33

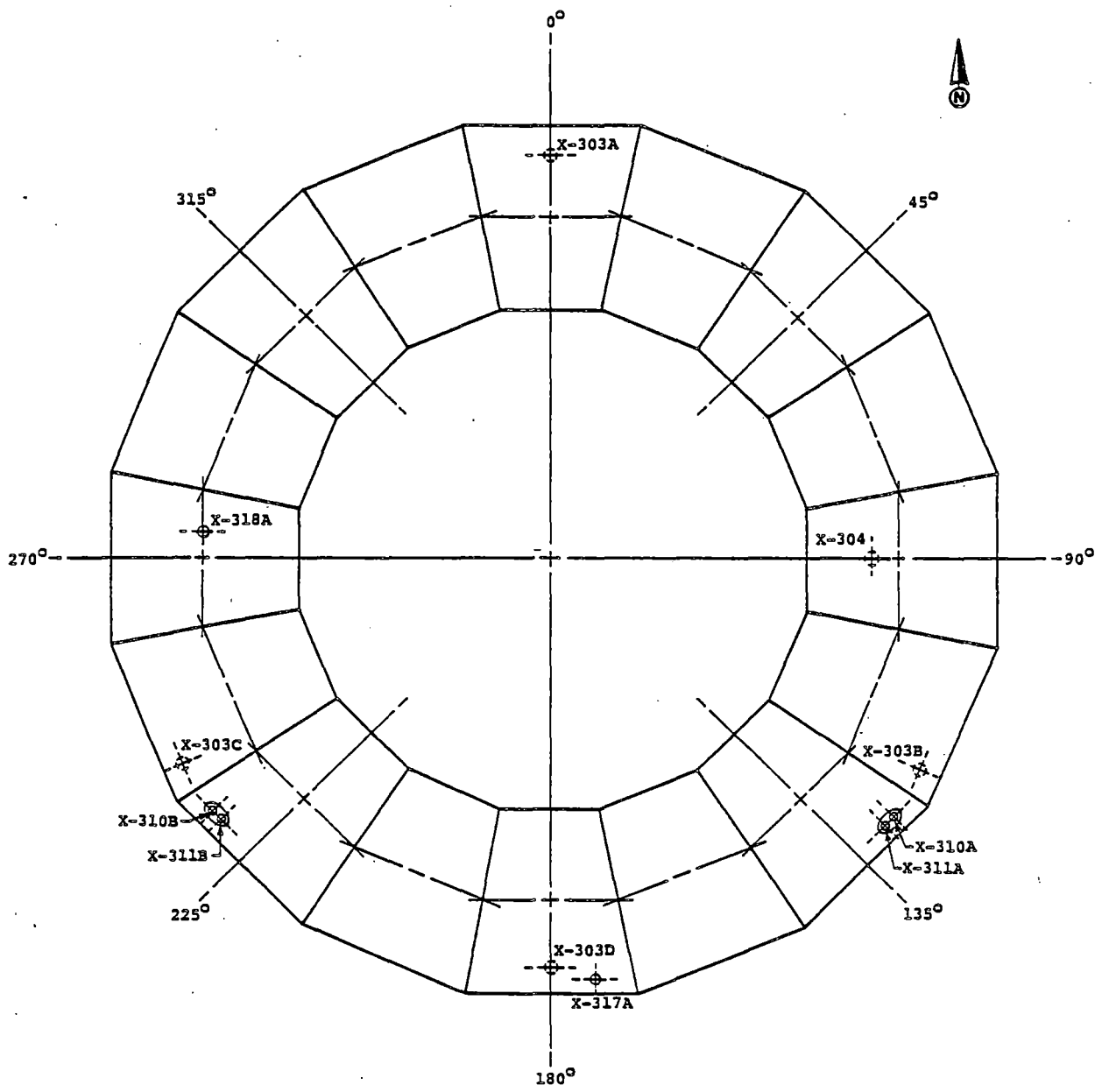


Figure 1-2.1-21

ESSENTIAL TAP PENETRATION LOCATIONS ON SUPPRESSION CHAMBER -
PLAN VIEW (DRESDEN UNIT 3)

COM-02-041-1
 Revision 0

1-2.34

1-2.2

Operating Parameters

Plant operating parameters are used to determine many of the hydrodynamic loads utilized in the reevaluation of the Dresden Units 2 and 3 suppression chamber design. Table 1-2.2-1 is a summary of the primary containment operating parameters used for the analysis of the Dresden Units 2 and 3 hydrodynamic loads.

COM-02-041-1
Revision 0

1-2.35

Table 1-2.2-1

PRIMARY CONTAINMENT OPERATING PARAMETERS

COMPONENTS	CONDITION/ITEM	VALUE
DRYWELL	FREE AIR VOLUME ⁽¹⁾	158,236 ft ³ +0% -10%
	NORMAL OPERATING PRESSURE	HIGH 1.5 psig LOW 1.0 psig
	NORMAL OPERATING TEMPERATURE	NOMINAL BULK 135 ^o F
	NORMAL OPERATING RELATIVE HUMIDITY RANGE	HIGH 100% LOW 20%
	PRESSURE SCRAM INITIATION SET POINT	2.0 psig ±0.2 psig
	DESIGN INTERNAL PRESSURE	62 psig
	DESIGN EXTERNAL PRESSURE MINUS INTERNAL PRESSURE	2.0 psid
	DESIGN TEMPERATURE	281 ^o F
SUPPRESSION CHAMBER	POOL VOLUME	MIN (LOW WATER LEVEL) 112,203 ft ³ MAX (HIGH WATER LEVEL) 115,655 ft ³
	FREE AIR VOLUME ⁽²⁾	MIN (LOW WATER LEVEL) 116,645 ft ³ MAX (HIGH WATER LEVEL) 120,097 ft ³
	LOCA VENT SYSTEM DOWNCOMER SUBMERGENCE	MIN (LOW WATER LEVEL) 3.67 ft MAX (HIGH WATER LEVEL) 4.00 ft
	WATER LEVEL BELOW TORUS CENTERLINE	MIN (LOW WATER LEVEL) 0.458 ft MAX (HIGH WATER LEVEL) 0.125 ft
	SUPPRESSION POOL SURFACE EXPOSED TO SUPPRESSION CHAMBER AIRSPACE	10,092.7 ft ²
	NORMAL OPERATING PRESSURE RANGE	HIGH = 0.2 psig LOW = -0.2 psig
	NORMAL OPERATING TEMPERATURE RANGE OF SUPPRESSION POOL	HIGH = 95 ^o F (TECH SPEC) LOW = 70 ^o F

COM-02-041-1
Revision 0

1-2.36

Table 1-2.2-1

PRIMARY CONTAINMENT OPERATING PARAMETERS

(Concluded)

COMPONENTS	CONDITION/ITEM	VALUE
SUPPRESSION CHAMBER	NORMAL OPERATING TEMPERATURE RANGE OF SUPPRESSION CHAMBER FREE AIR VOLUME	HIGH = 95°F LOW = 70°F
	NORMAL OPERATING RELATIVE HUMIDITY RANGE	HIGH = 100% LOW = 20%
	DESIGN INTERNAL PRESSURE	62 psig
	EXTERNAL PRESSURE MINUS INTERNAL PRESSURE	1 psid
	DESIGN TEMPERATURE	281°F
	NORMAL OPERATING PRESSURE DIFFERENTIAL (DRYWELL-TO-WETWELL)	1.0 psi
DOWNCOMERS	INSIDE DIAMETER AT DISCHARGE	2.01 ft ID
	OUTSIDE DIAMETER AT DISCHARGE	2.05 ft OD
	TOTAL NUMBER OF DOWNCOMERS	96
CONTAINMENT	LONG-TERM POST-LOCA PRIMARY CONTAINMENT LEAK RATE	MAX 2.0%/day
	DRYWELL-TO-WETWELL LEAKAGE	MAX 89.8 scfm
	SOURCE BYPASSING SUPPRESSION POOL WATER	
	SERVICE WATER TEMPERATURE LIMITS	MAX NORMAL 105°F (TECH SPEC) MIN NORMAL 85°F

NUMBER OF SAFETY/ ⁽⁴⁾ SAFETY RELIEF VALVES	SET POINT (psig)	CAPACITY AT 103% OF SET POINT (lbm/hr)
SAFETY 2 (3)	1112	598,000
RELIEF 2 (3)	1135	610,000
VALVES 1 (3)	1125 ±1%	604,000
SAFETY 2	1240 ±1%	642,100
VALVES 2	1250 ±1%	647,200
4	1260 ±1%	652,400

- (1) INCLUDES FREE AIR VOLUME OF THE LOCA VENT SYSTEM.
- (2) DOES NOT INCLUDE FREE AIR VOLUME OF THE LOCA VENT SYSTEM.
- (3) ADS VALVES.
- (4) BOTH SRV'S AND RV'S WILL BE REFERRED TO AS SRV'S THROUGHOUT THIS REPORT.

PLANT UNIQUE ANALYSIS CRITERIA

This section describes the acceptance criteria for the hydrodynamic loads and structural evaluations used in the plant unique analysis.

The acceptance criteria used in the PUA were developed from the NRC review of the long-term program LDR, the PUAAG, and the supporting analytical and experimental programs conducted by the Mark I Owners Group. These criteria are documented in NUREG-0661 for both hydrodynamic load definition and structural applications. Sections 1 and 2 of NUREG-0661 give introduction and background; Section 3 presents a detailed discussion of the hydrodynamic load evaluation; Section 4 presents the structural and mechanical analyses and acceptance criteria, and Appendix A presents the hydrodynamic acceptance criteria.

Appendix A of NUREG-0661 resulted from the NRC evaluation of the load definition procedures for suppression pool hydrodynamic loads, which were proposed by the Mark I Owners Group for use in their plant unique analyses. This NRC evaluation addressed only those events or event combinations involving suppression pool hydrodynamic loads. Unless specified otherwise, all loading conditions or structural analysis techniques used in the PUA, but not addressed in NUREG-0661, are in accordance with the Dresden Units 2 and 3 safety analysis report (SAR) (Reference 5). The NRC hydrodynamic loads acceptance criteria are used with a coupled fluid-structure analytical model.

Wherever feasible, the conservative hydrodynamic acceptance criteria of NUREG-0661 were incorporated directly into the detailed plant unique load determinations and associated structural analyses. Where this simple, direct approach resulted in unrealistic hydrodynamic loads, more detailed plant unique analyses were performed. Many of these analyses have indicated that a specific interpreta-

tion of the generic rules was well founded. These specific applications of the generic hydrodynamic acceptance criteria are identified in the following sections and are discussed in greater detail in Section 1-4.0.

1-3.1.1 LOCA-Related Load Applications

The hydrodynamic loads criteria are based on the NRC review of and revision to experimentally-formulated hydrodynamic loads. Pool swell loads derived from plant unique quarter-scale two-dimensional tests are used to obtain net torus uploads, downloads, and local pressure distributions. Vent system impact and drag loads resulting from pool swell effects are also based on experimental results, using analytical techniques where appropriate.

Condensation oscillation and chugging loads were derived from FSTF results. Downcomer loads are based on test data, using comparisons of plant unique and FSTF dynamic load factors.

The acceleration drag volumes used in determining loads on submerged structures are calculated based upon the values in published technical literature rather than on the procedure which might be inferred from NUREG-0661, where the structure is idealized as a cylindrical section for both velocity and acceleration drag (see Section 1-4.1-5).

Condensation oscillation and post-chug torus shell and submerged structure loads are defined in terms of 50 harmonics. Random phasing of the loading harmonics is assumed, based on FSTF data and subsequent analysis (see Section 1-4.1.7.1).

NUREG-0661 states that the fluid-structure interaction (FSI) effect on CO and chugging loads on submerged structures can be accounted for by adding the shell boundary accelerations to the local fluid acceleration. For Dresden Units 2 and 3, the FSI effects for a given structure are included by adding the pool fluid acceleration at the location of the structure rather than the shell boundary acceleration (see Section 1-4.1.7.3).

NUREG-0661 states that the multiple downcomer load during chugging should be based on an exceedance probability of 10^{-4} per loss-of-coolant accident. This exceedance probability is used in the analysis.

The analysis techniques for SRV loads were developed to generically define T-quencher air clearing loads on the torus. However, a number of Mark I licensees have indicated that the generic load definition procedures are overly conservative for their plant design, especially when the procedures are coupled with conservative structural analysis techniques. To allow for these special cases, the NRC has stipulated requirements whereby in-plant tests could be used to derive the plant specific structural response to the SRV air clearing loads on the torus and submerged structures.

Because of the various phenomena associated with the air clearing phase of SRV discharge, some form of analysis procedure is necessary to extrapolate from test conditions to the design cases. Therefore, the NRC requirements are predicated on formulating a coupled load-structure analysis technique which is calibrated to the plant specific conditions for the simplest form of discharge (i.e., single valve, first actuation) and then applied to the design basis event conditions.

The SRV torus shell loads are evaluated using the alternate approach of NUREG-0661, which allows the use of in-plant SRV tests to calibrate a coupled load- structure analytical model. This method utilizes shell pressure waveforms more characteristic of those observed in tests. A series of in-plant SRV tests were performed at Dresden 2 which confirmed that the computed loadings and predicted structural responses for SRV discharges are conservative (see Section 1-4.2.3).

For SRV bubble-induced drag loads on submerged structures, a bubble pressure multiplier which bounds the maximum peak positive bubble pressure and the maximum bubble pressure differential across the quencher observed during the Monticello T-quencher tests is used (see Section 1-4.2.4).

1-3.1.3 Other Considerations

As part of the PUA, each licensee is required to either demonstrate that previously submitted pool temperature response analyses are sufficient or provide plant specific pool temperature response analyses to assure that SRV discharge transients will not exceed specified pool temperature limits. A suppression pool temperature monitoring system is also required to ensure that the suppression pool bulk temperature is within the allowable limits set forth in the plant technical specifications. Section 1-5.0 discusses specific implementation of these considerations.

Several loads are classified as secondary loads because of their inherent low magnitudes. These loads include seismic slosh pressure loads, post-pool swell wave loads, asymmetric pool swell pressure loads on the torus as a whole, sonic and compression wave loads, and downcomer air clearing loads. These secondary loads are treated as negligible compared to other loads in the PUA, which is in accordance with Appendix A of NUREG-0661.

1-3.2

Component Analysis: Structural Acceptance Criteria

Section 4.0 of NUREG-0661 presents the NRC evaluation of the generic structural and mechanical acceptance criteria and of the general analysis techniques proposed by the Mark I Owners Group for use in the plant unique analyses. Because the Mark I facilities were designed and constructed at different times, there are variations in the codes and standards to which they were constructed and subsequently licensed. For this reassessment of the suppression chamber, the criteria described in this subsection were developed to provide a consistent and uniform basis for acceptability. In this evaluation, references to "original design criteria" mean those specific criteria in the Dresden Units 2 and 3 original containment data specifications (References 6 and 7).

COM-02-041-1
Revision 0

1-3.9

1-3.2.1 Classification of Components

The structures described in Section 1-1.1 were categorized according to their functions to assign the appropriate service limits. The general components of a Mark I suppression chamber have been classified in accordance with Section III of the ASME Boiler and Pressure Vessel Code, as specified in NUREG-0661.

1-3.2.2 Service Level Assignments

The criteria used in the plant unique analyses to evaluate the acceptability of the existing Mark I containment designs or to provide the basis for any plant modifications follow Section III of the ASME Boiler and Pressure Vessel Code through the Summer 1977 Addenda.

Service Limits

The service limits are defined in terms of the Winter 1976 Addenda of the ASME Code, which introduced Levels A, B, C, and D. The selection of specific service limits for each load combination was dependent on the functional requirements of the component analyzed and the nature of the applied load. Tables 1-3.2-1 and 1-3.2-2 provide the assignments of service levels for each load combination. Reference 2 describes details regarding service level assignments and other aspects of Tables 1-3.2-1 and 1-3.2-2.

Table 1-3.2-1

EVENT COMBINATIONS AND SERVICE LEVELS FOR CLASS MC
COMPONENTS AND INTERNAL STRUCTURES

EVENT COMBINATIONS	SRV	SRV + EQ		SBA IBA		SBA + EQ IBA + EQ				SBA+SRV IBA+SRV		SBA + SRV + EQ IBA + SRV + EQ				DBA		DBA + EQ				DBA+SRV		DBA + EQ + SRV				
		0	S	CO, CH	CO, CH	CO, CH	CO, CH	CO, CH	CO, CH	PS (1)	CO, CH	PS	CO, CH	PS	CO, CH	PS	CO, CH	PS	CO, CH	PS	CO, CH	PS	CO, CH	PS	CO, CH	PS	CO, CH	
TYPE OF EARTHQUAKE		0	S			0	S	0	S			0	S	0	S			0	S	0	S					S	0	S
COMBINATION NUMBER		1	2	3	4	5	6	7	8	9	10	11	12	13	14	15	16	17	18	19	20	21	22	23	24	25	26	27
NORMAL (2)	N	X	X	X	X	X	X	X	X	X	X	X	X	X	X	X	X	X	X	X	X	X	X	X	X	X	X	X
EARTHQUAKE	EQ	X	X	X			X	X	X	X			X	X	X	X			X	X	X	X			X	X	X	X
SRV DISCHARGE	SRV	X	X	X							X	X	X	X	X	X							X	X(7)	X	X	X(7)	X(7)
LOCA THERMAL	T _A				X	X	X	X	X	X	X	X	X	X	X	X	X	X	X	X	X	X	X	X	X	X	X	X
LOCA REACTIONS	R _A				X	X	X	X	X	X	X	X	X	X	X	X	X	X	X	X	X	X	X	X	X	X	X	X
LOCA QUASI-STATIC PRESSURE	P _A				X	X	X	X	X	X	X	X	X	X	X	X	X	X	X	X	X	X	X	X	X	X	X	X
LOCA POOL SWELL	P _{PS}																X		X	X			X		X	X		
LOCA CONDENSATION OSCILLATION	P _{CO}					X			X	X		X			X	X			X		X		X				X	X
LOCA CHUGGING	P _{CH}					X			X	X		X			X	X			X		X		X				X	X
STRUCTURAL ELEMENT	ROW																											
EXTERNAL CLASS MC	TORUS, EXTERNAL VENT PIPE, BELLOWS, DRYWELL (AT VENT), ATTACHMENT WELDS, TORUS SUPPORTS, SEISMIC RESTRAINTS	1	A	B	C	A	A	B	C	B	C	A	A	B	C	B	C	A	B	C	C	C	C	C	C	C	C	C
INTERNAL VENT PIPE	GENERAL AND ATTACHMENT WELDS	2	A	B	C	A	A	B	C	B	C	A	A	B	C	B	C	A	B	C	C	C	C	C	C	C	C	C
	AT PENETRATIONS (e.g., HEADER)	3	A	B	C	A	A	B	C	B	C	A	A	B	C	B	C	A	B	C	C	C	C	C	C	C	C	C
VENT HEADER	GENERAL AND ATTACHMENT WELDS	4	A	B	C	A	A	B	C	B	C	A	A	B	C	B	C	A	B	C	C	C	C	C	C	C	C	C
	AT PENETRATIONS (e.g., DOWNCOMERS)	5	A	B	C	A	A(4)	B	C	B(4)	C	A	A(4)	B	C	B(4)	C	A	B	C	C	C	C	C	C	C	C	C
DOWNCOMERS	GENERAL AND ATTACHMENT WELDS	6	A	B	C	A	A	B	C	B	C	A	A	B	C	B	C	A	B	C	C	C	C	C	C	C	C	C
INTERNAL SUPPORTS		7	A	B	C	A	A	B	C	B	C	A	A	B	C	B	C	A	B	C	C	C	C	C	C	C	C	C
INTERNAL STRUCTURES	GENERAL	8	A	B	C	A	A	C	D	C	D	C	C	D	E	D	E	E	E	E	E	E	E	E	E	E	E	E
	VENT DEFLECTOR	9	A	B	C	A	A	C	D	C	D	C	C	D	D	D	D	D	D	D	D	D	D	D	D	D	D	D

NOTES TO TABLE 1-3.2-1

- COM-02-041-1
Revision 0
- (1) REFERENCE 3 STATES "WHERE THE DRYWELL-TO-WETWELL PRESSURE DIFFERENTIAL IS NORMALLY UTILIZED AS A LOAD MITIGATOR, AN ADDITIONAL EVALUATION SHALL BE PERFORMED WITHOUT SRV LOADINGS BUT ASSUMING LOSS OF THE PRESSURE DIFFERENTIAL." IN THE ADDITIONAL EVALUATION LEVEL D SERVICE LIMITS SHALL APPLY FOR ALL STRUCTURAL ELEMENTS EXCEPT ROW 8 INTERNAL STRUCTURES, WHICH NEED NOT BE EVALUATED.
 - (2) NORMAL LOADS (N) CONSIST OF THE COMBINATION OF DEAD LOADS, LIVE LOADS, COLUMN PRESET LOADS, THERMAL EFFECTS DURING OPERATION, AND PIPE REACTIONS DURING OPERATION.
 - (3) EVALUATION OF PRIMARY-PLUS-SECONDARY STRESS INTENSITY RANGE (NE-3221.4) AND OF FATIGUE (NE-3221.5) IS NOT REQUIRED.
 - (4) WHEN CONSIDERING THE LIMITS ON LOCAL MEMBRANE STRESS INTENSITY (NE-3221.2) AND PRIMARY-MEMBRANE-PLUS-PRIMARY-BENDING STRESS (NE-3221.3), THE S_{mc} VALVE MAY BE REPLACED BY $1.3 S_{mc}$.

(NOTE: THE MODIFICATION TO THE LIMITS DOES NOT AFFECT THE NORMAL LIMITS ON PRIMARY-PLUS-SECONDARY STRESS INTENSITY RANGE (NE-3221.4 OR NE-3228.3) NOR THE NORMAL LIMITS ON FATIGUE EVALUATION (NE-3221.5(e) OR APPENDIX II-1500). THE MODIFICATION IS THAT THE LIMITS ON LOCAL MEMBRANE STRESS INTENSITY (NE-3221.2) AND ON PRIMARY-MEMBRANE-PLUS-PRIMARY BENDING STRESS INTENSITY (NE-3221.3) HAVE BEEN MODIFIED BY USING $1.3 S_{mc}$ IN PLACE OF THE NORMAL S_{mc} .

THIS MODIFICATION IS A CONSERVATIVE APPROXIMATION TO RESULTS FROM LIMIT ANALYSIS TESTING AS REPORTED IN REFERENCE 2 AND IS CONSISTENT WITH THE REQUIREMENTS OF NE-3228.2.

- 1-3.13
- (5) SERVICE LEVEL LIMITS SPECIFIED APPLY TO THE OVERALL STRUCTURAL RESPONSE OF THE VENT SYSTEM. AN ADDITIONAL EVALUATION WILL BE PERFORMED TO DEMONSTRATE THAT SHELL STRESSES DUE TO THE LOCAL POOL SWELL IMPINGEMENT PRESSURES DO NOT EXCEED SERVICE LEVEL C LIMITS.
 - (6) FOR THE SUPPRESSION CHAMBER SHELL, THE S_{mc} VALUE MAY BE REPLACED BY $1.0 S_{mc}$ TIMES THE DYNAMIC LOAD FACTOR DERIVED FROM THE TORUS STRUCTURAL MODEL. AS AN ALTERNATIVE, THE 1.0 MULTIPLIER MAY BE REPLACED BY THE PLANT UNIQUE RATIO OF THE SUPPRESSION CHAMBER DYNAMIC FAILURE PRESSURE TO THE STATIC FAILURE PRESSURE.
 - (7) SRV ACTUATION IS ASSUMED TO OCCUR COINCIDENT WITH THE POOL SWELL EVENT. ALTHOUGH SRV ACTUATION CAN OCCUR LATER IN THE DBA, THE RESULTING AIR LOADING ON THE SUPPRESSION CHAMBER SHELL IS NEGLIGIBLE SINCE THE AIR AND WATER INITIALLY IN THE LINE WILL BE CLEARED AS THE DRYWELL-TO-WETWELL WP INCREASES DURING THE DBA TRANSIENT.

Table 1-3.2-2

EVENT COMBINATIONS AND SERVICE LEVELS
FOR CLASS 2 AND 3 PIPING

EVENT COMBINATIONS		SRV	SRV + EQ		SBA IBA		SBA + EQ IBA + EQ				SBA+SRV IBA+SRV		SBA + SRV + EQ IBA + SRV + EQ				DBA		DBA + EQ				DBA+SRV		DBA + EQ + SRV				
			0	S	CO, CH	0	S	CO, CH	0	S	0	S	CO, CH	0	S	0	S	PS (1)	CO, CH	PS	CO, CH	PS	CO, CH	PS	CO, CH	0	S	0	S
TYPE OF EARTHQUAKE			0	S			0	S	0	S			0	S	0	S			0	S	0	S			0	S	0	S	
COMBINATION NUMBER		1	2	3	4	5	6	7	8	9	10	11	12	13	14	15	16	17	18	19	20	21	22	23	24	25	26	27	
LOADS	NORMAL (2)	N	X	X	X	X	X	X	X	X	X	X	X	X	X	X	X	X	X	X	X	X	X	X	X	X	X	X	
	EARTHQUAKE	EQ		X	X			X	X	X	X			X	X	X	X		X	X	X	X			X	X	X	X	
	SRV DISCHARGE	SRV	X	X	X						X	X	X	X	X	X							X	X(6)	X	X	X(6)	X(6)	
	THERMAL	T _A	X	X	X	X	X	X	X	X	X	X	X	X	X	X	X	X	X	X	X	X	X	X	X	X	X	X	X
	PIPE PRESSURE	P _A	X	X	X	X	X	X	X	X	X	X	X	X	X	X	X	X	X	X	X	X	X	X	X	X	X	X	X
	LOCA POOL SWELL	P _{PS}															X		X	X			X		X	X			
	LOCA CONDENSATION OSCILLATION	P _{CO}				X			X	X		X			X	X		X			X			X			X		
LOCA CHUGGING	P _{CH}				X			X	X		X			X	X		X			X	X		X			X	X		
STRUCTURAL ELEMENT		ROW																											
ESSENTIAL PIPING SYSTEMS	WITH IBA/DBA	10	B	B (3)	B (3)	B (4)	B (4)	B (4)	B (4)	B (4)	B (4)	B (4)	B (4)	B (4)	B (4)	B (4)	B (4)	B (4)	B (4)	B (4)	B (4)	B (4)	B (4)	B (4)	B (4)	B (4)	B (4)	B (4)	
	WITH SBA	11				B (3)	B (3)	B (4)	B (4)	B (4)	B (4)	B (3)	B (3)	B (4)	B (4)	B (4)													
NONESENTIAL PIPING SYSTEMS	WITH IBA/DBA	12	B	C (5)	D (5)	D (5)	D (5)	D (5)	D (5)	D (5)	D (5)	D (5)	D (5)	D (5)	D (5)	D (5)	D (5)	D (5)	D (5)	D (5)	D (5)	D (5)	D (5)	D (5)	D (5)	D (5)	D (5)	D (5)	
	WITH SBA	13				C (5)	C (5)	D (5)	D (5)	D (5)	D (5)	D (5)	D (5)	D (5)	D (5)	D (5)													

NOTES TO TABLE 1-3.2-2

- (1) REFERENCE 3 STATES "WHERE A DRYWELL-TO-WETWELL PRESSURE DIFFERENTIAL IS NORMALLY UTILIZED AS A LOAD MITIGATOR, AN ADDITIONAL EVALUATION SHALL BE PERFORMED WITHOUT SRV LOADINGS BUT ASSUMING THE LOSS OF THE PRESSURE DIFFERENTIAL." SERVICE LEVEL D LIMITS SHALL APPLY FOR ALL STRUCTURAL ELEMENTS OF THE PIPING SYSTEM FOR THIS EVALUATION. THE ANALYSIS NEED ONLY BE ACCOMPLISHED TO THE EXTENT THAT INTEGRITY OF THE FIRST PRESSURE BOUNDARY ISOLATION VALUE IS DEMONSTRATED.
- (2) NORMAL LOADS (N) CONSIST OF DEAD LOADS (D).
- (3) AS AN ALTERNATIVE, THE $1.2 S_h$ LIMIT IN EQUATION 9 OF NC-3652.2 MAY BE REPLACED BY $1.8 S_h$, PROVIDED THAT ALL OTHER LIMITS ARE SATISFIED. FATIGUE REQUIREMENTS ARE APPLICABLE TO ALL COLUMNS, WITH THE EXCEPTION OF 16, 18, 19, 22, 24 AND 25.
- (4) FOOTNOTE 3 APPLIES EXCEPT THAT INSTEAD OF USING $1.8 S_h$ IN EQUATION 9 OF NC-3652.2, $2.4 S_h$ IS USED.
- (5) EQUATION 10 OF NC OR ND-3659 WILL BE SATISFIED, EXCEPT THE FATIGUE REQUIREMENTS ARE NOT APPLICABLE TO COLUMNS 16, 18, 19, 22, 24 AND 25 SINCE POOL SWELL LOADINGS OCCUR ONLY ONCE. IN ADDITION, IF OPERABILITY OF AN ACTIVE COMPONENT IS REQUIRED TO ENSURE CONTAINMENT INTEGRITY, OPERABILITY OF THAT COMPONENT MUST BE DEMONSTRATED.
- (6) SRV ACTUATION IS ASSUMED TO OCCUR COINCIDENT WITH THE POOL SWELL EVENT. ALTHOUGH SRV ACTUATION CAN OCCUR LATER IN THE DBA, THE RESULTING AIR LOADING ON THE SUPPRESSION CHAMBER SHELL IS NEGLIGIBLE SINCE THE AIR AND WATER INITIALLY IN THE LINE WILL BE CLEARED AS THE DRYWELL-TO-WETWELL ΔP INCREASES DURING THE DBA TRANSIENT.

COM-02-041-1
Revision 0

1-3.15

1-3.2.3 Other Considerations

The general structural analysis techniques proposed by the Mark I Owners Group are utilized with sufficient detail to account for all significant structural response modes and are consistent with the methods used to develop the loading functions defined in the load definition report. For those loads considered in the original design but not redefined by the LDR, either the results of the original analysis are used or a new analysis is performed, based on the methods employed in the original plant design.

The damping values used in the analysis of dynamic loading events are those specified in Regulatory Guide 1.61, "Damping Values for Seismic Design of Nuclear Power Plants," which is in accordance with NUREG-0661.

The structural responses resulting from two dynamic phenomena are combined by either the absolute sum or the SRSS method. The combined state of the stress results in the maximum stress intensity.

1-4.0

HYDRODYNAMIC LOADS METHODOLOGY AND EVENT SEQUENCE
SUMMARY

This section presents the load definition procedures used to develop the Dresden Units 2 and 3 hydrodynamic loads and is organized in accordance with NUREG-0661, Section 3. Table 1-4.0-1 provides a cross-reference between the sections of this PUAR and the sections of Appendix A of NUREG-0661, where each load or event is addressed.

COM-02-041-1
Revision 0

1-4.1

Table 1-4.0-1

PLANT UNIQUE ANALYSIS/NUREG-0661 LOAD SECTIONS
CROSS-REFERENCE

LOAD/EVENT	PUA SECTION	NUREG-0661 APPENDIX A SECTION
CONTAINMENT PRESSURE AND TEMPERATURE RESPONSE	1-4.1.1	2.0
VENT SYSTEM DISCHARGE LOADS	1-4.1.2	2.2
POOL SWELL LOADS ON TORUS SHELL	1-4.1.3	2.3 & 2.4
POOL SWELL LOADS ON ELEVATED STRUCTURES	1-4.1.4	2.6 - 2.10
POOL SWELL LOADS ON SUBMERGED STRUCTURES	1-4.1.5 & 1-4.1.6	2.14.1 & 2.14.2
CONDENSATION OSCILLATION LOADS ON TORUS SHELL	1-4.1.7	2.11.1
CONDENSATION OSCILLATION LOADS ON DOWNCOMERS AND VENT SYSTEM	1-4.1.7	2.11.2
CONDENSATION OSCILLATION LOADS ON SUBMERGED STRUCTURES	1-4.1.7	2.14.5
CHUGGING LOADS ON TORUS SHELL	1-4.1.8	2.12.1
CHUGGING LOADS ON DOWNCOMERS	1-4.1.8	2.12.2
CHUGGING LOADS ON SUBMERGED STRUCTURES	1-4.1.8	2.14.6
SRV ACTUATION CASES	1-4.2.1	2.13.7
SRV DISCHARGE LINE CLEARING LOADS	1-4.2.2	2.13.2 & 2.13.1
SRV LOADS ON TORUS SHELL	1-4.2.3	2.13.3
SRV LOADS ON SUBMERGED STRUCTURES	1-4.2.4	2.14.3 & 2.14.4
DESIGN BASIS ACCIDENT	1-4.3.1	3.2.1
INTERMEDIATE BREAK ACCIDENT	1-4.3.2	3.2.1
SMALL BREAK ACCIDENT	1-4.3.3	3.2.1

COM-02-041-1
Revision 0

1-4.2

This subsection describes the procedures used to define the Dresden Units 2 and 3 LOCA-related hydrodynamic loads. The sources of structural loads generated during a LOCA are primarily a result of the following conditions.

- Pressures and temperatures within the drywell, vent system, and wetwell
- Fluid flow through the vent system
- Initial LOCA bubble formation in the pool and the resulting displacement of water resulting in pool swell
- Steam flow into the suppression pool (CO and chugging).

For postulated pipe breaks inside the drywell, three LOCA categories are considered. These three categories, selected on the basis of break size, are referred to as a design basis accident (DBA), an intermediate break accident (IBA), and a small break accident (SBA).

The DBA for the Mark I containment design is the instantaneous guillotine rupture of the largest pipe in the primary system (recirculation suction line). This LOCA leads to a specific combination of dynamic, quasi-static and static loads. However, the DBA does not represent the limiting case for all loads and structural responses. Consequently, an IBA and a SBA are also evaluated. The IBA is evaluated as a 0.1 ft² instantaneous liquid line break in the primary system, and the SBA is evaluated as a 0.01 ft² instantaneous steam line break in the primary system.

1-4.1.1 Containment Pressure and Temperature Response

The drywell and suppression chamber transient pressure and temperature responses are calculated using the "General Electric Company Pressure Suppression Containment Analytical Model" (Reference 8). This analytical model calculates the thermodynamic response of the drywell, vent system, and suppression chamber volumes to mass and energy released from the primary system following a postulated loss-of-coolant accident.

The containment pressure and temperature analyses are performed in accordance with Appendix A of NUREG-0661 and are documented in Reference 9.

1-4.1.2 Vent System Discharge Loads

Of the three postulated LOCA categories, the DBA causes the most rapid pressurization of the containment system, the largest vent system mass flow rate, and therefore, the most severe vent system thrust loads. The pressurization of the containment for the IBA and SBA is much less rapid than for the design basis accident. Thus, the resulting vent system thrust loads for the SBA and IBA are bounded by the DBA thrust loads. Consequently, vent system thrust loads are only evaluated for the design basis accident.

Reaction loads occur on the vent system (main vent, vent header, and downcomers) following a LOCA due to pressure imbalances between the vent system and the surrounding torus airspace, and due to forces resulting from changes in linear momentum.

The LDR thrust equations consider these forces due to pressure distributions and momentum to define horizontal and vertical thrust forces. These equations are included in the analytical procedures applied to the main vents, vent header, and downcomer portions of the vent system.

Because main vents and downcomers are located symmetrically about the center of the vent system, the horizontal vent system thrust loads cancel each other, resulting in a zero effective horizontal vent system thrust load.

The bases, analytical procedures, and assumptions used to calculate thrust loads are described in the load definition report. The Dresden Units 2 and 3 plant unique DBA thrust loads for the main vent, the vent header, and downcomers were developed using both an operating and zero initial drywell-to-wetwell pressure differential. The thrust loads used in this PUA are documented in Reference 9.

Volume 3 of the PUAR presents the analysis of the vent system. The vent system discharge loads are developed in accordance with Appendix A of NUREG-0661.

1-4.1.3 Pool Swell Loads on the Torus Shell

During the postulated LOCA, the air initially in the drywell and vent system is injected into the suppression pool, producing a downward reaction force on the torus followed by an upward reaction force. These vertical loads create a dynamic imbalance of forces on the torus, which acts in addition to the weight of the water applied to the torus. This dynamic force history lasts for only a few seconds.

The bases, assumptions, and justifications for the pool swell loads on the torus shell due to the DBA are described in the load definition report. The pool swell loads on the torus shell are based on a series of CECO unique tests conducted in the OSTF (Reference 10), which are applicable to Dresden Units 2 and 3. The results from these OSTF tests are documented in Reference 10. The pool swell loads on the torus shell used in the PUA are based on the information in Reference 10, with the addition of the upload and download margins specified in Appendix A of NUREG-0661.

From the plant unique average submerged pressure and the torus air pressure-time histories, the local average submerged pressure transients at different locations on the shell are calculated using the LDR methodology and the criteria given in NUREG-0661.

In order to perform pool swell analysis of the torus shell and supports, shell loads are divided into static and dynamic components. This is accomplished by subtracting the airspace pressures from the average submerged pressures.

Torus shell loads development procedures, methodology, and assumptions are in accordance with Appendix A of NUREG-0661, with the exception of the download margin. In this case, a more conservative value than that specified in NUREG-0661 was used.

1-4.1.4 Pool Swell Loads on Elevated Structures

This subsection describes the load definition procedures used to define the following hydrodynamic loads on the main vent line and other structures initially above normal water level.

- Pool Swell Impact and Drag Loads
- Froth Impingement Loads, Region I
- Froth Impingement Loads, Region II
- Pool Fallback Loads
- Froth Fallback Loads

Volumes 3 and 4 of this PUAR present the analysis of the effect of pool swell loads on elevated structures.

1-4.1.4.1 Impact and Drag Loads on the Vent System

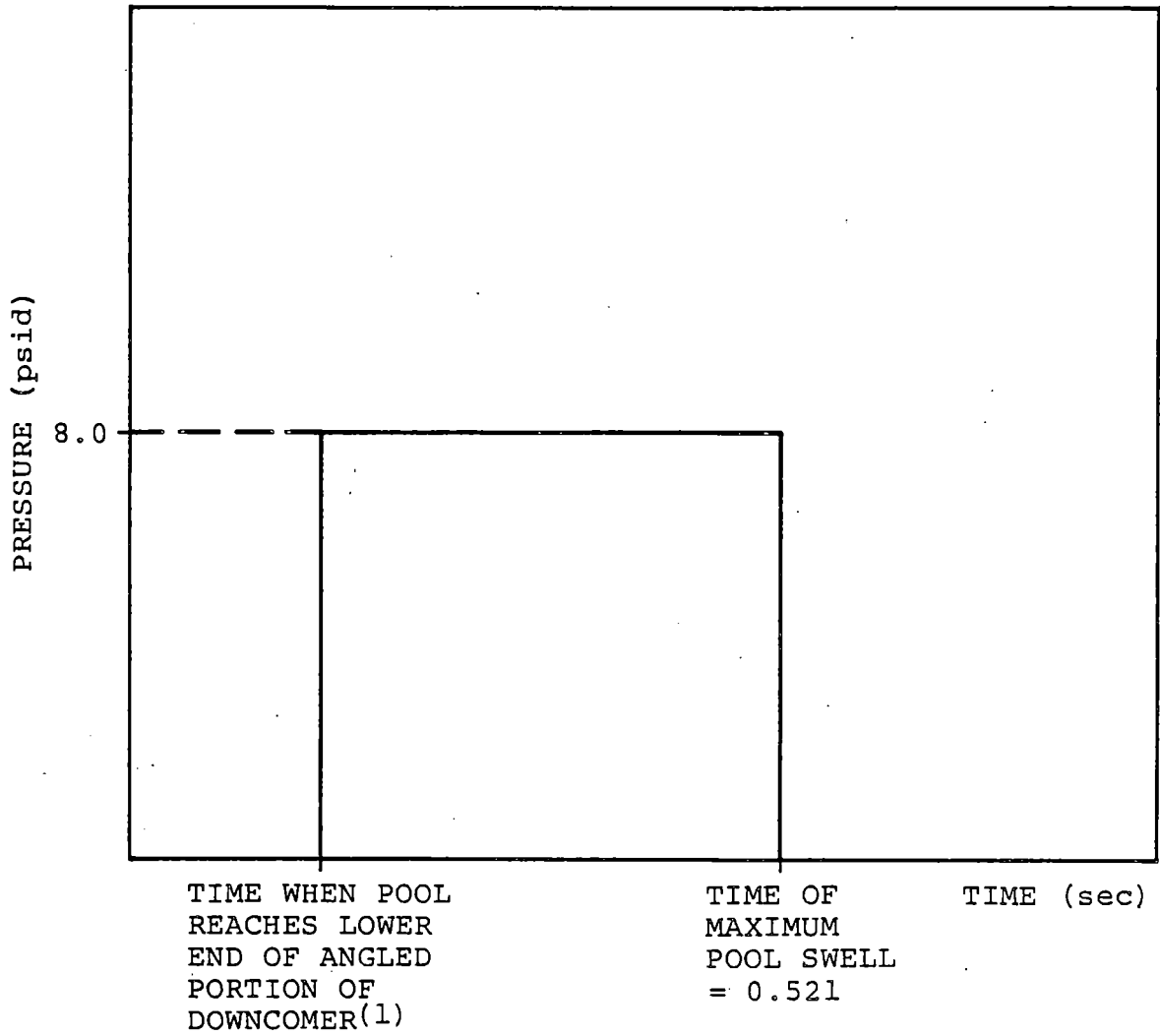
In the event of a postulated design basis LOCA, the pool surface rises during the pool swell phase and impacts structures in its path. The resulting loading condition of primary interest is the impact on the vent system. The impact phenomenon consists of two events: (1) the impact of the pool on the structure, and (2) the drag on the structure as the pool flows past it following impact. The load definition includes both the impact and drag portions of the loading transient.

The vent system components which are potentially impacted during pool swell include the main vents, spherical junctions, vent header, the vent header deflector, and the downcomers. The vent header will experience pool swell impact and drag loads for two reasons: (1) the deflector does not protect the vent header in the vicinity of the spherical junctions, and (2) the pool surface "wraps around" the deflector pipe and partially impacts the vent system. The vent system pool swell impact and drag loads were developed from plant unique quarter-scale tests with a deflector in place (Reference 10).

A generic pressure transient is specified for the downcomers and is assumed to apply uniformly over the bottom 50° of the angled portion of the downcomer. The load amplitude is 8.0 psid and Figures 1-4.1-1 and 1-4.1-2 show how it is applied.

The vent header deflector loads are developed on a plant unique basis. The LDR provides the bases, assumptions, and justifications for vent header deflector impact loads. Reference 9 presents the full-scale loads for the deflector used at Dresden. These loads are based on a zero initial drywell-to-wetwell pressure differential and include the load definition requirements specified in Appendix A of NUREG-0661. These loads are conservatively used for both zero and operating initial drywell-to-wetwell conditions. The vent header deflector load definition is in accordance with Appendix A of NUREG-0661.

Pool swell impact and drag loads on the main vent line and spherical junction are calculated using the procedure specified in Appendix A of NUREG-0661. The pool swell loads on the vent header, the downcomers, and the vent header deflector are also calculated in accordance with Appendix A of NUREG-0661.



(1) THE TIME OF INITIAL IMPACT IS DEPENDENT ON THE DOWNCOMER LOCATION. THESE TIMES ARE PRESENTED IN VOLUME 3.

Figure 1-4.1-1

DOWNCOMER IMPACT AND DRAG PRESSURE TRANSIENT

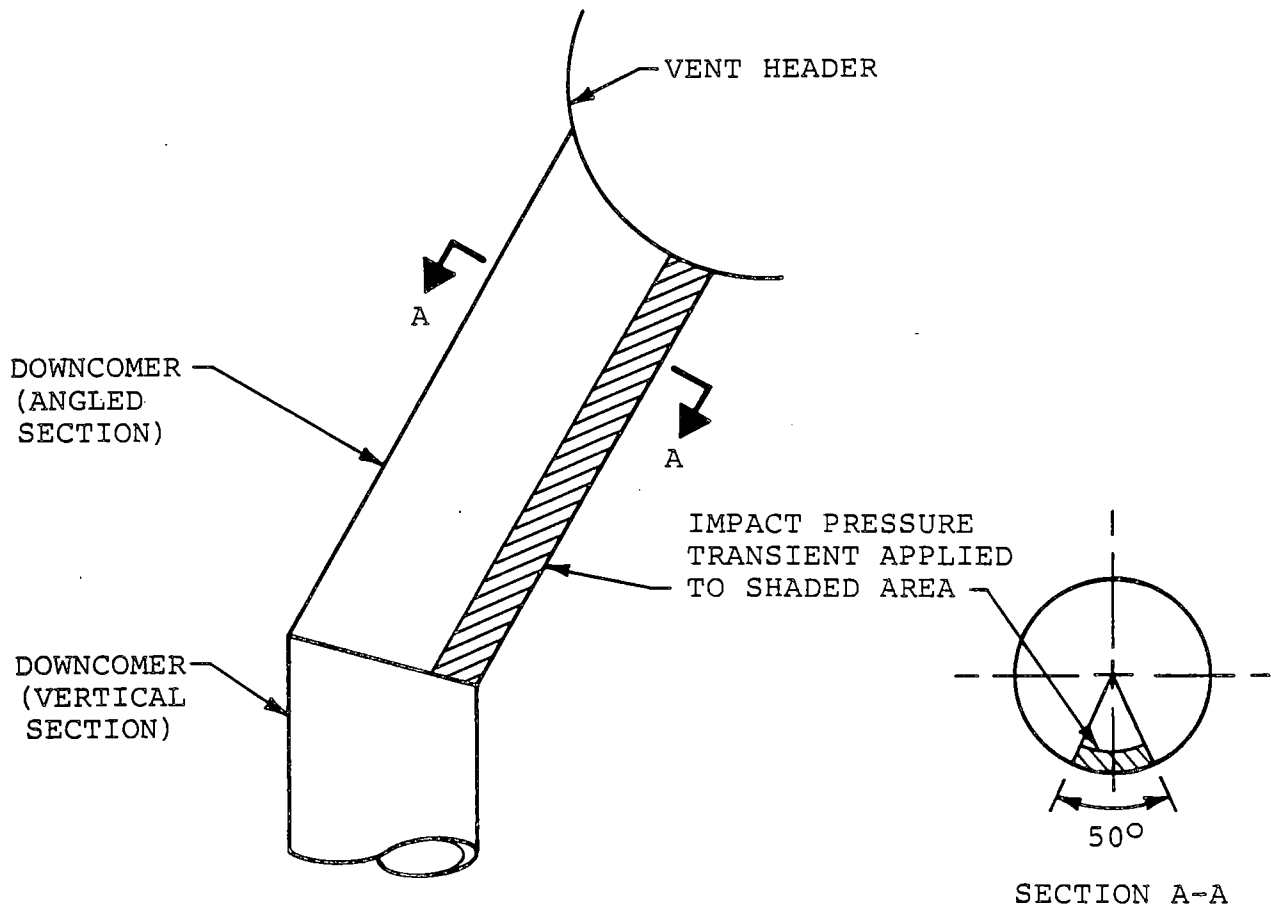


Figure 1-4.1-2
APPLICATION OF IMPACT AND DRAG PRESSURE
TRANSIENT TO DOWNCOMER

COM-02-041-1
 Revision 0

1-4.14

1-4.1.4.2 Impact and Drag Loads on Other Structures

As the pool surface rises due to the bubbles forming at the downcomer exits, it may impact structures located in the wetwell airspace. In the present context, "other structures" are defined as all structures located above the initial pool surface, exclusive of the vent system.

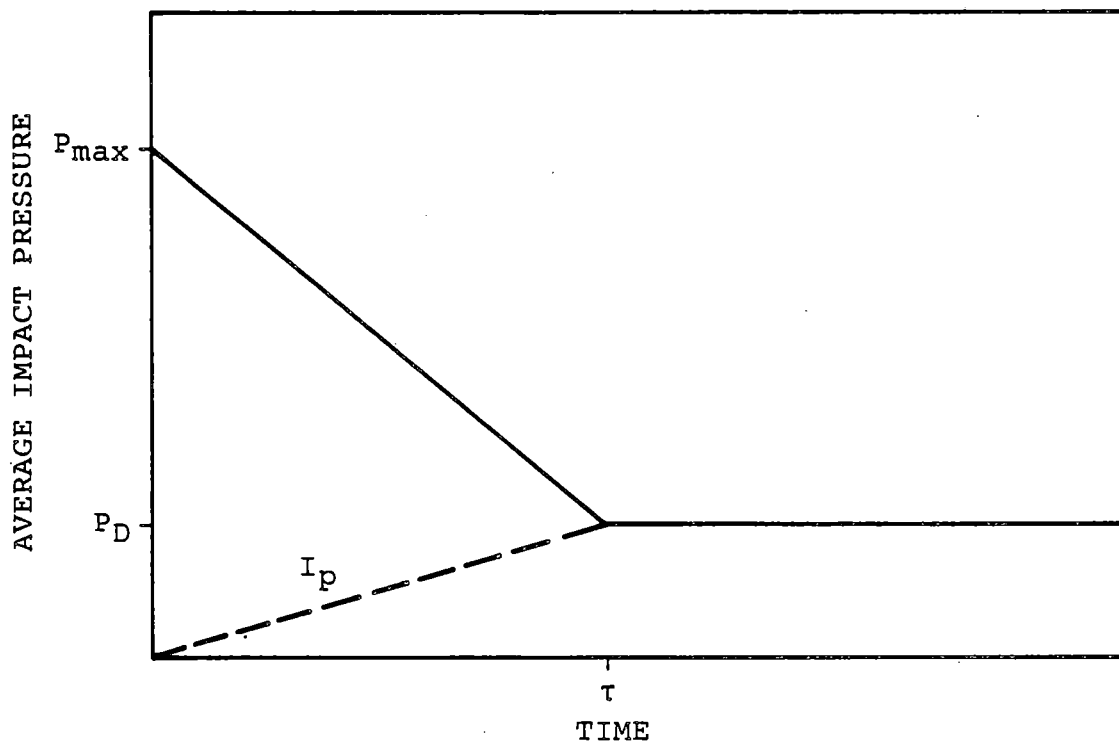
The LDR presents the bases, assumptions, and methodology used in determining the pool swell impact and drag loads on structures located above the pool surface. These load specifications correspond to impact on "rigid" structures. When performing structural dynamic analysis, the "rigid body" impact loads are applied. However, the mass of the impacted structure is adjusted by adding the hydrodynamic mass of impact, except for gratings. The value of hydrodynamic mass is obtained using the methods described in the load definition report.

In performing the structural dynamic analysis, drag following impact is included in the forcing function (Figures 1-4.1-3 and 1-4.1-4). The transient calculation is continued until the maximum stress in the structure is identified.

Impact and drag loads development and application
are in accordance with Appendix A of NUREG-0661.

COM-02-041-1
Revision 0

1-4.16



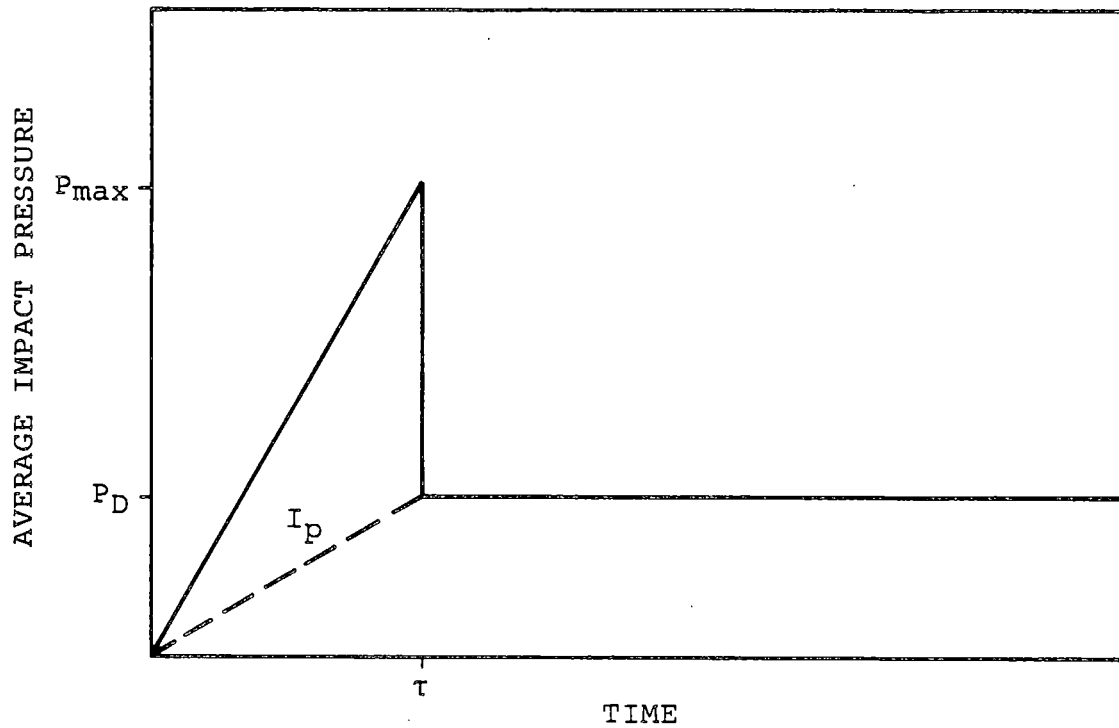
WHERE

I_p = IMPULSE OF IMPACT PER UNIT AREA

τ = PULSE DURATION

Figure 1-4.1-3

PULSE SHAPE FOR WATER IMPACT ON CYLINDRICAL TARGETS



WHERE

I_p = IMPULSE OF IMPACT PER UNIT AREA

τ = PULSE DURATION

Figure 1-4.1-4

PULSE SHAPE FOR WATER IMPACT ON FLAT TARGETS

1-4.1.4.3 Pool Swell Froth Impingement Loads

During the final stages of the pool swell phase of a DBA LOCA, the rising pool breaks up into a two-phase froth of air and water. This froth rises above the pool surface and may impinge on structures within the torus airspace. Subsequently, when the froth falls back, it creates froth fallback loads. Froth may be generated by two mechanisms, described below.

Region I Froth

As the rising pool strikes the bottom of the vent header deflector, a froth spray which travels upward and to both sides of the vent header is formed. This is defined as the Region I froth impingement zone (Figure 1-4.1-5).

Region II Froth

A portion of the water above the expanding air bubble becomes detached from the bulk pool and travels vertically upward. This water is influenced only by its own inertia and gravity. The "bubble breakthrough" creates a froth which rises into the

airspace beyond the maximum bulk pool swell height. This is defined as the Region II froth impingement zone (Figure 1-4.1-6).

The LDR methods are used to define the froth impingement loads for Region I. For the Region I froth formation, the LDR method assumes the froth density to be 20% of full water density for structures with maximum cross-section dimensions of less than 1', and a proportionally lower density for structures greater than 1'. The load is applied as a step function for a duration of 80 milliseconds in the direction most critical to the structure within the region of load application.

The froth density of Region II is assumed to be 100% of water density for structures or sections of structures with a maximum cross-sectional dimension less than or equal to 1', 25% of water density for structures greater than 1', and 10% of water density for structures located within the projected region directly above the vent header. The load is applied as a rectangular pulse with a duration of 100 milliseconds in the direction most critical to the structure within the region of load application.

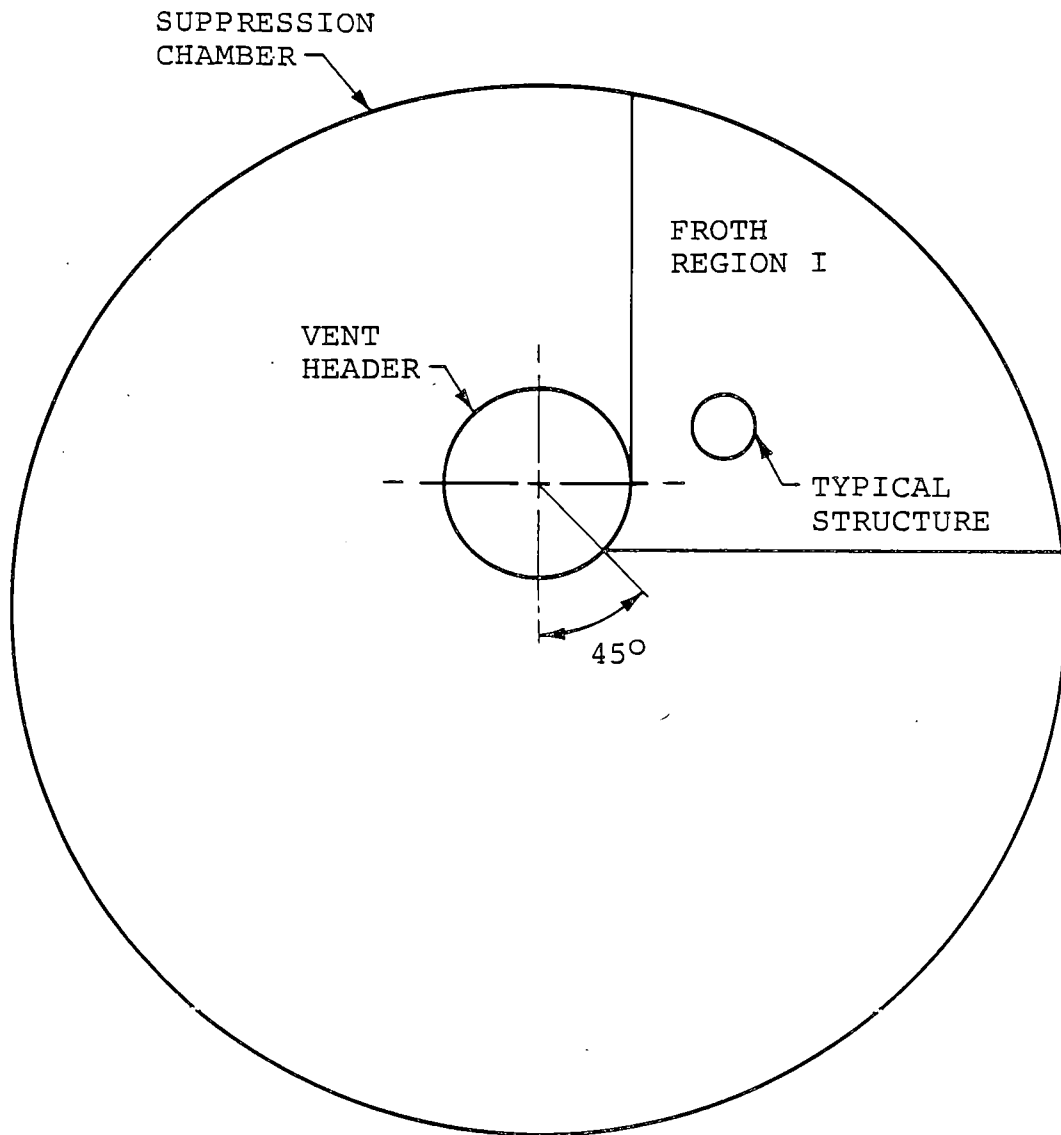
For some structures, the procedures described above result in unrealistically conservative loads. In these situations, the alternate procedure outlined in Appendix A of NUREG-0661 is used. This procedure consists of calculating Region I froth loads from high-speed QSTF movies. In this case, the froth source velocity, mean jet angle, and froth density in Region I are derived from a detailed analysis of the QSTF plant specific high-speed films.

With either methodology for Region I, the vertical component of the source velocity is decelerated to the elevation of the target structure to obtain the froth impingement velocity. The load is applied in the direction most critical to the structure within the sector obtained from QSTF movies. The QSTF movies were used to determine whether a structure had been impinged by Region I froth. Uncertainty limits for each parameter are applied to assure a conservative load specification.

The froth fallback pressure is based on the conservative assumption that all of the froth fallback momentum is transferred to the structure. The froth

velocity is calculated by allowing the froth to fall freely from the height of the upper torus shell directly above the subject structure. The froth fallback pressure is applied uniformly to the upper projected area of the structure being analyzed in the direction most critical to the behavior of the structure. The froth fallback is specified to start when the froth impingement load ends and lasts for 1.0 second. The range of direction of application is downward ± 45 degrees from the vertical.

The pool swell froth impingement and froth fallback loads used in the PUA are in accordance with Appendix A of NUREG-0661.



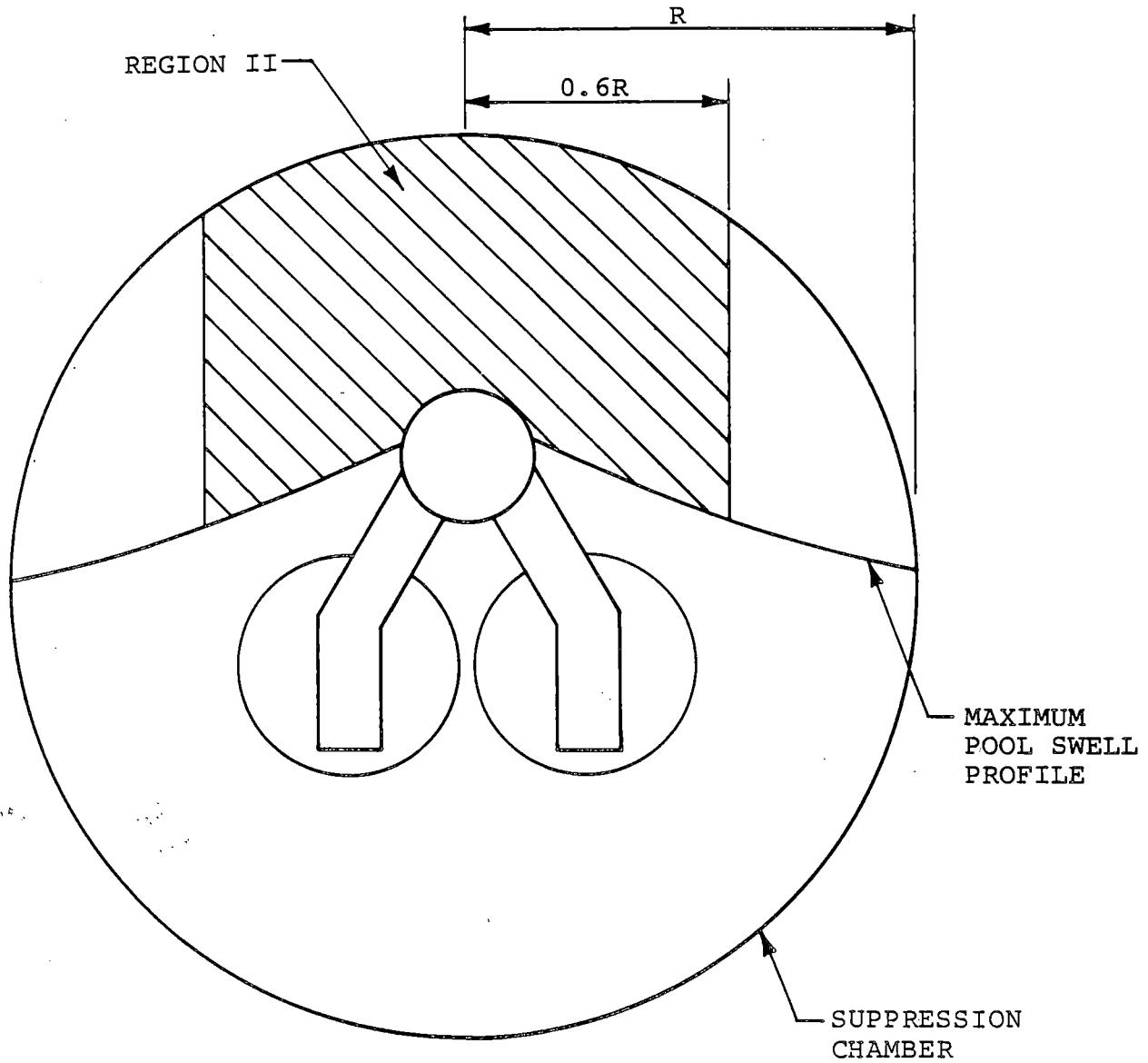
1. REGION IS SYMMETRICAL ON BOTH SIDES OF VENT HEADER.

Figure 1-4.1-5

FROTH IMPINGEMENT ZONE - REGION I

COM-02-041-1
Revision 0

1-4.23



1. REGION IS SYMMETRICAL ON BOTH SIDES OF VENT HEADER.

Figure 1-4.1-6

FROTH IMPINGEMENT ZONE - REGION II

COM-02-041-1
Revision 0

1-4.24

1-4.1.4.4 Pool Fallback Loads

This subsection describes pool fallback loads which apply to structures within the torus that are below the upper surface of the pool at its maximum height and above the downcomer exit level. After the pool surface has reached maximum height as a result of pool swell, it falls back under the influence of gravity and creates drag loads on structures inside the torus shell. The structures affected are between the maximum bulk pool swell height and the downcomer exit level, or immersed in an air bubble extending beneath the downcomer exit level.

For structures immersed in the pool, the drag force during fallback (as described in the LDR) is the sum of standard drag (proportional to the velocity squared) and acceleration drag (proportional to the acceleration). For structures which are beneath the upper surface of the pool but within the air bubble, there is an initial load associated with resubmergence of the structure by either an irregular impact with the bubble-pool interface or a process similar to froth fallback. This initial load is bounded by the standard drag because conservative

assumptions are made in calculating the standard drag.

The load calculation procedure, as described in the LDR, requires determination of the maximum pool swell height above the height of the top surface of the structure. Freefall of the bulk fluid from this height is assumed to occur, producing both standard drag and acceleration drag. The total drag is calculated to be the sum of the two.

The LDR procedure results in a conservative calculation of the velocity since it is unlikely that any appreciable amount of pool fluid will be in freefall through this entire distance. The maximum pool swell height is determined from the QSTF plant unique tests (Reference 10).

The procedures outlined in Appendix A of NUREG-0661 are used to account for interference effects associated with both standard and acceleration drag forces.

Structures which may be enveloped by the LOCA bubble are evaluated for potential fallback loads as a

result of bubble collapse to ensure that such loads are not larger than the LOCA bubble drag loads (Section 1-4.1.6).

The fallback load is applied uniformly over the upper projected surface of the structure in the direction most critical to the behavior of the structure. The range of ± 45 degrees from the vertical is applied to both the radial and longitudinal planes of the torus.

The procedures used to determine pool fallback loads in the PUA are in accordance with Appendix A of NUREG-0661.

As the drywell pressurizes during a postulated DBA LOCA, the water slug initially standing in the submerged portion of the downcomer vents is accelerated downward into the suppression pool. As the water slug enters the pool, it forms a jet which could potentially load structures which are intercepted by the discharge. Forces due to the pool acceleration and velocity induced by the advancing jet front are also included in the analysis.

The LOCA water jet loads affect structures which are enclosed by the jet boundaries and last from the time that the jet first reaches the structure until the last particle of the water slug passes the structure. Pool motion can create loads on structures which are within the region of motion for the duration of the water jet. The assumptions included in the methodology are presented in the load definition report.

The calculation procedure used to obtain LOCA jet loads is based on experimental data obtained from tests performed at the Quarter-Scale Test Facility

(Reference 10) utilizing Dresden plant parameters, which are representative of both Dresden units, and on the analytical model described in Reference 1. Figures 1-4.1-7 and 1-4.1-8 show plant unique downcomer clearing information, obtained experimentally during the QSTF testing in the form of LOCA jet fluid displacement-, velocity-, and acceleration-time histories.

As the jet travels through the pool, the particles at the rear of the water slug, which were discharged from the downcomer at higher velocities, catch up with particles at the front of the water slug, which were discharged at lower velocities. When this "overtaking" occurs, both particles are assumed to continue on at the higher velocity. As the rear particles catch up to the particles in front, the jet becomes shorter and wider. When the last fluid particle leaving the downcomer catches up to the front of the jet, the jet dissipates.

Forces due to pool motion induced by the advancing jet are calculated for structures that are within four downcomer diameters below the downcomer exit elevation. The flow field, standard drag, and

acceleration drag are calculated using the equations in the load definition report.

Structures that are within four downcomer diameters below the downcomer exit elevation will sustain a loading, first from the flow field induced by the jet, then from the jet itself if it is within the cross-section of the jet. Forces resulting from the flow field are due to standard drag and acceleration drag. The force from the jet is due to standard drag only, since particles within the jet travel at a constant discharge velocity (i.e., there is no acceleration).

The standard drag force on the submerged structure is computed based on the normal component of velocity intercepting the structure, the projected area of the structure intercepted by the normal component of velocity, and the jet or flow field area.

For LOCA water jet loads, downcomers are modeled as jet sources for submerged structures based on the location of the structure.

Structures are divided into several sections, following the procedure given in the LDR and the

criteria given in NUREG-0661. For each section, the location, acceleration drag volume, drag coefficient, and orientation are input into the LOCA jet model.

The LOCA water jet loads on circular, cross-sectional structures due to standard and acceleration drag are developed in accordance with Appendix A of NUREG-0661. For structures with sharp corners, these drag loads are calculated considering forces on an equivalent cylinder of diameter $D_{eq} = 2^{1/2} L_{max}$, where L_{max} is the maximum transverse dimension. For acceleration drag, this technique results in unrealistic loads on some structures such as I-beams due to the significant increase in the acceleration drag volume. In these cases, the acceleration drag volumes in Table 1-4.1-1 are used in the acceleration drag load calculation. A literature search concluded that these acceleration drag volumes are appropriate in this application. References 11 and 12 show that the values in this table are applicable for the cases evaluated in this analysis. The LOCA water jet load is a transient load and is therefore applied dynamically.

Table 1-4.1-1

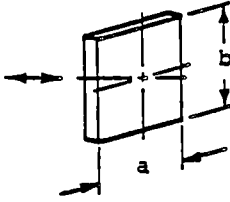
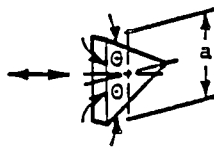

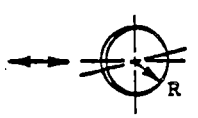
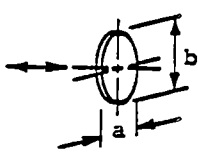
HYDRODYNAMIC MASS AND ACCELERATION DRAG VOLUMES
FOR TWO-DIMENSIONAL STRUCTURAL COMPONENTS
 (LENGTH L FOR ALL STRUCTURES)

BODY	SECTION THROUGH BODY AND UNIFORM FLOW DIRECTION	HYDRODYNAMIC MASS	ACCELERATION DRAG VOLUME V_A	
CIRCLE		$\rho\pi R^2 L$	$2\pi R^2 L$	
ELLIPSE		$\rho\pi a^2 L$	$\pi a(a+b)L$	
ELLIPSE		$\rho\pi b^2 L$	$\pi b(a+b)L$	
PLATE		$\rho\pi a^2 L$	$\pi a^2 L$	
RECTANGLE		$\frac{a}{b}$		
		10	1.14 $\rho\pi a^2 L$	$aL(4b+a)$
		5	1.21 $\rho\pi a^2 L$	$aL(4b+1.14\pi a)$
		2	1.36 $\rho\pi a^2 L$	$aL(4b+1.21\pi a)$
		1	1.51 $\rho\pi a^2 L$	$aL(4b+1.36\pi a)$
		1/2	1.70 $\rho\pi a^2 L$	$aL(4b+1.51\pi a)$
		1/5	1.98 $\rho\pi a^2 L$	$aL(4b+1.70\pi a)$
DIAMOND		$\frac{a}{b}$		
		2	0.85 $\rho\pi a^2 L$	$aL(2b+0.85\pi a)$
		1	0.76 $\rho\pi a^2 L$	$aL(2b+0.76\pi a)$
		1/2	0.67 $\rho\pi a^2 L$	$aL(2b+0.67\pi a)$
I-BEAM		$\frac{a}{c} = 2.6$ $\frac{b}{c} = 3.6$		
		2.11 $\rho\pi a^2 L$	$(2.11\pi a^2 + 2c(2a+b-c))L$	

Table 1-4.1-1

HYDRODYNAMIC MASS AND ACCELERATION DRAG VOLUMES
FOR TWO-DIMENSIONAL STRUCTURAL COMPONENTS
(LENGTH L FOR ALL STRUCTURES)

(Concluded)

BODY	BODY AND FLOW DIRECTION	HYDRODYNAMIC MASS	ACCELERATION DRAG VOLUME V_A
RECTANGULAR PLATE		b/a	
		1 0.478 $\rho\pi a^2 b/4$	$0.478\pi a^2 b/4$
		1.5 0.680 $\rho\pi a^2 b/4$	$0.680\pi a^2 b/4$
		2 0.840 $\rho\pi a^2 b/4$	$0.840\pi a^2 b/4$
		2.5 0.953 $\rho\pi a^2 b/4$	$0.953\pi a^2 b/4$
		3 $\rho\pi a^2 b/4$	$\pi a^2 b/4$
∞ $\rho\pi a^2 b/4$	$\pi a^2 b/4$		
TRIANGULAR PLATE		$\frac{\rho a^3 (\tan \theta)^{3/2}}{3\pi}$	$\frac{a^3 (\tan \theta)^{3/2}}{3\pi}$
SPHERE		$\rho 2\pi R^3/3$	$2\pi R^3/3$
CIRCULAR DISK		$\rho 8R^3/3$	$8R^3/3$
ELLIPTICAL DISK		b/a	
		3 0.9 $\rho\pi b a^2/6$	0.9
		2 0.826 $\rho\pi b a^2/6$	$0.826\pi b a^2/6$
		1.5 0.748 $\rho\pi b a^2/6$	$0.748\pi b a^2/6$
		1.0 0.637 $\rho\pi b a^2/6$	$0.637\pi b a^2/6$

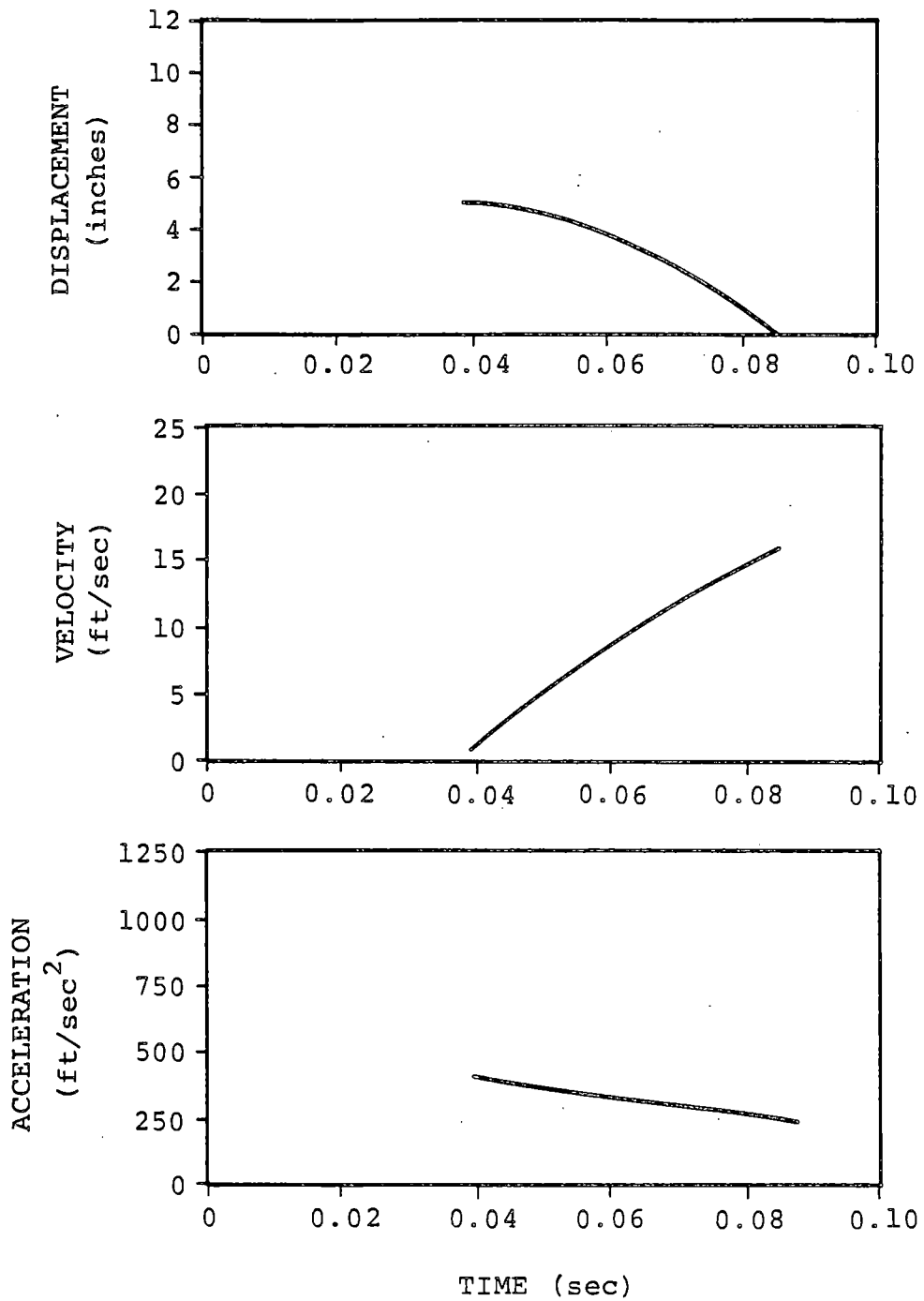


Figure 1-4.1-7

QUARTER-SCALE DOWNCOMER WATER SLUG EJECTION,
DRESDEN, TEST 3 - OPERATING DIFFERENTIAL PRESSURE

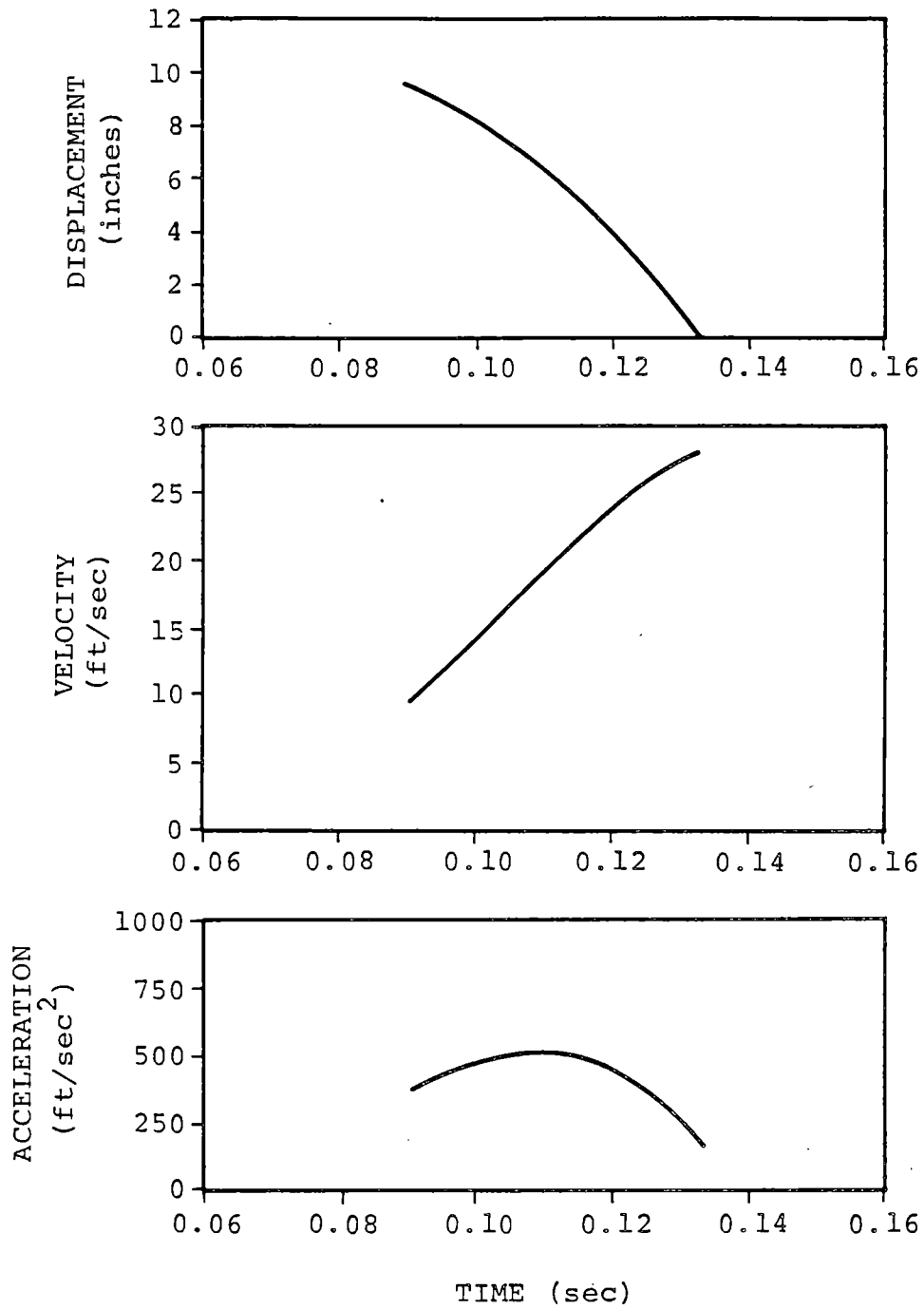


Figure 1-4.1-8

QUARTER-SCALE DOWNCOMER WATER SLUG EJECTION,
DRESDEN, TEST 5 - ZERO DIFFERENTIAL PRESSURE

During the initial phase of the DBA, pressurized drywell air is purged into the suppression pool through the submerged downcomers. After the vent clearing phase of a DBA, a single bubble is formed around each downcomer. During the bubble growth period, unsteady fluid motion is created within the suppression pool. During this period, all submerged structures will be exposed to transient hydrodynamic loads.

The bases of the flow model and load evaluation for the definition of LOCA bubble-induced loads on submerged structures are presented in Section 4.3.8 of the load definition report.

After contact between bubbles of adjacent downcomers, the pool swell flow field above the downcomer exit elevation is derived from OSTF plant unique tests (Reference 10). After bubble contact, the load will act only vertically. This pool swell drag load is computed using the method described in Section 1-4.1.4.2.

The parameters which affect load determination are torus geometry, downcomer locations, and thermodynamic properties. Table 1-4.1-2 presents these plant specific data. Figures 1-4.1-9 and 1-4.1-10 show the DBA plant unique transient drywell pressure-time histories, which are inputs into the model.

The torus is modeled as a rectangular cell with dimensions given in Table 1-4.1-2. The structures are divided into sections and the loads on each section are calculated following the procedure given in the LDR and the criteria given in NUREG-0661.

The procedure used for calculating drag loads on structures with circular and sharp-cornered cross-sections is in accordance with Appendix A of NUREG-0661. For some structures with sharp corners such as I-beams, the acceleration drag volumes are calculated using the information in Table 1-4.1-1.

The LOCA bubble loads are transient loads and are therefore applied dynamically. Volume 4 of the PUAR

presents the plant specific loads for internal structures.

COM-02-041-1
Revision 0

1-4.38

Table 1-4.1-2

PLANT UNIQUE PARAMETERS FOR
LOCA BUBBLE DRAG LOAD DEVELOPMENT - ZERO AND
OPERATING DRYWELL-TO-WETWELL PRESSURE DIFFERENTIAL

PARAMETER		VALUE
NUMBER OF DOWNCOMERS		6 ⁽²⁾
WATER DEPTH IN TORUS (ft)		14.875
CELL	WIDTH (ft)	30.0
	LENGTH (ft)	21.682
VERTICAL DISTANCE FROM DOWNCOMER EXIT TO TORUS CENTERLINE (ft)		4.125
DOWNCOMER	INSIDE RADIUS (ft)	1.00
	SUBMERGENCE (ft)	4.00
UNDISTURBED PRESSURE AT BUBBLE CENTER ELEVATION BEFORE THE BUBBLE APPEARS (psia)		16.67
		17.42 ⁽¹⁾
INITIAL DRYWELL	PRESSURE BEFORE LOCA (psia)	15.5
		15.25 ⁽¹⁾
	TEMPERATURE BEFORE LOCA (°F)	135
OVERALL VENT PIPE LOSS COEFFICIENT		5.17
INITIAL LOCA BUBBLE WALL VELOCITY (ft/sec)		7.83
		13.53 ⁽¹⁾

(1) FOR ZERO PRESSURE DIFFERENTIAL ONLY.

(2) NUMBER OF DOWNCOMERS MODELED DUE TO SYMMETRY.

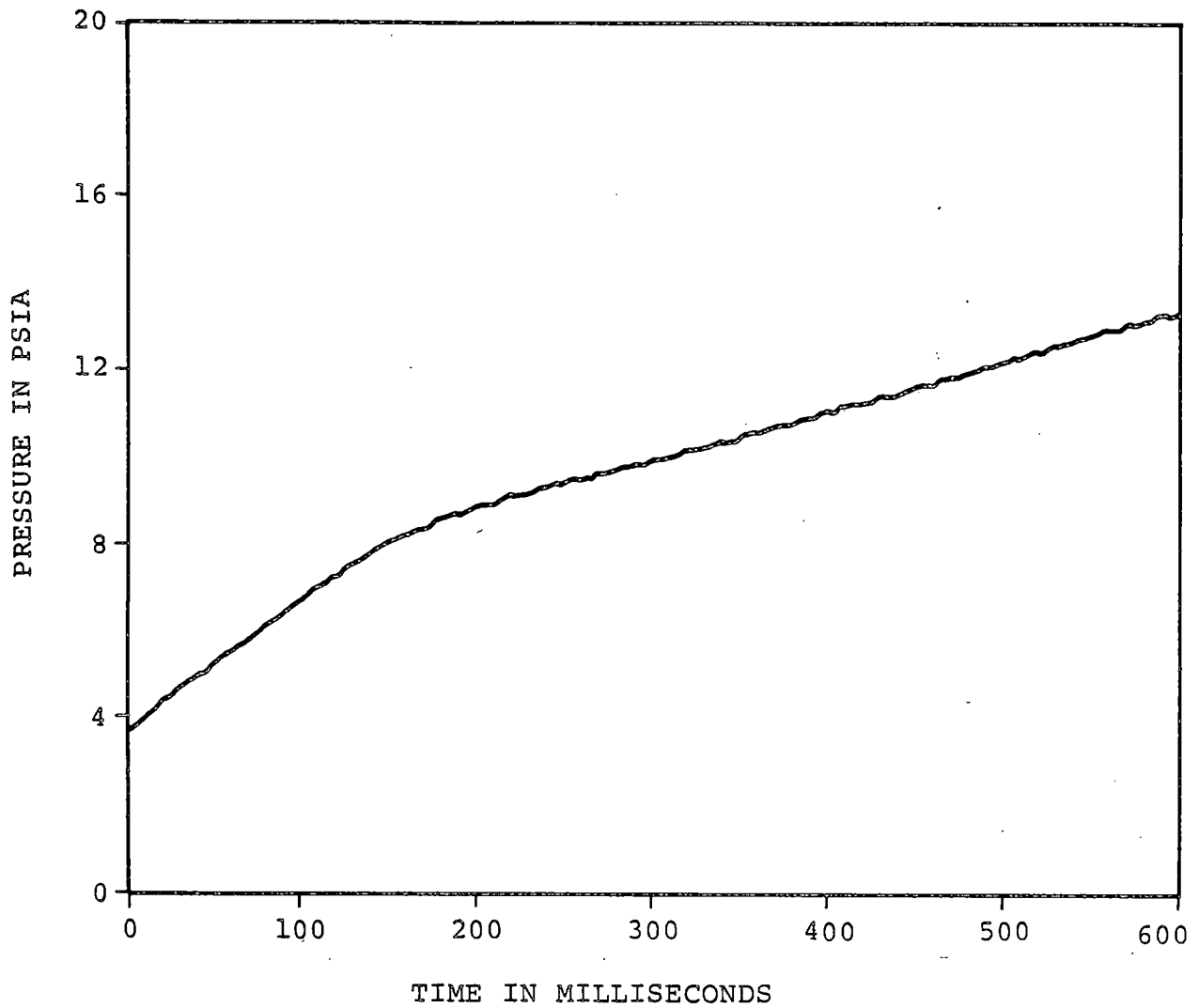


Figure 1-4.1-9

QUARTER-SCALE DRYWELL PRESSURE TIME-HISTORY -
OPERATING DIFFERENTIAL PRESSURE

COM-02-041-1
Revision 0

1-4.40

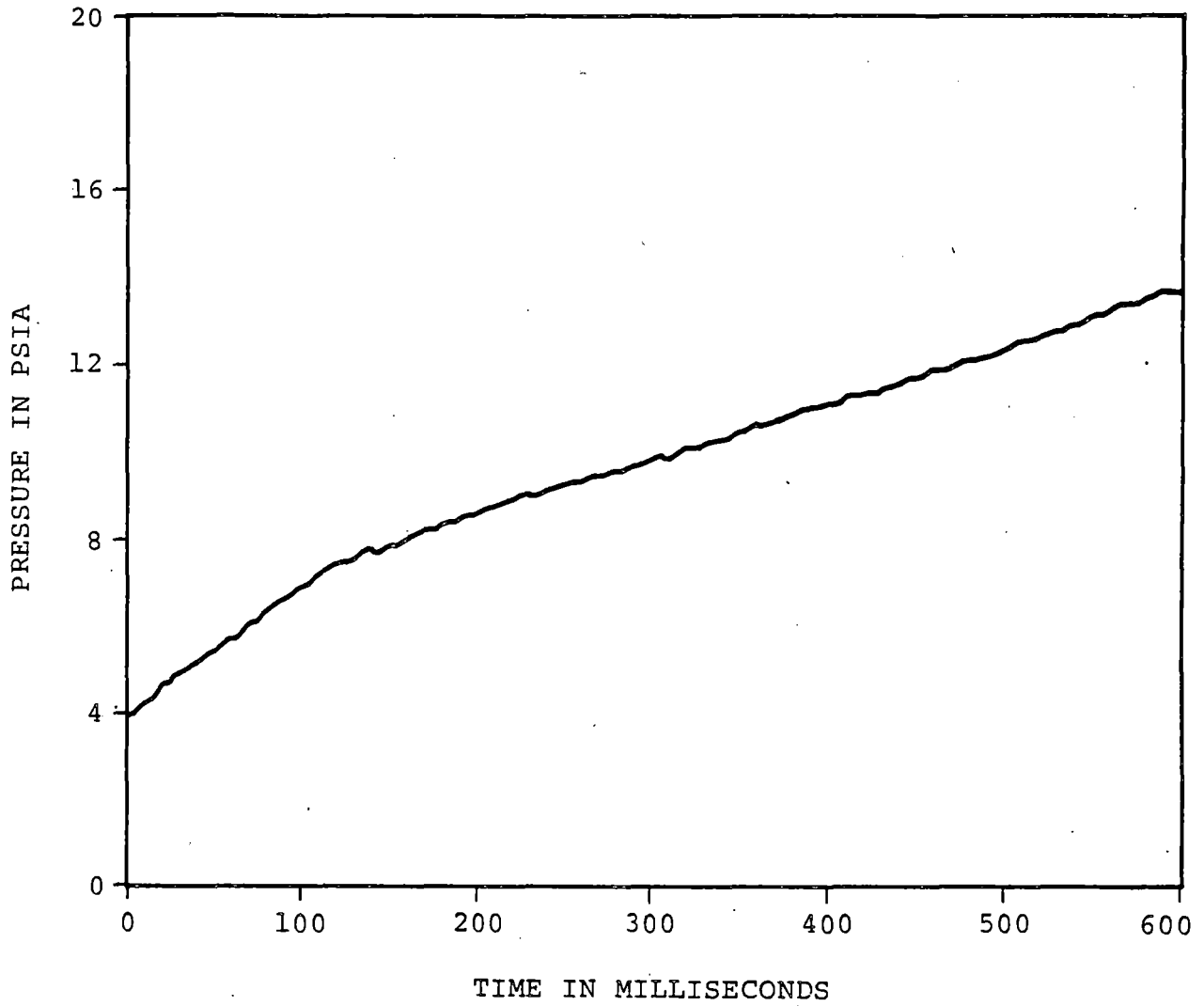


Figure 1-4.1-10

QUARTER-SCALE DRYWELL PRESSURE
TIME-HISTORY - ZERO DIFFERENTIAL PRESSURE

COM-02-041-1
Revision 0

1-4.41

1-4.1.7 Condensation Oscillation Loads

This subsection describes the CO loads on the various structures and components in the suppression chamber.

Following the pool swell transient of a postulated LOCA, there is a period during which condensation oscillations occur at the downcomer exit. Condensation oscillations are associated with the pulsating movement of the steam-water interface, caused by variations in the condensation rate at the downcomer exit. These condensation oscillations cause periodic pressure oscillations on the torus shell, submerged structures, and in the vent system. The loads specified for CO are based on the FSTF tests (References 13, 14, and 15). The LDR and NUREG-0661 discuss the bases, assumptions, and methodology for computation of the CO loads.

1-4.1.7.1 CO Loads on the Torus Shell

Loads on the submerged portion of the torus shell during the CO phenomenon consist of pressure oscillations superimposed on the prevailing local static pressures.

The CO load on the torus shell is a rigid wall load specified in terms of the pressure at the torus bottom dead center. It is used in conjunction with a flexible wall coupled fluid-structure torus model. The LDR load definition for CO consists of 50 harmonic loadings with amplitudes which vary with frequency. Three alternate rigid wall pressure amplitude variations in the range of 4 to 16 hertz are specified in the load definition report. A fourth alternate load case is also considered, based on the results of Test M12 from the supplemental test series conducted at the FSTF (References 14 and 15). Table 1-4.1-3 and Figure 1-4.1-11 give the rigid wall pressure amplitude variation with frequency. The alternate frequency spectrum which produces the maximum total response is used for analysis.

The effects of all harmonics must be summed to obtain the total response of the structure. Random phasing of the loading harmonics is assumed, based on experimental observations and subsequent analysis.

The implementation of the random phasing approach for the structural evaluation is accomplished by multiplying the absolute sum of the responses of all 50 harmonics by a scale factor. This scale factor is calculated using cumulative distribution function (CDF) curves of the responses at 14 locations on the FSTF torus shell. Each of the CDF curves is generated using 200 sets of random phase angles. Using this approach, a scale factor of 0.65 is developed which results in a nonexceedance probability (NEP) of 84% at a confidence level of 90% (Table 1-4.1-4). This scale factor is applied to the absolute sum of the responses of all 50 harmonics for all Dresden Units 2 and 3 torus shell locations evaluated.

The implementation of the random phasing approach for TAP is accomplished by using a set of random phase angles for all 50 harmonics. The effects of each harmonic loading are summed to obtain the total

response. This response is then multiplied by a scale factor to reach the desired non-exceedance probability. For CO Load Alternates 1, 2 and 3, a scale factor of 1.3 is used to yield an 84% NEP at a confidence level of 90%. For Alternate 4, a scale factor of 1.15 is used to yield a 50% NEP at a confidence level of 90%.

Table 1-4.1-4 compares measured and calculated FSTF response to CO loads. The calculated FSTF response in this table is determined using CO Load Alternates 1, 2, and 3 and the random phasing approach described above. The calculated response is greater than the measured response in all cases, demonstrating the conservatism of this approach. Although not shown in Table 1-4.1-4, CO Load Alternate 4 adds approximately 20% to the calculated shell response. Thus, using Alternate 4 in the Dresden Units 2 and 3 analysis contributes additional conservatism to the comparison shown in Table 1-4.1-4. This is due to the calculated response for Alternates 1, 2, and 3 already bounding the measured response for Alternate 4, which uses M12.

Table 1-4.1-5 specifies the onset times and durations for condensation oscillation. Test results

indicate that for the postulated IBA, CO loads are bounded by chugging loads. Test results also indicate that for the postulated SBA, CO loads are not significant; therefore, none is specified.

The longitudinal CO pressure distribution along the torus centerline is uniform. The cross-sectional variation of the torus wall pressure varies linearly with elevation, from zero at the water surface to the maximum at the torus bottom (Figure 1-4.1-12).

Since torus dimensions and the number of downcomers vary, the magnitude of the CO load differs for each Mark I plant. A multiplication factor was developed to account for the effect of the pool-to-vent area ratio. This factor is 0.98 for Dresden Units 2 and 3 and was developed using the method described in the LDR (Figures 1-4.1-12 and 1-4.1-13). The Dresden plant unique CO load is determined by multiplying the amplitude of the baseline rigid wall load (Table 1-4.1-3) by this factor. Since this factor is close to unity, a factor of 1.0 was conservatively used.

Table 1-4.1-3

DBA CONDENSATION OSCILLATION TORUS
SHELL PRESSURE AMPLITUDES

FREQUENCY INTERVALS (Hz)	MAXIMUM PRESSURE AMPLITUDE (psi)			
	ALTERNATE 1	ALTERNATE 2	ALTERNATE 3	ALTERNATE 4
0-1	0.29	0.29	0.29	0.25
1-2	0.25	0.25	0.25	0.28
2-3	0.32	0.32	0.32	0.33
3-4	0.48	0.48	0.48	0.56
4-5	1.86	1.20	0.24	2.71
5-6	1.05	2.73	0.48	1.17
6-7	0.49	0.42	0.99	0.97
7-8	0.59	0.38	0.30	0.47
8-9	0.59	0.38	0.30	0.34
9-10	0.59	0.38	0.30	0.47
10-11	0.34	0.79	0.18	0.49
11-12	0.15	0.45	0.12	0.38
12-13	0.17	0.12	0.11	0.20
13-14	0.12	0.08	0.08	0.10
14-15	0.06	0.07	0.03	0.11
15-16	0.10	0.10	0.02	0.08
16-17	0.04	0.04	0.04	0.04
17-18	0.04	0.04	0.04	0.05
18-19	0.04	0.04	0.04	0.03
19-20	0.27	0.27	0.27	0.34
20-21	0.20	0.20	0.20	0.23
21-22	0.30	0.30	0.30	0.49
22-23	0.34	0.34	0.34	0.37
23-24	0.33	0.33	0.33	0.31
24-25	0.16	0.16	0.16	0.22

Table 1-4.1-3

DBA CONDENSATION OSCILLATION TORUSSHELL PRESSURE AMPLITUDES

(Concluded)

FREQUENCY INTERVALS (Hz)	MAXIMUM PRESSURE AMPLITUDE (psi)			
	ALTERNATE 1	ALTERNATE 2	ALTERNATE 3	ALTERNATE 4
25-26	0.25	0.25	0.25	0.50
26-27	0.58	0.58	0.58	0.51
27-28	0.13	0.13	0.13	0.39
28-29	0.19	0.19	0.19	0.27
29-30	0.14	0.14	0.14	0.09
30-31	0.08	0.08	0.08	0.08
31-32	0.03	0.03	0.03	0.07
32-33	0.03	0.03	0.03	0.05
33-34	0.03	0.03	0.03	0.04
34-35	0.05	0.05	0.05	0.04
35-36	0.08	0.08	0.08	0.07
36-37	0.10	0.10	0.10	0.11
37-38	0.07	0.07	0.07	0.06
38-39	0.06	0.06	0.06	0.05
39-40	0.09	0.09	0.09	0.03
40-41	0.33	0.33	0.33	0.08
41-42	0.33	0.33	0.33	0.19
42-43	0.33	0.33	0.33	0.19
43-44	0.33	0.33	0.33	0.13
44-45	0.33	0.33	0.33	0.18
45-46	0.33	0.33	0.33	0.30
46-47	0.33	0.33	0.33	0.18
47-48	0.33	0.33	0.33	0.19
48-49	0.33	0.33	0.33	0.17
49-50	0.33	0.33	0.33	0.21

Table 1-4.1-4

FSTF RESPONSE TO CONDENSATION OSCILLATION

RESPONSE QUANTITY	CALCULATED FSTF RESPONSE AT 84% NEP(1)	MAXIMUM MEASURED FSTF RESPONSE		
		M8	M11B	M12
BOTTOM DEAD CENTER AXIAL STRESS (ksi)	3.0	2.3	1.6	2.7
BOTTOM DEAD CENTER HOOP STRESS (ksi)	3.7	2.6	1.4	2.9
BOTTOM DEAD CENTER DISPLACEMENT (in)	0.17	0.11	0.08	0.14
INSIDE COLUMN FORCE (kips)	184	93	68	109
OUTSIDE COLUMN FORCE (kips)	208	110	81	141

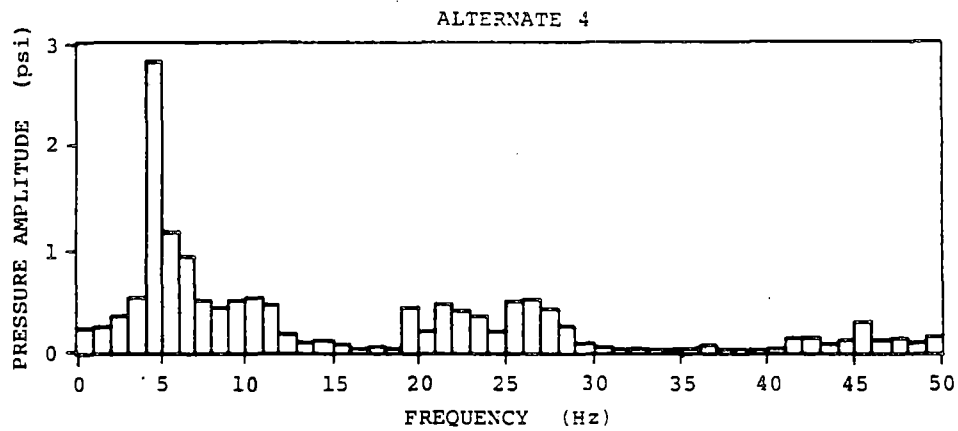
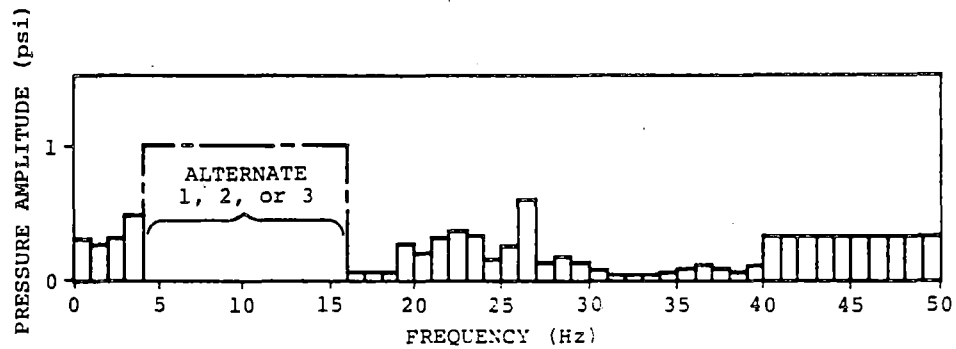
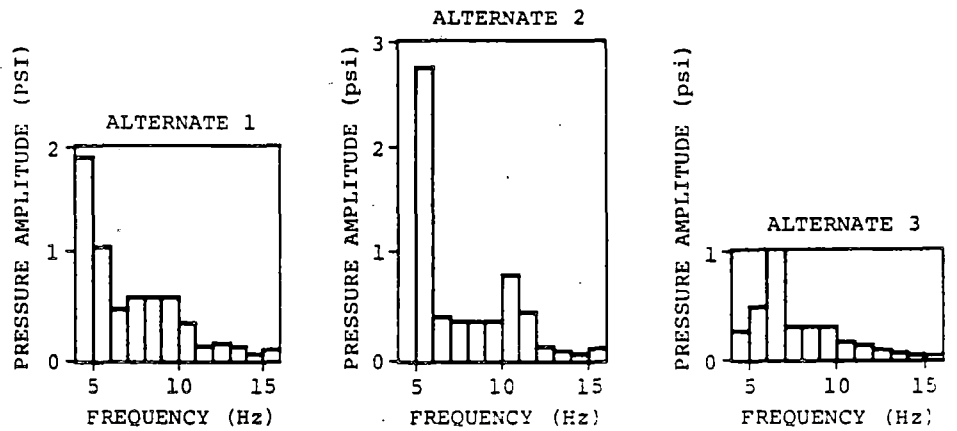
(1) USING CO LOAD ALTERNATES 1, 2, AND 3.

Table 1-4.1-5

CONDENSATION OSCILLATION ONSET AND DURATION

BREAK SIZE	ONSET TIME AFTER BREAK	DURATION AFTER ONSET
DBA	5 SECONDS	30 SECONDS
IBA	5 SECONDS ⁽¹⁾	300 SECONDS ⁽¹⁾
SBA	NOT APPLICABLE	NOT APPLICABLE

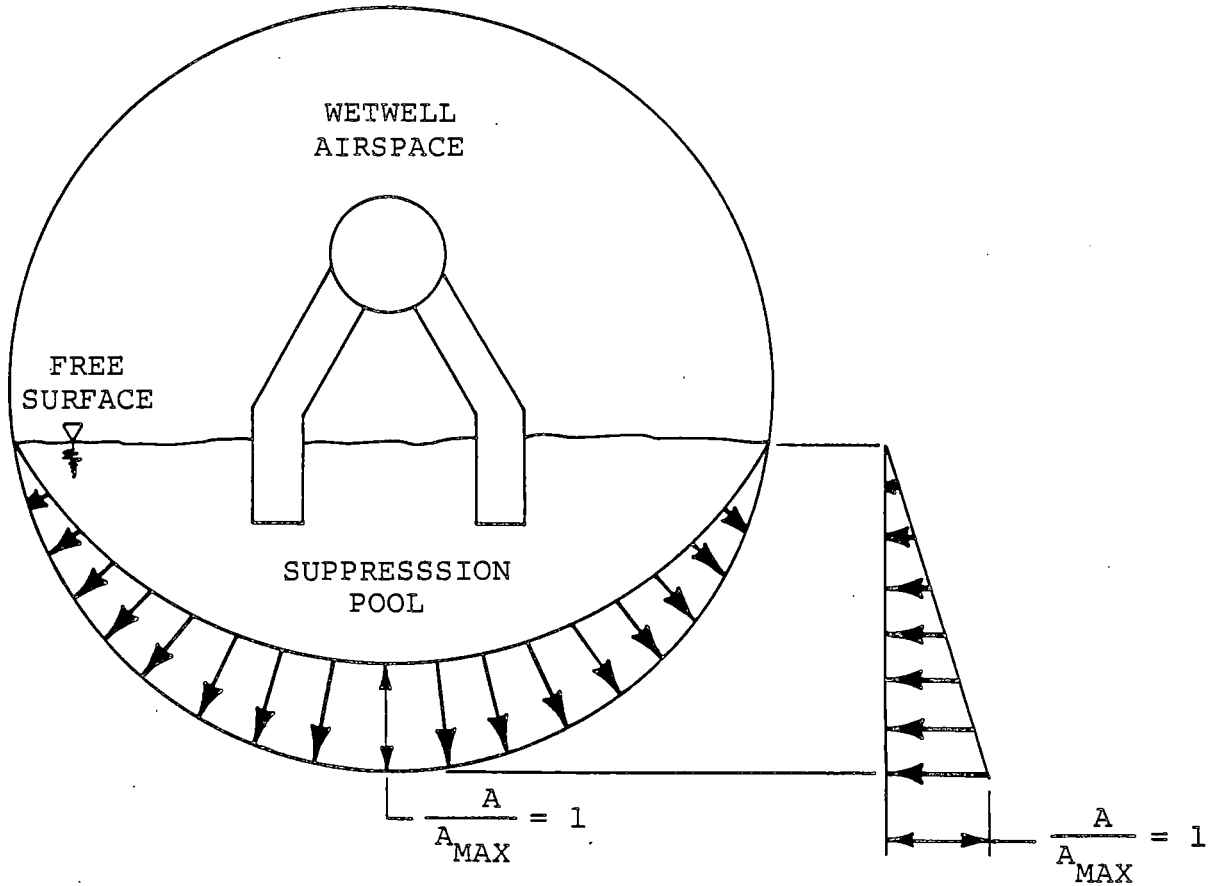
1. FOR THE IBA, CHUGGING LOADS AS DEFINED IN SECTION 1-4.1.8.2 ARE USED.



ALL AMPLITUDES REPRESENT ONE-HALF OF THE PEAK-TO-PEAK AMPLITUDE.

Figure 1-4.1-11

CONDENSATION OSCILLATION BASELINE RIGID WALL PRESSURE
AMPLITUDES ON TORUS SHELL BOTTOM DEAD CENTER



1. A = LOCAL PRESSURE OSCILLATION AMPLITUDE.
2. A_{MAX} = MAXIMUM PRESSURE OSCILLATION AMPLITUDE (AT TORUS BOTTOM DEAD CENTER).

Figure 1-4.1-12

MARK I CONDENSATION OSCILLATION -
TORUS VERTICAL CROSS-SECTIONAL DISTRIBUTION
FOR PRESSURE OSCILLATION AMPLITUDE

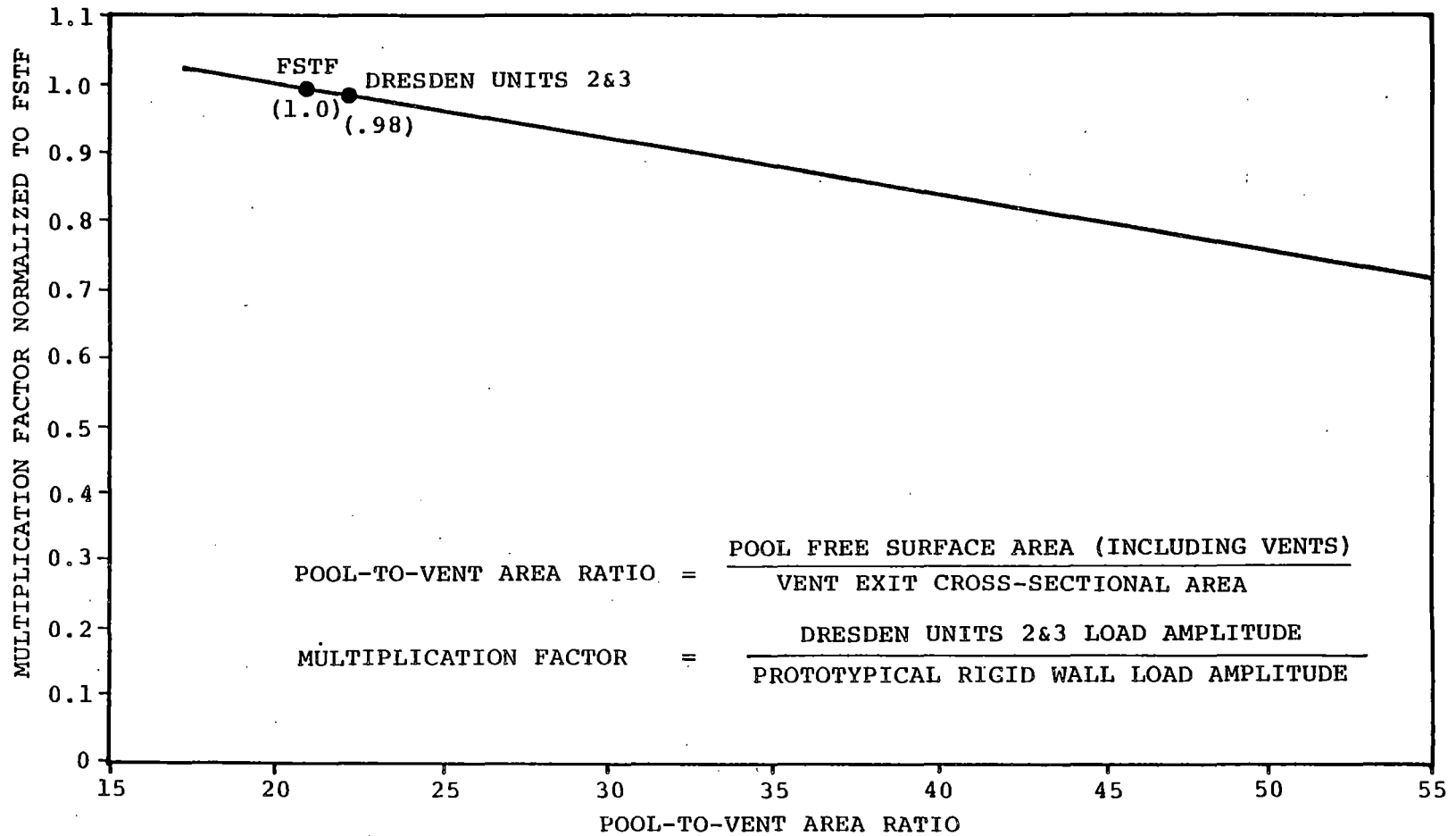


Figure 1-4.1-13

MARK I CONDENSATION OSCILLATION - MULTIPLICATION FACTOR TO
ACCOUNT FOR THE EFFECT OF THE POOL-TO-VENT AREA RATIO

1-4.1.7.2 CO Loads on the Downcomer and Vent System

Downcomer Dynamic Loads

The downcomers experience loading during the CO phase of a blowdown. The procedure for defining the dynamic portion of this loading for both a DBA and an IBA is presented in this section. Condensation oscillation loads do not occur for the SBA. The bases, assumptions, and loading definition details are presented in the load definition report.

The downcomer dynamic load involves two components:

- (1) an internal pressure load of equal magnitude in each downcomer in a pair, and
- (2) a differential pressure load between downcomers in a pair.

Both the internal pressure load and the differential pressure load have three frequency bands over which they are applied. Figure 1-4.1-14 shows a typical downcomer and a schematic of downcomer loading conditions during the CO phase of a blowdown.

Table 1-4.1-6 lists the downcomer internal pressure loads for the DBA CO period. Figure 1-4.1-15 shows the internal pressure load and the three frequency bands over which it is applied. The dominant downcomer frequency is determined from a harmonic analysis, where the dominant downcomer frequency is shown to occur in the frequency range of the second CO downcomer load harmonic (see Volume 3). The first and third CO downcomer load harmonics are therefore applied at frequencies equal to 0.5 and 1.5 times the value of the dominant downcomer frequency.

Table 1-4.1-7 defines the downcomer differential pressure loads for the DBA CO period. Application of the dominant harmonic differential pressures is the same as for the internal pressure application previously discussed. Figure 1-4.1-16 shows the differential pressure amplitudes and frequency ranges.

Figure 1-4.1-17 shows how the downcomer CO dynamic loads are applied to the different downcomer pairs on the Dresden Units 2 and 3 vent header system. The total response of the downcomer-vent header

intersection to the CO dynamic load is the sum of the responses from the internal and differential pressure components. All eight load cases are evaluated, and the case with the maximum response is used for analysis.

Table 1-4.1-8 provides the downcomer internal pressure loads for the IBA CO period. Figure 1-4.1-18 shows these downcomer internal pressure load values and the range of application. Table 1-4.1-9 gives the downcomer differential pressure loads for the IBA CO period. The procedure used to evaluate the IBA CO downcomer loads is the same as that used for the DBA CO downcomer loads. The load cases for the IBA loads are also the same as for the DBA loads; therefore, Figure 1-4.1-17 is used.

Vent System Loads

Loads on the vent system during the CO phenomenon result from harmonic pressure oscillations superimposed on the prevailing local static pressures in the vent system.

Condensation oscillation loads are specified for all three major components of the vent system: (1) the main vents, (2) the vent header, and (3) the downcomers (Table 1-4.1-10). As determined from FSTF data, these loads are generic and thus directly applicable to all Mark I plants.

In addition to the oscillating pressure described above, a uniform static pressure is applied to the main vents, vent header, and the downcomers to account for the nominal submergence of the downcomers.

Table 1-4.1-6

DOWNCOMER INTERNAL PRESSURE LOADS
FOR DBA CONDENSATION OSCILLATION

FREQUENCY	PRESSURE (psi)	APPLIED FREQUENCY RANGE (Hz)
DOMINANT	3.6	4-8
SECOND HARMONIC	1.3	8-16
THIRD HARMONIC	0.6	12-24

Table 1-4.1-7

DOWNCOMER DIFFERENTIAL PRESSURE LOADS FOR DBA
CONDENSATION OSCILLATION

FREQUENCY	PRESSURE (psi)	APPLIED FREQUENCY RANGE (Hz)
DOMINANT	2.85	4-8
SECOND HARMONIC	2.6	8-16
THIRD HARMONIC	1.2	12-24

Table 1-4.1-8

DOWNCOMER INTERNAL PRESSURE LOADS FOR IBA
CONDENSATION OSCILLATION

FREQUENCY	PRESSURE (psi)	APPLIED FREQUENCY RANGE (Hz)
DOMINANT	1.1	6-10
SECOND HARMONIC	0.8	12-20
THIRD HARMONIC	0.2	18-30

Table 1-4.1-9

DOWNCOMER DIFFERENTIAL PRESSURE LOADS FOR IBA
CONDENSATION OSCILLATION

FREQUENCY	PRESSURE (psi)	APPLIED FREQUENCY RANGE (Hz)
DOMINANT	0.2	6-10
SECOND HARMONIC	0.2	12-20
THIRD HARMONIC	0.2	18-30

Table 1-4.1-10

CONDENSATION OSCILLATION LOADS
ON THE VENT SYSTEM

COMPONENTS		DBA	IBA
MAIN VENT AND VENT HEADER	AMPLITUDE	±2.5 psi	±2.5 psi
	FREQUENCY RANGE	AT FREQUENCY OF MAXIMUM RESPONSE IN 4-8 Hz RANGE	AT FREQUENCY OF MAXIMUM RESPONSE IN 6-10 Hz RANGE
	FORCING FUNCTION	SINUSOIDAL	SINUSOIDAL
	SPATIAL DISTRIBUTION	UNIFORM	UNIFORM
DOWNCOMERS	AMPLITUDE	±5.5 psi	±2.1 psi
	FREQUENCY RANGE	AT FREQUENCY OF MAXIMUM RESPONSE IN 4-8 Hz RANGE	AT FREQUENCY OF MAXIMUM RESPONSE IN 6-10 Hz RANGE
	FORCING FUNCTION	SINUSOIDAL	SINUSOIDAL
	SPATIAL DISTRIBUTION	UNIFORM	UNIFORM

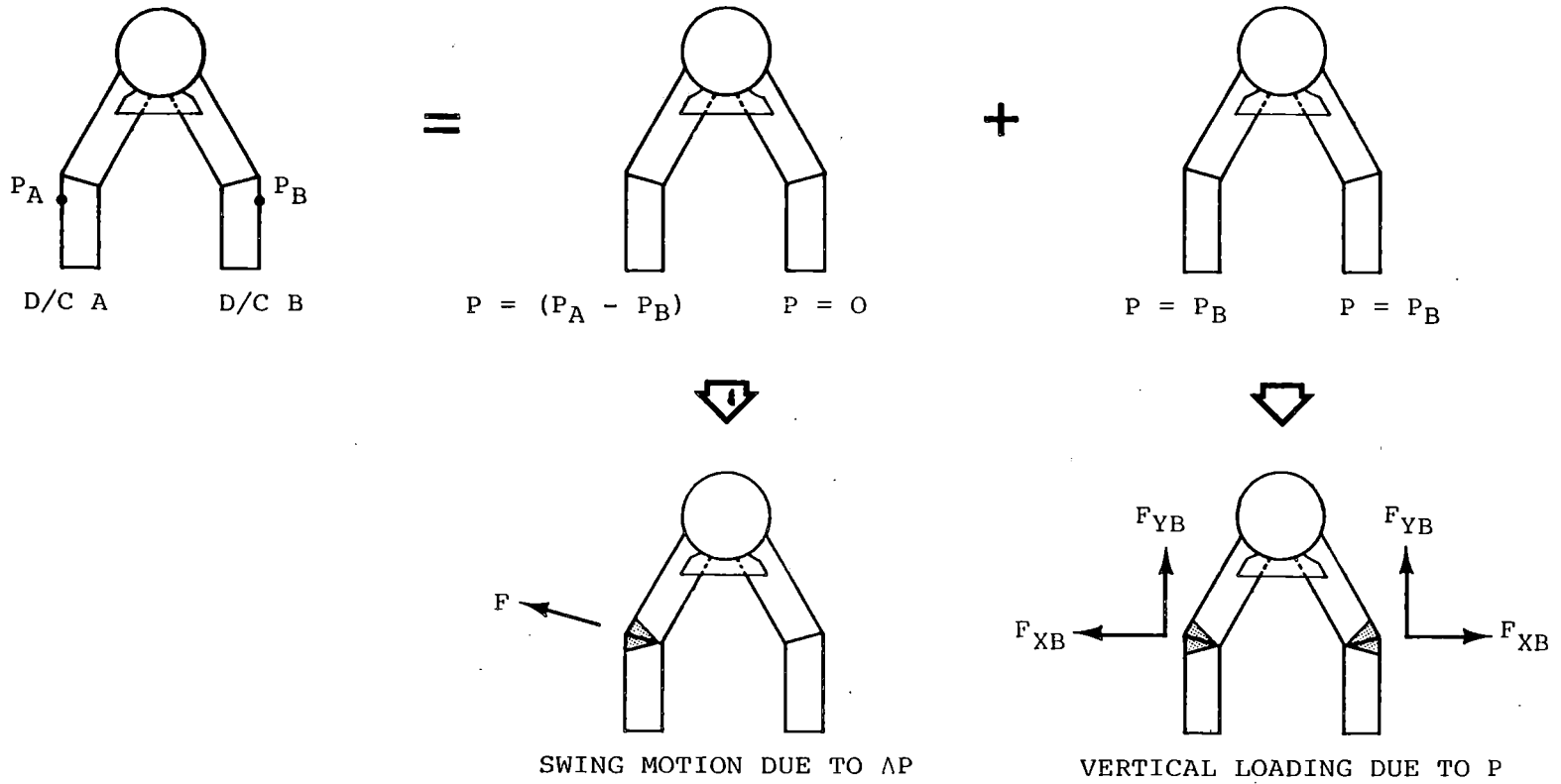
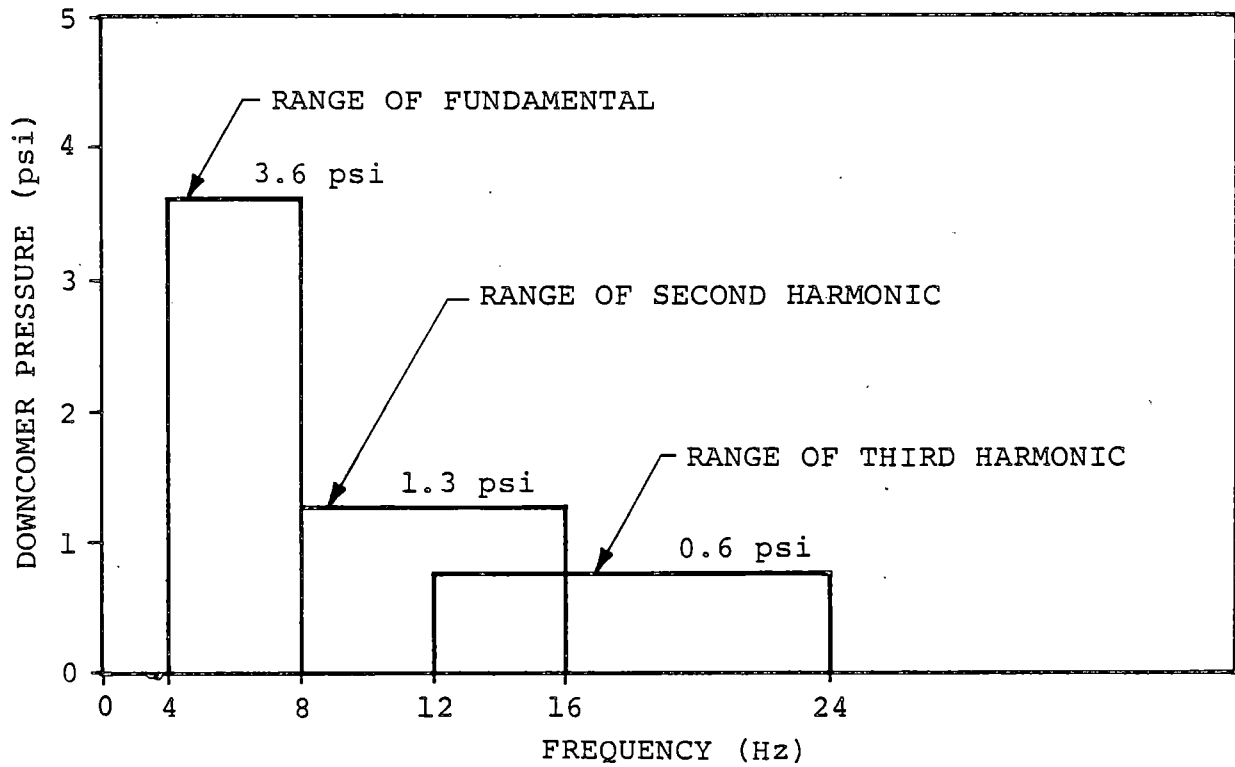


Figure 1-4.1-14

DOWNCOMER DYNAMIC LOAD



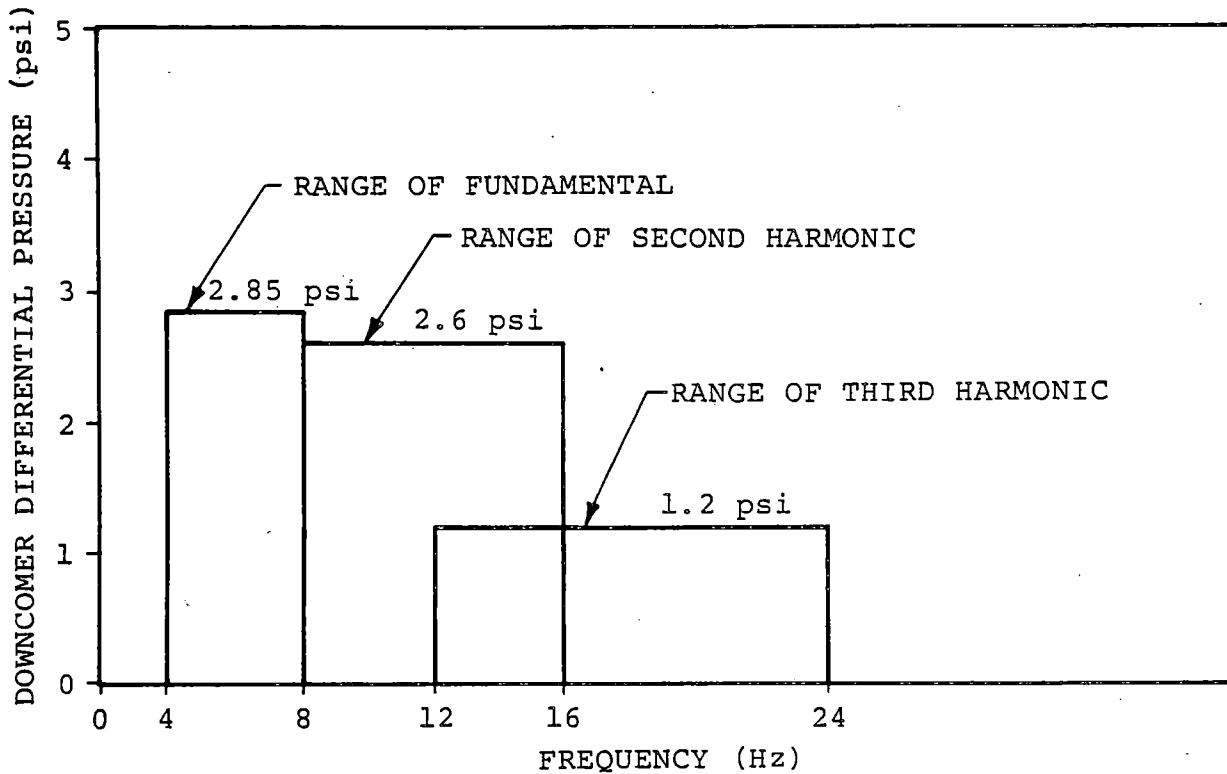
1. THE AMPLITUDES SHOWN ARE HALF-RANGE (ONE-HALF OF THE PEAK-TO-PEAK VALUE).

Figure 1-4.1-15

DOWNCOMER PAIR INTERNAL PRESSURE LOADING FOR DBA CO

COM-02-041-1
Revision 0

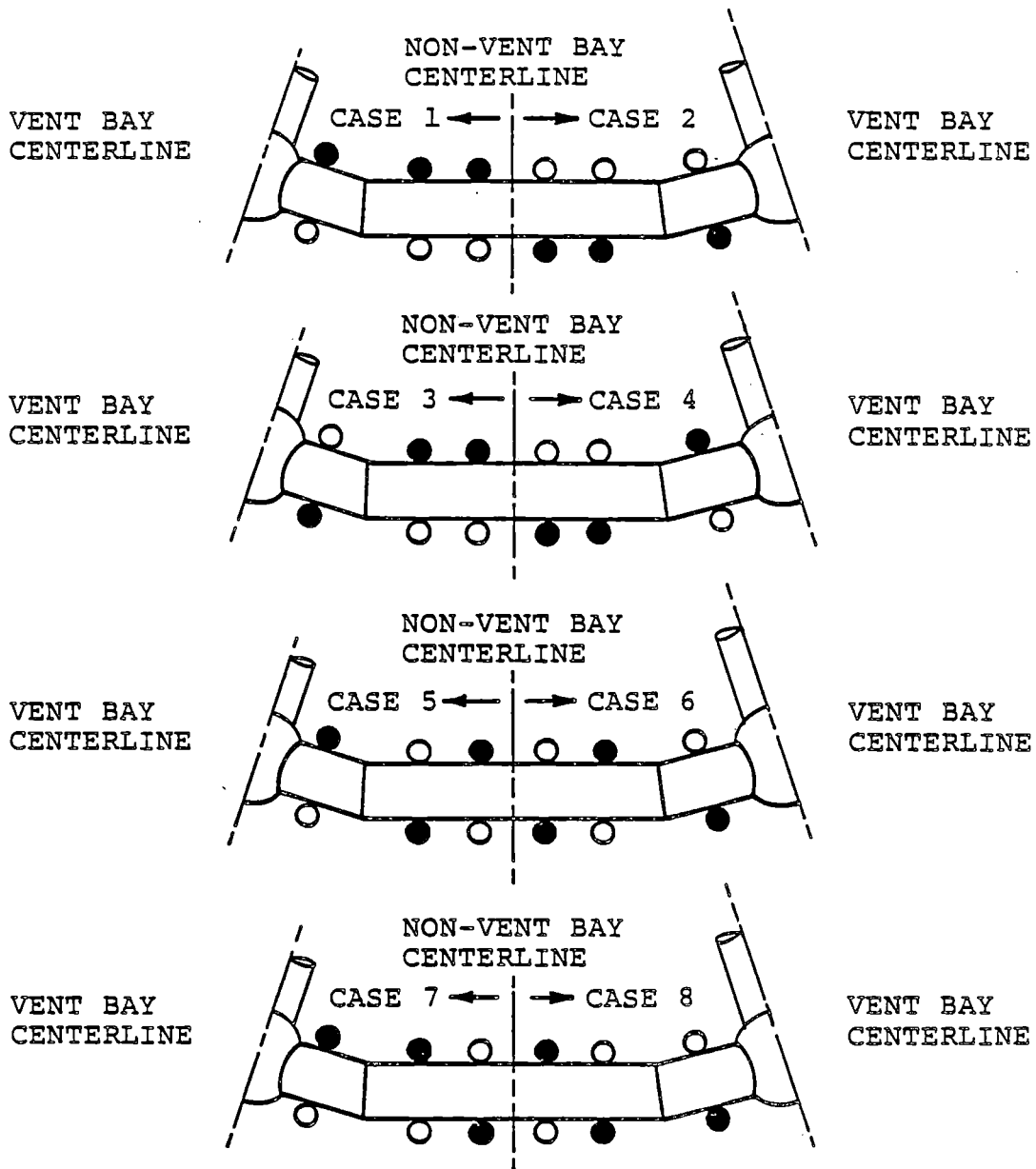
1-4.64



1. THE AMPLITUDES SHOWN ARE HALF-RANGE (ONE-HALF OF THE PEAK-TO-PEAK VALUE).

Figure 1-4.1-16

DOWNCOMER PAIR DIFFERENTIAL PRESSURE LOADING FOR DEA CO



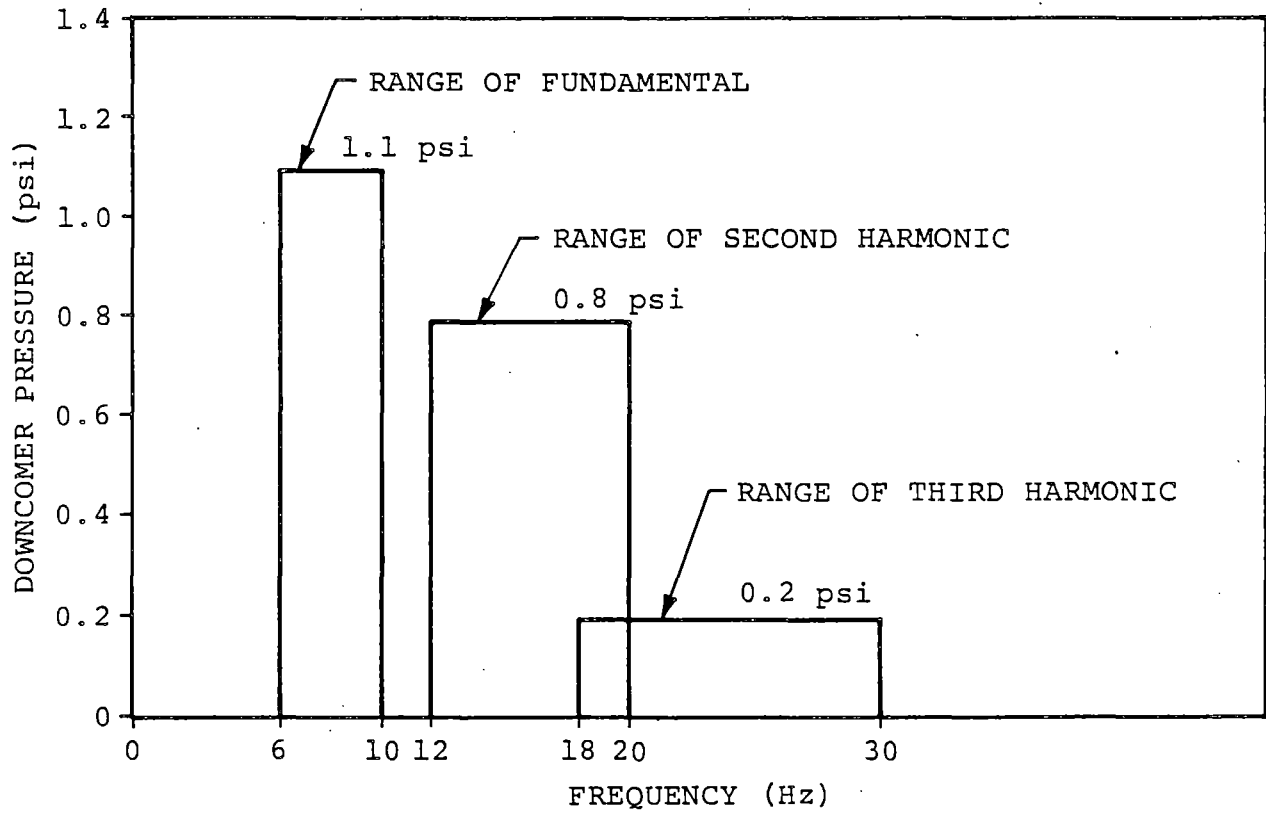
1. ● D/C WITH INITIAL DIFFERENTIAL PRESSURE LOAD.
2. ALL D/C'S HAVE INTERNAL PRESSURE LOAD IN PHASE WITH DIFFERENTIAL PRESSURE LOAD.
3. ANALYZED ALL EIGHT CASES - USED MAXIMUM RESPONSE FOR DESIGN.

Figure 1-4.1-17

DOWNCOMER CO DYNAMIC LOAD APPLICATION

COM-02-041-1
Revision 0

1-4.66



1. THE AMPLITUDES SHOWN ARE HALF-RANGE (ONE-HALF OF THE PEAK-TO-PEAK VALUE).

Figure 1-4.1-18

DOWNCOMER INTERNAL PRESSURE LOADING FOR IBA CO

1-4.1.7.3 CO Loads on Submerged Structures

The CO phase of the postulated LOCA induces bulk pool motion, creating drag loads on structures submerged in the pool. The basis of the flow model used to determine CO loads on submerged structures is presented in the load definition report.

Condensation oscillations are described by fluid sources located at the downcomer vent exits. The average source strengths are determined from wall load measurements. By using potential flow theory and the method of images to account for the effects of solid walls and the free surface, the velocity and acceleration flow fields within the torus are established. For each structure, the loads are computed using both the average source strength applied at all downcomers and the maximum source strength applied at the nearest downcomer.

The FSI effects are included when the local fluid acceleration is less than twice the boundary acceleration. Pool fluid accelerations are computed within the torus using frequency-decomposed, radial shell accelerations obtained from the torus analysis

described in Volume 2. The FSI effects for a given structure are computed using the pool fluid accelerations at the actual location of the structure.

Drag forces on submerged structures can be separated into two components: (1) standard drag, and (2) acceleration drag. The sum of these two effects gives the total drag load on a submerged structure. The calculations for CO loads on submerged structures use the same procedure used for calculating LOCA bubble-induced drag loads on submerged structures. Acceleration drag volumes for some structures with sharp corners (e.g., I-beams) are calculated using equations from Table 1-4.1-1 instead of volumes derived by circumscribed cylinders, as noted in Section 1-4.1.5.

Presented in Table 1-4.1-11 are the source amplitudes used for CO loads on submerged structures, which are in accordance with NUREG-0661. The source forcing function has the form of a sinusoidal wave characterized by the appropriate amplitude and frequency taken from Table 1-4.1-11. The LDR defines the total drag force as the summation of the

resulting responses from all 50 harmonics. As described in Section 1-4.1.7.1, the summation is performed to achieve a NEP of 84%.

COM-02-041-1
Revision 0

1-4.70

Table 1-4.1-11

AMPLITUDES AT VARIOUS FREQUENCIES
FOR CONDENSATION OSCILLATION SOURCE FUNCTION
FOR LOADS ON SUBMERGED STRUCTURES

FREQUENCY (Hz)	AMPLITUDE (ft ³ /sec ²)	FREQUENCY (Hz)	AMPLITUDE (ft ³ /sec ²)
0-1	28.38	26-27	56.75
1-2	24.46	27-28	12.72
2-3	31.31	28-29	18.59
3-4	46.97	29-30	13.70
4-5	182.00	30-31	7.83
5-6	267.13	31-34	2.94
6-7	96.87	34-35	4.89
7-10	57.73	35-36	7.83
10-11	77.30	36-37	9.79
11-12	44.03	37-38	6.85
12-13	16.63	38-39	5.87
13-14	11.74	39-40	8.81
14-15	6.85	40-41	32.29
15-16	9.79	41-42	32.29
16-19	3.91	42-43	32.29
19-20	26.42	43-44	32.29
20-21	19.57	44-45	32.29
21-22	29.36	45-46	32.29
22-23	33.27	46-47	32.29
23-24	32.29	47-48	32.29
24-25	15.66	48-49	32.29
25-26	24.46	49-50	32.29

This subsection describes the chugging loads on the various structures and components in the Dresden Units 2 and 3 suppression chamber.

Chugging occurs during a postulated LOCA when the steam flow through the vent system falls below the rate necessary to maintain steady condensation at the downcomer exits. The corresponding flowrates for chugging are less than those of the CO phenomenon. During chugging, steam bubbles form at the downcomer exits, oscillate as they grow to a critical size (approximately downcomer diameter), and begin to collapse independently in time. The resulting load on the torus shell due to a chug cycle consists of a low frequency oscillation (pre-chug) which corresponds to the oscillating bubbles at the downcomer exit as they grow, followed by a higher frequency "ring-out" of the torus shell-pool water system (post-chug) in response to the collapsing bubbles (Figure 1-4.1-19).

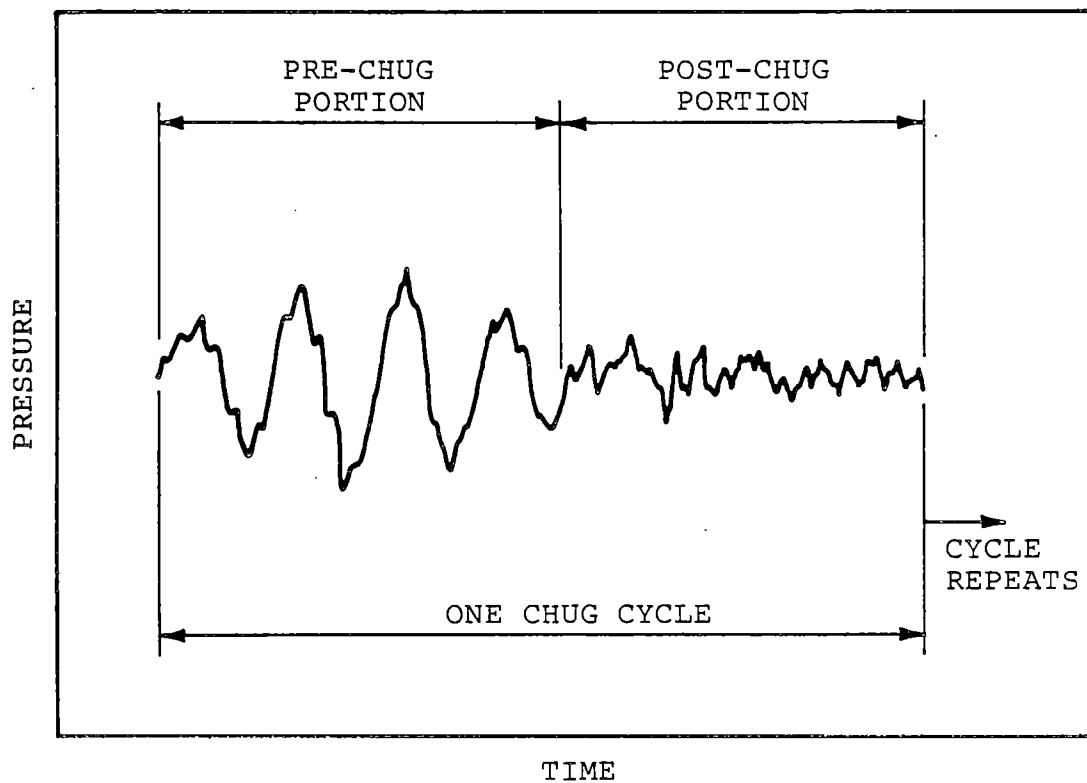


Figure 1-4.1-19

TYPICAL CHUG AVERAGE PRESSURE TRACE ON THE TORUS SHELL

COM-02-041-1
Revision 0

1-4.73

1-4.1.8.1 Chugging Loads on the Torus Shell

During the chugging regime of a postulated LOCA, the chugging loads on the torus shell occur as a series of chug cycles. The chugging load cycles are divided into pre-chug and post-chug portions. The bases for pre-chug and post-chug rigid wall load definitions are presented in the load definition report.

For the pre-chug portion of the chug cycle, both symmetric and asymmetric loading conditions are used to conservatively account for any randomness in the chugging phenomenon. The asymmetric loading is based on both low and high amplitude chugging data conservatively distributed around the torus in order to maximize the asymmetric loading.

In order to bound the post-chug portion of the chug cycle, symmetric loads are used. Asymmetric loads are not specified since any azimuthal response would be governed by the asymmetric pre-chug low frequency load specification.

Presented in Table 1-4.1-12 are the chugging onset times and durations for the DBA, IBA, and SBA, which are in accordance with the load definition report. Dresden Units 2 and 3 utilize motor-driven feedwater pumps, and the IBA scenario for this configuration is described in Section 2.2 of the load definition report. For the SBA, the automatic depressurization system (ADS) is assumed to initiate 600 seconds after the break and the reactor is assumed to be depressurized 600 seconds after ADS initiation, when chugging ends. For the IBA, the reactor is assumed to be depressurized 200 seconds after ADS initiation, when chugging ends. Table 1-4.1-12 shows these chugging durations.

a. Pre-Chug Load

The symmetric pre-chug torus shell pressure load is specified as ± 2 psi, applied uniformly along the torus longitudinal axis. Figure 1-4.1-20 shows the longitudinal distribution of the asymmetric pre-chug pressure load, which varies from ± 0.4 to ± 2.0 psi. The pre-chug cross-sectional distribution for both symmetric and asymmetric cases is the same as

for CO (Figure 1-4.1-21). The pre-chug loads are applied at the structural frequency in the range of 6.9 to 9.5 hertz. Table 1-4.1-12 shows the pre-chug load of 0.5 second duration is applied at 1.4 second intervals for the appropriate total chugging duration.

b. Post-Chug Load

Table 1-4.1-13 and Figure 1-4.1-20 define the amplitude versus frequency variation for the post-chug torus shell pressure load. The load is applied uniformly along the torus longitudinal axis. The cross-sectional variation is the same for CO and pre-chug loads (Figure 1-4.1-21). The steady-state responses from the application of the pressure amplitudes at each frequency given in Figure 1-4.1-22 are summed. The summation is performed for the CO load as described in Section 1-4.1.7.1. Table 1-4.1-12 shows the post-chug load of 0.5 second duration is applied at 1.4 second intervals for the appropriate total chugging duration.

Table 1-4.1-12

CHUGGING ONSET AND DURATION

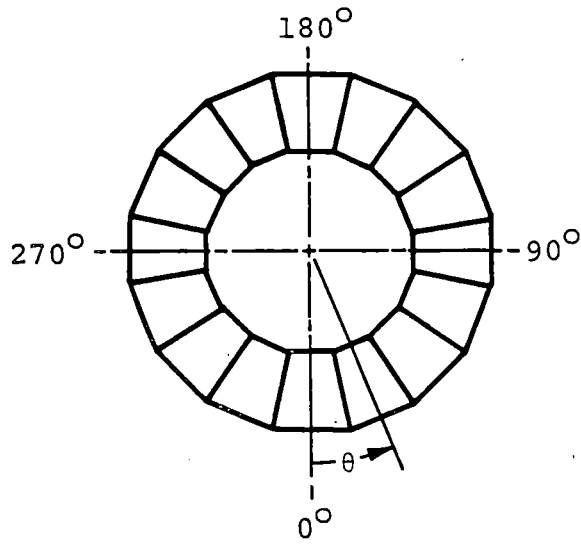
BREAK SIZE	ONSET TIME AFTER BREAK	DURATION AFTER ONSET
DBA	35 SECONDS	30 SECONDS
IBA	905 SECONDS	200 SECONDS
SBA	300 SECONDS	900 SECONDS

Table 1-4.1-13

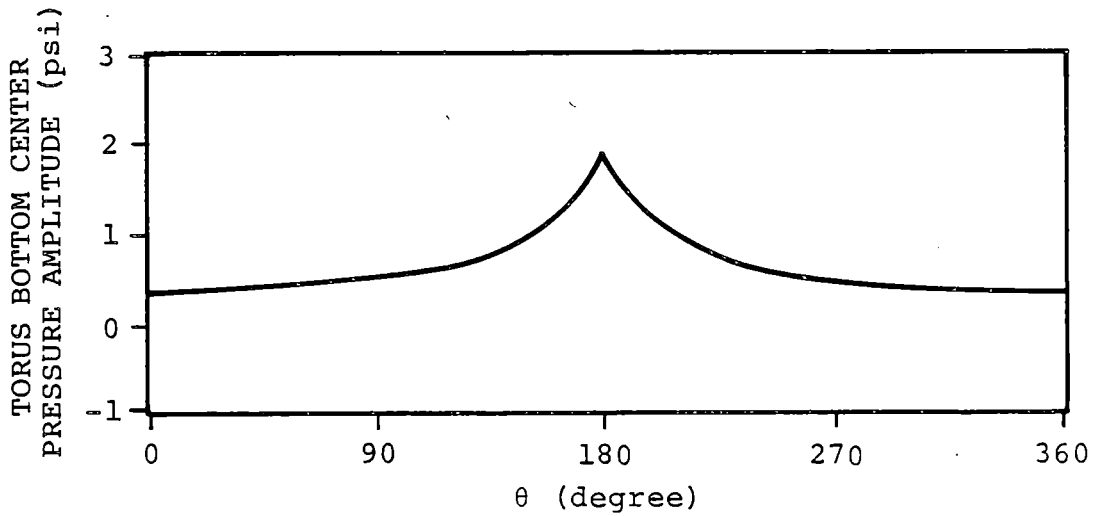
POST-CHUG RIGID WALL PRESSURE AMPLITUDES
ON TORUS SHELL BOTTOM DEAD CENTER

FREQUENCY RANGE (1) (Hz)	PRESSURE (psi)	FREQUENCY RANGE (1) (Hz)	PRESSURE (psi)
0-1	0.04	25-26	0.04
1-2	0.04	26-27	0.28
2-3	0.05	27-28	0.18
3-4	0.05	28-29	0.12
4-5	0.06	29-30	0.09
5-6	0.05	30-31	0.03
6-7	0.10	31-32	0.02
7-8	0.10	32-33	0.02
8-9	0.10	33-34	0.02
9-10	0.10	34-35	0.02
10-11	0.06	35-36	0.03
11-12	0.05	36-37	0.05
12-13	0.03	37-38	0.03
13-14	0.03	38-39	0.04
14-15	0.02	39-40	0.04
15-16	0.02	40-41	0.15
16-17	0.01	41-42	0.15
17-18	0.01	42-43	0.15
18-19	0.01	43-44	0.15
19-20	0.04	44-45	0.15
20-21	0.03	45-46	0.15
21-22	0.05	46-47	0.15
22-23	0.05	47-48	0.15
23-24	0.05	48-49	0.15
24-25	0.04	49-50	0.15

(1) HALF-RANGE (= ONE-HALF PEAK-TO-PEAK AMPLITUDE).



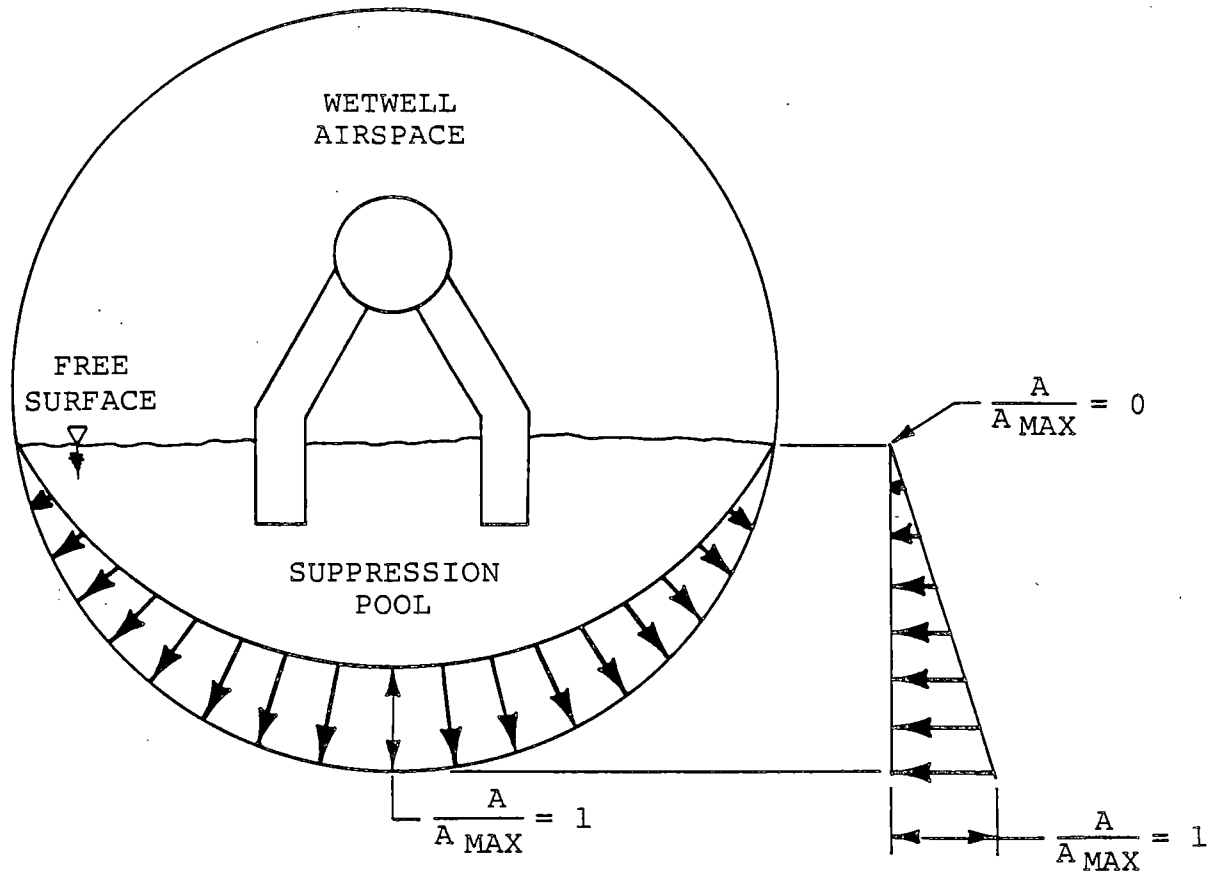
PLAN VIEW OF TORUS



1. THE AMPLITUDE SHOWN HERE REPRESENTS ONE-HALF OF THE PEAK-TO-PEAK AMPLITUDE.
2. HIGHEST VALUE IN BAY APPLIED OVER THE ENTIRE BAY.

Figure 1-4.1-20

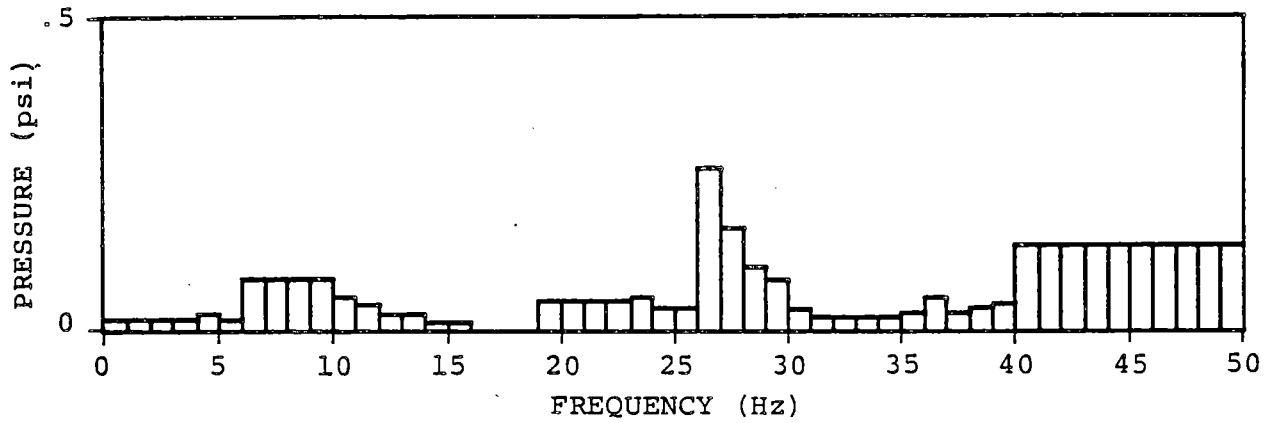
MARK I CHUGGING - TORUS ASYMMETRIC LONGITUDINAL
DISTRIBUTION FOR PRESSURE AMPLITUDE



1. A = LOCAL PRESSURES OSCILLATION AMPLITUDE.
2. A_{MAX} = MAXIMUM PRESSURE OSCILLATION AMPLITUDE (AT TORUS BOTTOM DEAD CENTER).

Figure 1-4.1-21

MARK I CHUGGING - TORUS VERTICAL CROSS-SECTIONAL
DISTRIBUTION FOR PRESSURE AMPLITUDE



1. THE AMPLITUDE SHOWN HERE REPRESENTS ONE-HALF OF THE PEAK-TO-PEAK AMPLITUDE.

Figure 1-4.1-22

POST-CHUG RIGID WALL PRESSURE AMPLITUDES
ON TORUS SHELL BOTTOM DEAD CENTER

COM-02-041-1
 Revision 0

1-4.81

1-4.1.8.2 Chugging Downcomer Lateral Loads

During the chugging phase of a postulated LOCA, vapor bubbles which form at the downcomer exit collapse suddenly and intermittently to produce lateral loads on the downcomer. This section presents the procedure for defining the dynamic portion of this loading for a DBA, an IBA, and a small break accident.

The basis for the chugging lateral load definition is the data obtained from the instrumented downcomers of the Mark I Full-Scale Test Facility. The load definition was developed for, and is directly applicable to, downcomer pairs which are untied. Based on FSTF observations, this load definition is also applicable to tied downcomers.

The FSTF downcomer lateral loads are defined as resultant static-equivalent loads (RSEL) which, when applied statically to the end of the downcomer, reproduce the measured bending response near the downcomer-vent header junction at any given time.

The loads associated with chugging obtained from the FSTF data are scaled to determine plant specific loads for Dresden Units 2 and 3. The maximum downcomer design load, histograms of load reversals, and the maximum vent system loading produced by synchronous chugging of the downcomers are determined from the FSTF loads.

NUREG-0661 states that the force per downcomer should be based on a probability of exceedance of 10^{-4} per LOCA for multiple downcomers during chugging. This requirement relates to the potential for a number of downcomers experiencing a lateral load in the same direction at the same time. The correlation between load magnitude and probability level was derived from a statistical analysis of FSTF data. A probability of exceedance of 10^{-4} per LOCA bounds all the load cases up to about 120 downcomers during chugging at the same time in a given plant. Dresden Units 2 and 3 have only 96 downcomers; therefore, a probability of exceedance of 10^{-4} per LOCA is conservative and is used for the two chugging load cases (Figure 1-4.1-23).

For fatigue evaluation of the downcomers, the required stress reversals at the downcomer-vent header junction are obtained from the FSTF RSEL reversal histograms. The plant unique junction stress reversals are obtained by scaling the FSTF RSEL reversals by the ratio of the chugging duration specified for Dresden Units 2 and 3 to that of the full-scale test facility. Table 1-4.1-12 specifies chugging durations for the DBA, IBA, and small break accident.

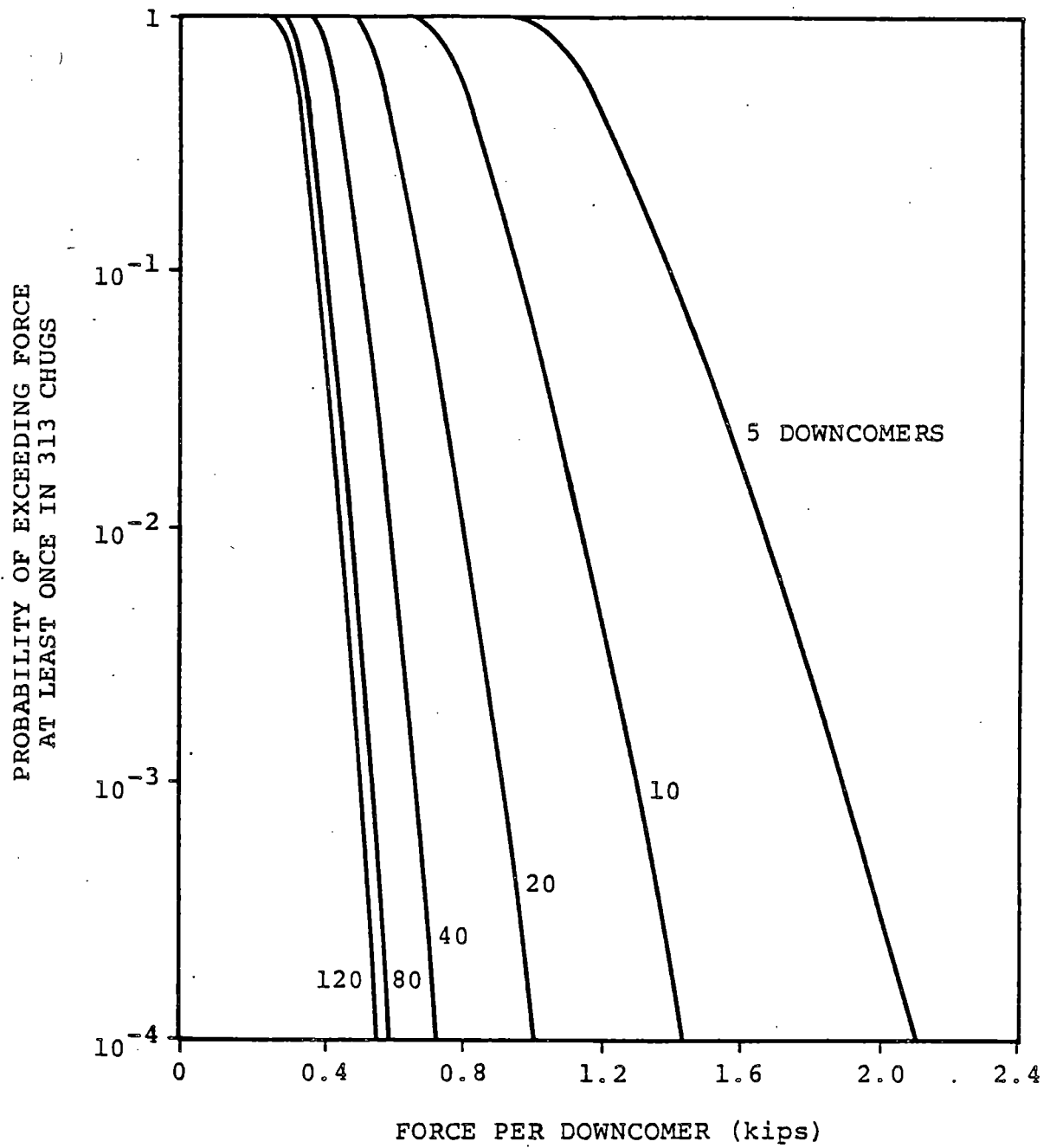


Figure 1-4.1-23

PROBABILITY OF EXCEEDING A GIVEN FORCE PER DOWNCOMER
FOR DIFFERENT NUMBERS OF DOWNCOMERS

COM-02-041-1
 Revision 0

1-4.85

1-4.1.8.3. Chugging Loads on Submerged Structures

Chugging at the downcomer exits induces bulk water motion, and therefore creates drag loads on structures submerged in the pool. The submerged structure load definition method for chugging follows that used to predict drag forces caused by condensation oscillations (see Section 1-4.1.7.3), except that the source strength for chugging is proportional to the wall load measurement corresponding to the chugging regime.

The LDR presents the bases and assumptions of the flow model for the chugging load definition. Table 1-4.1-14 presents the source amplitudes for pre-chug and post-chug regimes.

The load development procedure for chugging loads on submerged structures is the same as presented in Section 1-4.1.7.3 for CO loads and is in accordance with NUREG-0661. The responses from the 50 harmonics are summed as described in Section 1-4.1.7.1. Acceleration drag volumes for structures with sharp corners (e.g., I-beams) are calculated using equations from Table 1-4.1-1. Fluid-structure

interaction effects are included as described in
Section 1-4.1.7.3.

COM-02-041-1
Revision 0

1-4.87

Table 1-4.1-14

AMPLITUDES AT VARIOUS FREQUENCIES FOR CHUGGING
SOURCE FUNCTION FOR LOADS ON SUBMERGED STRUCTURES

CHUGGING	FREQUENCY (Hz)	AMPLITUDE (ft ³ /sec ²)
PRE	6.9 - 9.5	195.70
POST	0-2	11.98
	2-3	10.36
	3-4	9.87
	4-5	17.40
	5-6	17.00
	6-10	18.88
	10-11	87.90
	11-12	76.18
	12-13	41.01
	13-14	35.89
	14-15	6.82
	15-16	6.20
	16-17	3.14
	17-18	4.18
	18-19	2.94
	19-20	16.82
20-21	17.53	
21-22	30.67	

Table 1-4.1-14

AMPLITUDES AT VARIOUS FREQUENCIES FOR CHUGGING
SOURCE FUNCTION FOR LOADS ON SUBMERGED STRUCTURES

(Concluded)

CHUGGING	FREQUENCY (Hz)	AMPLITUDE (ft ³ /sec ²)
POST	22-24	92.39
	24-25	134.50
	25-26	313.84
	26-27	377.83
	27-28	251.89
	28-29	163.32
	29-30	116.66
	30-31	43.14
	31-32	21.57
	32-33	37.91
	33-34	50.54
	34-35	42.54
	35-36	61.87
	36-37	41.95
	37-38	20.97
	38-39	24.47
39-40	29.37	
40-50	224.90	

Safety Relief Valve Discharge Loads

This section discusses the procedures used to determine loads created when one or more SRV's is actuated.

When a SRV actuates, pressure and thrust loads are exerted on the SRV DL piping and the T-quencher discharge device. In addition, the expulsion of water followed by air into the suppression pool through the T-quencher results in pressure loads on the submerged portion of the torus shell and in drag loads on submerged structures.

The T-quencher utilized in Dresden Units 2 and 3 is a plant unique version of the Mark I T-quencher described in the load definition report. The Dresden Units 2 and 3 T-quencher has 12", Schedule 160 arms which are connected to the ramshead. The T-quencher is located at the centerline of the torus and is offset 1'-1" from bay centerline (Figure 1-2.1-16). The SRV DL is slanted from the vertical going into the ramshead. Figures 1-4.2-1 and 1-4.2-2 show the details of the hole distribution along the arm and illustrate the geometry of the SRV DL, ramshead, and T-quencher connection.

Volume 5 of this PUAR provides a detailed description of the SRVDL, T-quencher, and their related support structures.

As allowed in Section 2.13.9 of Appendix A of NUREG-0661, plant unique SRV testing at Dresden Unit 2 has been performed to confirm that the computed loadings and predicted structural responses for SRV discharges are conservative for Dresden Units 2 and 3.

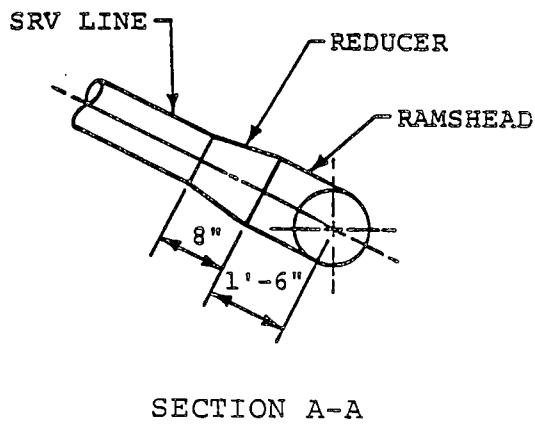
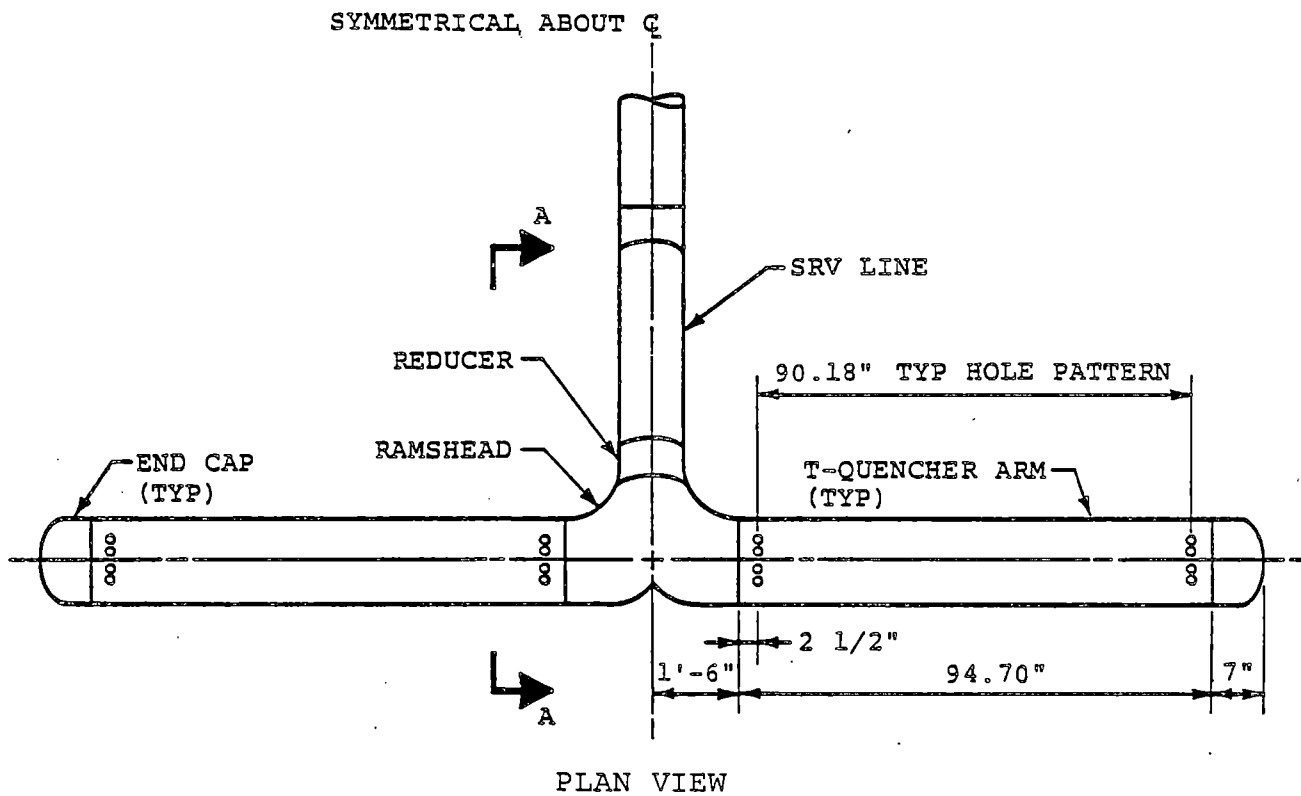
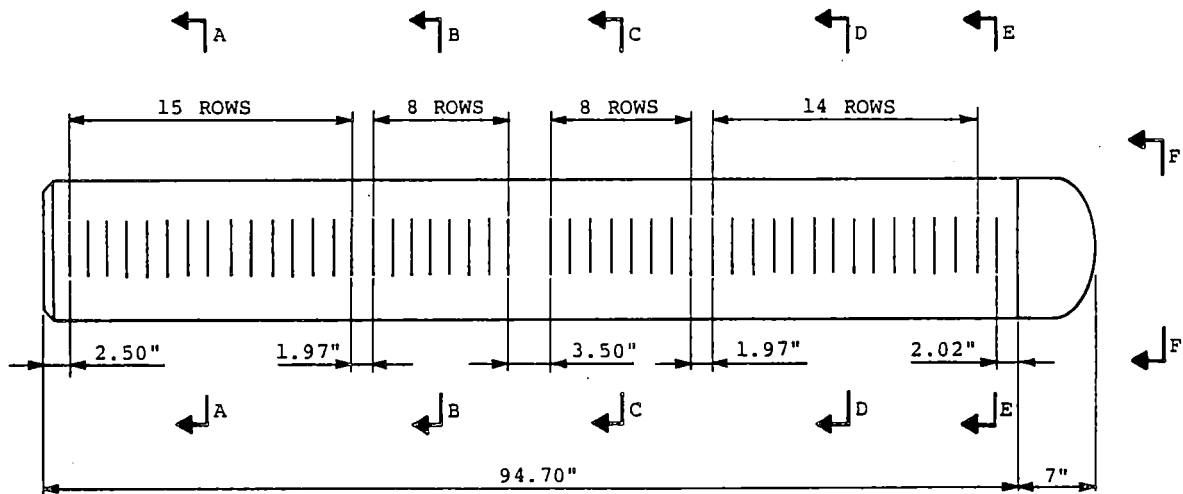


Figure 1-4.2-1

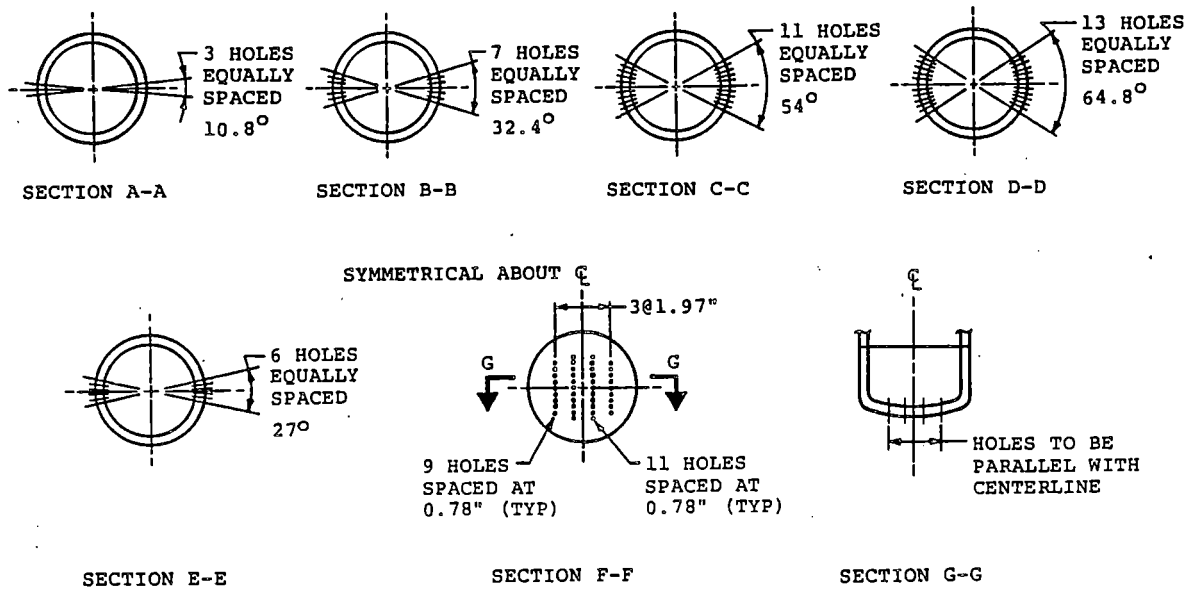
T-QUENCHER AND SRV LINE

COM-02-041-1
Revision 0

1-4.92



TYPICAL T-QUENCHER HOLES
WITH ENDCAP HOLES



1. ALL HOLE PATTERNS SYMMETRICAL ABOUT \mathcal{C} .
2. ALL HOLES ARE 0.391" IN DIAMETER.
3. SPACINGS NOT SHOWN ARE 1.97"

Figure 1-4.2-2

ELEVATION AND SECTION VIEWS OF
T-QUENCHER ARM HOLE PATTERNS

1-4.2.1 SRV Actuation Cases

This section provides a discussion on the selection of SRV discharge cases considered for design load evaluations. The load cases summarized in Table 1-4.2-1 are described as follows.

Load Case A1.1 (Normal Operating Conditions (NOC), First Actuation)

The first actuation of a SRV may occur under normal operating conditions; i.e., the SRVDL is cold, there is air in the drywell, and the water in the SRV is at its normal operating level.

Load Case A1.2 (SBA/IBA, First Actuation)

First actuation of SRV(s) is assumed to occur at the predicted time of ADS actuation. At this time, the SRVDL is full of air at the pressure corresponding to the drywell pressure minus the vacuum breaker set point. The water level inside the line is depressed below the normal operating level because the drywell

pressure is higher than the wetwell pressure by a pressure differential equal to the down-comer submergence.

Load Case Al.3 (DBA, First Actuation)

The same assumptions are used as for Case Al.1, except for SRV flowrate. This load case is bounded by Case Al.1.

Load Case B (First Actuation, Leaking SRV)

First actuation of a SRV may occur under NOC for leaking safety relief valves. For T-quenchers, Load Case Al.1 bounds the leaking SRV load.

Load Case C3.1 (NOC, Subsequent Actuation, Normal Water Leg)

After the SRV is closed following a first actuation (Case Al.1), the steam in the line is condensed, causing a rapid pressure drop which draws water back into the line. At the same time, the vacuum breaker allows air from the drywell to enter the discharge line. The

air repressurizes the line and the water refloods to a point which is higher than its equilibrium height, and oscillates back to its equilibrium point. A subsequent actuation is assumed to occur after the water level oscillations have damped out and the water leg has returned to the normal water level.

Load Case C3.2 (SBA/IBA, Subsequent Actuation)

Following SRV closure after the first actuation (Case A1.2) in the SBA/IBA, the water refloods back into the line while air from the drywell flows through the vacuum breaker into the SRV discharge line. The SRV is assumed to actuate after the water level oscillations have damped out and the level has stabilized at a point determined by the drywell-to-wetwell ΔP minus the vacuum breaker set point.

Load Case C3.3 (SBA/IBA, Subsequent Actuation, Steam in SRVDL)

This case differs from the previous case in that during the reflood transient, steam,

instead of air, flows through the vacuum breaker. Thus, the line contains very little air and the loading imposed on the torus shell from this subsequent SRV actuation is bounded by Case C3.2.

The SRVDL water leg is assumed at its equilibrium height for all subsequent actuation SRV cases. The time after the first valve closure when the equilibrium height is reestablished is calculated using the LDR SRVDL reflood model. Dresden Units 2 and 3 primary system transient analyses are used to confirm that more than the minimum required time is available for the SRVDL water leg to return to the equilibrium position. To further insure that the SRVDL water leg will be at its equilibrium height for all subsequent SRV actuation cases, Dresden Units 2 and 3 will have delay logic on the two lowest-set relief valves to allow this water leg to clear after initial actuation. For the steam-in-the-drywell conditions, a steam-water convective heat transfer coefficient of 2×10^5 BTU/hr·ft²·°R is used. This conservative coefficient is based on the results of a literature survey on chugging and the downcomer water column rise characteristics

during chugging in the Mark I Full-Scale Test Facility.

The number of SRV's predicted to actuate for each of the above conditions is maximized in performing the Dresden Units 2 and 3 structural evaluations, documented in the remaining volumes of the plant unique analysis report. Section 1-4.3 describes the other hydrodynamic loads which must be combined with SRV loads.

Table 1-4.2-1

SRV LOAD CASE/INITIAL CONDITIONS

DESIGN INITIAL CONDITION, LOAD CASE	ANY ONE VALVE	ADS VALVES	MULTIPLE VALVES (1)
NOC, FIRST ACTUATION	A1.1		A3.2
SBA/IBA, FIRST ACTUATION	A1.2	A2.2	A3.2
DBA, FIRST ACTUATION ⁽²⁾	A1.3		
NOC, LEAKING SRV ⁽³⁾			B3.1 ⁽⁴⁾
NOC, SUBSEQUENT ACTUATION			C3.1
SBA/IBA, SUBSEQUENT ACTUATION, AIR IN SRVDL			C3.2
SBA/IBA, SUBSEQUENT ACTUATION, STEAM IN SRVDL			C3.3

- (1) THE NUMBER (ONE OR MORE) AND LOCATION OF VALVES ASSUMED TO ACTUATE ARE DETERMINED BY PLANT UNIQUE ANALYSIS.
- (2) THIS ACTUATION IS ASSUMED TO OCCUR COINCIDENT WITH THE POOL SWELL EVENT. ALTHOUGH SRV ACTUATION CAN OCCUR LATER IN THE DBA, THE RESULTING AIR LOADING ON THE TORUS SHELL IS NEGLIGIBLE SINCE THE AIR AND WATER INITIALLY IN THE LINE WILL BE CLEARED AS THE DRYWELL-TO-WETWELL ΔP INCREASES DURING THE DBA TRANSIENT.
- (3) THIS IS APPLICABLE TO RAMSHEAD DISCHARGE ONLY.
- (4) ONLY ONE VALVE OF THE MULTIPLE GROUP IS ASSUMED TO LEAK.

1-4.2.2 SRV Discharge Line Clearing Loads

The flow of high pressure steam into the discharge line when a SRV opens results in the development of a pressure wave at the entrance to the line. During the early portion of this transient, a substantial pressure differential exists across the pressure wave. This pressure differential, plus momentum effects from steam (or water in initially submerged pipe runs) flowing around elbows in the line, results in transient thrust loads on the SRV discharge piping segments. These loads are considered in the design of SRV piping restraints, the SRV penetrations in the vent lines, and the T-quencher support system.

The LDR presents the bases, assumptions, and descriptions of the SRV discharge line clearing analytical model. The parameters affecting SRVDL clearing loads development are the SRVDL geometry, plant specific initial conditions for the SRV actuation cases, and the SRV mass flowrate. Table 1-4.2-2 presents plant specific initial conditions for various actuation cases. Table 1-4.2-3 presents common (but case-independent) SRVDL analysis input parameters. All calculation input procedures for

the SRVDL clearing model are consistent with the load definition report.

The line clearing model is used to obtain transient values for each SRV actuation case for each SRVDL for the following parameters or loads.

- SRVDL Pressures and Temperatures
- Thrust Loads on SRVDL Piping Segments
- T-quencher Internal Discharge Pressure and Temperature
- Water Slug Mass Flowrate
- Water Clearing Time, Velocity, and Acceleration

The values obtained for T-quencher discharge pressure and water clearing time are used as input to evaluate the torus shell loads (Section 1-4.2.3) and SRV air bubble drag loads (Section 1-4.2.4) on submerged structures. The water slug mass flowrate and acceleration are used as inputs to calculations of SRV water jet loads on submerged structures (Section 1-4.2.4).

The water clearing thrust load along the axis of the T-quencher (due to the uneven flowsplit in the ramshead), and the thrust load perpendicular to the T-quencher arms (due to a skewed air-water interface) are calculated as specified in the load definition report.

The calculation procedures, load definitions, and applications used for SRV water and air clearing thrust and all other SRV water clearing loads are in accordance with the LDR and Appendix A of NUREG-0661.

Table 1-4.2-2

PLANT UNIQUE INITIAL
CONDITIONS FOR ACTUATION CASES
USED FOR SRVDL CLEARING TRANSIENT LOAD DEVELOPMENT

PARAMETER	CASE A1.1	CASE A1.2	CASE C3.1	CASE C3.2
PRESSURE IN THE WETWELL (psia)	14.65	40.37	14.65	40.37
PRESSURE IN THE DRYWELL (psia)	15.65	42.1	15.65	42.1
ΔP VACUUM BREAKER (psid)	0.2	0.2	0.2	0.2
INITIAL PIPE WALL TEMPERATURE IN THE WETWELL AIRSPACE ($^{\circ}F$)	115	340	350	350
INITIAL PIPE WALL TEMPERATURE IN THE SUPPRESSION POOL ($^{\circ}F$)	90	130	90	130
INITIAL AIR PRESSURE IN SRVDL (psia)	15.45	41.9	15.45	41.9
INITIAL AIR DENSITY IN SRVDL (lbm/ft^3)	0.0725	0.1414	0.0515	0.1396
INITIAL WATER VOLUME IN SRVDL AND T-QUENCHER (ft^3)	12.945	12.023	12.945	12.023

Table 1-4.2-3

SRVDL ANALYSIS PARAMETERS

PARAMETER	VALUE
DESIGN SRV FLOW RATE (lbm/sec)	215.3
STEAM LINE PRESSURE (psia)	1200
STEAM DENSITY IN THE STEAM LINE (lbm/ft ³)	2.76
RATIO OF AREAS OF DISCHARGE DEVICE EXIT TO TOTAL T-QUENCHER ARM	1.183

Following SRV actuation, the air mass in the SRVDL is expelled into the suppression pool, forming many small air bubbles. These bubbles then coalesce into four larger bubbles which expand and contract as they rise and break through the pool surface. The positive and negative dynamic pressures developed within these bubbles result in an oscillatory, attenuated pressure loading on the torus shell.

The analytical model which is used to predict air bubble and torus shell boundary pressures resulting from SRV discharge is similar to that described in Reference 16. The analytical model in Reference 16 was modified slightly to more closely bound the magnitudes and time characteristics of pressures observed in the Monticello test. Figure 1-4.2-3 shows a comparison of the shell pressure-time history measured during the Monticello test to the shell pressure-time history computed using the revised analytical model. The comparison is shown for shell pressures at the bottom of the torus beneath the quencher, where the highest shell pressures were observed. Figure 1-4.2-3 shows that

the predicted shell pressures envelop those observed in the Monticello test.

The pressure-time history generated using the analytical model discussed above is used to perform a forced vibration analysis of the suppression chamber. The phenomena associated with SRV discharge into the suppression pool are characteristic of an initial value or free vibration condition rather than a forced vibration condition. Correction factors are applied to convert the forced vibration response to a free vibration response.

The correction factors are developed using single degree-of-freedom analogs. The factors vary with the ratio of load frequency to structural frequency and are applied to the response (displacement, velocity, and acceleration) associated with each structural mode. Figure 1-4.2-4 shows the modal correction factors (MCF) which are used in the suppression chamber evaluation.

The pressure magnitudes produced by the analytical model discussed previously were calibrated to envelop the maximum local shell pressures observed

in the Monticello test. This results in an overly conservative prediction of net vertical loads, as discussed in Section 3.10.2.9 of NUREG-0661. Net vertical load correction factors were developed by comparing net vertical pressure loads measured in the Monticello test with those predicted at test conditions. The factors were determined to be 0.70 for upward loads and 0.78 for downward loads.

Table 1-4.2-4 shows a comparison of shell membrane stresses and column forces observed in the Monticello test with those values predicted using the analytical methods and correction factors described above. The table shows that predicted forces and stresses conservatively bound the measured values at all locations. A series of in-plant tests were performed at Dresden Unit 2 in May 1981. These tests provided additional confirmation that the computed loadings and predicted structural response due to SRV discharge are conservative.

Table 1-4.2-4

COMPARISON OF ANALYSIS AND MONTICELLO TEST RESULTS

QUANTITY	LOCATION	ANALYSIS	TEST	<u>ANALYSIS</u> <u>TEST</u>
SUPPRESSION CHAMBER SHELL MEMBRANE STRESSES (ksi)	MIDBAY 90° FROM BDC REACTOR SIDE	2.8	0.6	4.7
	MIDBAY 52.5° FROM BDC REACTOR SIDE	2.3	1.1	2.1
	MIDBAY 12.4° FROM BDC OPPOSITE REACTOR	2.2	1.4	1.6
	MIDBAY 12.4° FROM BDC REACTOR SIDE	2.1	1.7	1.2
	MIDBAY 52.5° FROM BDC OPPOSITE REACTOR	2.5	1.1	2.3
	1/4 BAY 12.4° FROM BDC OPPOSITE REACTOR	2.2	1.4	1.6
TORUS COLUMN UPLIFT LOADS (kips)	INSIDE COLUMN	123.9	49.0	2.5
	OUTSIDE COLUMN	157.8	52.5	3.0
TORUS COLUMN DOWN LOADS (kips)	INSIDE COLUMN	152.9	64.5	2.4
	OUTSIDE COLUMN	178.2	78.5	2.3

COM-02-041-1
Revision 0

1-4.109

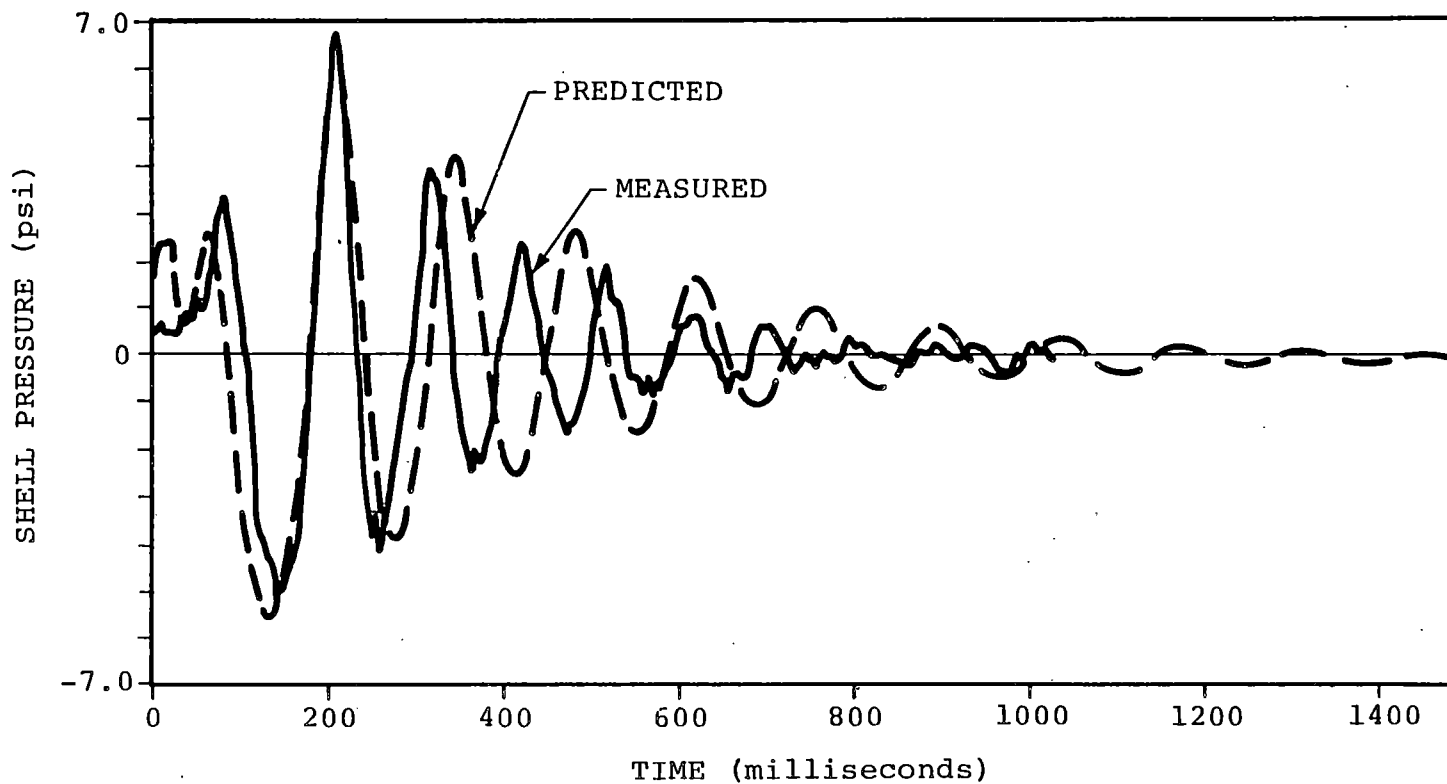


Figure 1-4.2-3

COMPARISON OF PREDICTED AND MEASURED SHELL PRESSURE
TIME-HISTORIES FOR MONTICELLO TEST 801

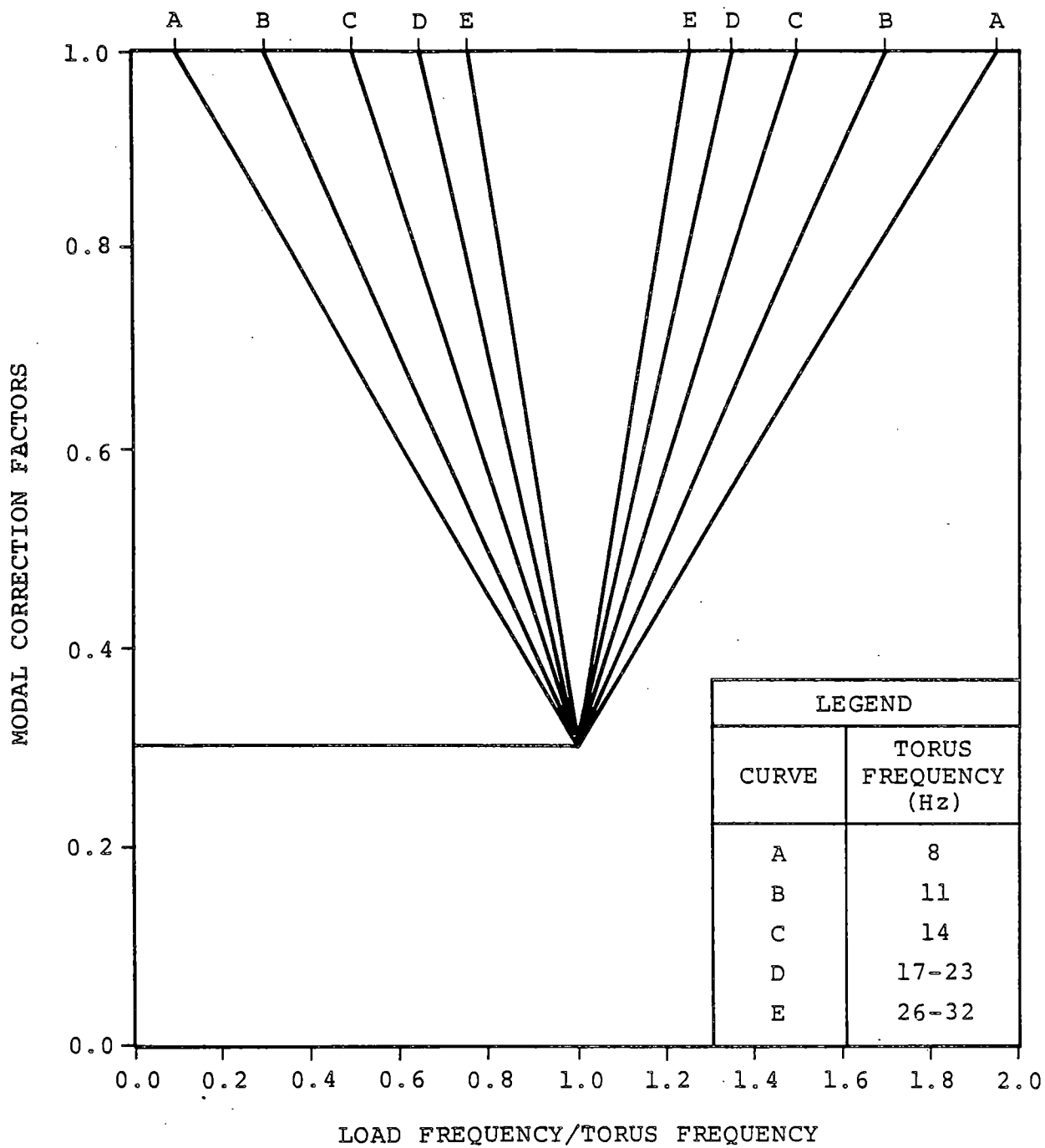


Figure 1-4.2-4

MODAL CORRECTION FACTORS FOR ANALYSIS
OF SRV DISCHARGE TORUS SHELL LOADS

COM-02-041-1
 Revision 0

1-4.110

This section addresses the load definition procedures for determining SRV loads on submerged structures due to T-quencher water jets and bubbles.

When a SRV is actuated, water initially contained in the submerged portion of the SRVDL is forced out of the T-quencher through holes in the arms, forming orifice jets. Some distance downstream, the orifice jets merge to form column jets. Further downstream, the column jets merge to form the quencher arm jets. As soon as the water flow through the arm hole ceases, the quencher arm jet velocity decreases rapidly and the jet penetrates a limited distance into the pool. The T-quencher water jets create drag loads on nearby submerged structures within the jet path.

Oscillating bubbles resulting from a SRV actuation create an unsteady three-dimensional flow field, and therefore induce acceleration and standard drag forces on the submerged structures in the suppression pool.

a. T-quencher Water Jet Loads

The T-quencher water jet model conservatively models the T-quencher water jet test data. The bases, justification, and assumptions for the Mark I T-quencher model are presented in Reference 1. The SRV T-quencher water jet analytical model calculation procedure and application are in accordance with Mark I LDR techniques. Figure 1-4.2-5 shows a plan view of the T-quencher arm jet sections.

b. SRV Bubble-Induced Drag Loads

The SRV bubble drag load development methodology, load definition, and application for the Dresden Units 2 and 3 PUA are performed utilizing Commonwealth Edison's T-quencher geometry (Figure 1-4.2-1). The techniques utilized in developing the Dresden Units 2 and 3 loads are in accordance with the LDR and Appendix A of NUREG-0661. Dynamic load factors are derived from Dresden's in-plant SRV test data.

A bubble pressure bounding factor based on Monticello test data in lieu of the LDR value of 2.5 is utilized for Dresden Units 2 and 3 SRV load development. A value of 1.75 produces results which bound the peak positive bubble pressure and maximum bubble pressure differential from both the Dresden and Monticello T-quencher test data. Using 1.75, the calculated values for Monticello are 9.9 psid and 18.1 psid, respectively. The predicted values correspond to the single valve actuation, normal water level, cold pipe case listed in Table 3.2 of Reference 16.

For submerged structures with sharp corners such as T-beams, I-beams, etc., the acceleration drag volumes are calculated using the methodology in Section 1-4.1.5.

The model described in Section 1-4.2.3 is used to determine drag loads on downcomers due to SRV bubble oscillation.

SYMMETRICAL ABOUT ζ

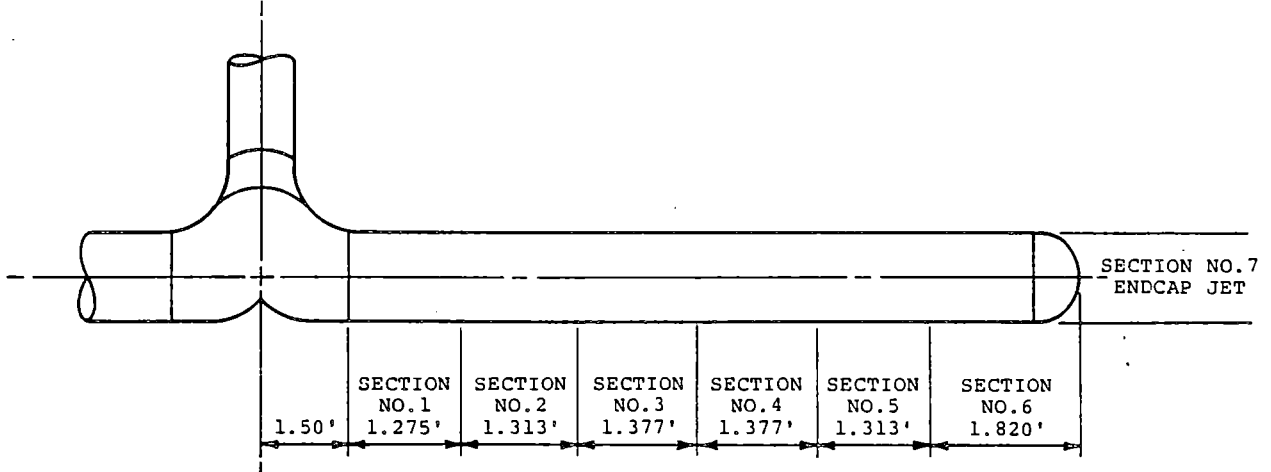


Figure 1-4.2-5

PLAN VIEW OF DRESDEN UNITS 2 AND 3
T-QUENCHER ARM JET SECTIONS

COM-02-041-1
Revision 0

1-4.114

Event Sequence

Not all of the suppression pool hydrodynamic loads discussed in this evaluation can occur at the same time. In addition, the load magnitudes and timing vary, depending on the accident scenario being considered. Therefore, it is necessary to construct a series of event combinations to describe the circumstances under which individual loads might combine.

Tables 1-3.2-1 and 1-3.2-2 show the event combinations used in the plant unique analysis. The combinations of load cases were determined from typical plant primary system and containment response analyses, with considerations for automatic actuation, manual actuation, and single active failures of the various systems in each event. This section describes the event sequences for the following postulated loss-of-coolant accidents.

- Design Basis Accident
- Intermediate Break Accident
- Small Break Accident

Table 1-4.3-1 identifies the SRV and LOCA loads which potentially affect structural components and identifies the appropriate section of this report defining the loads. For SRV piping and other structures within the wetwell, the locations of the structural components are considered to determine if any of the identified conditions affect the structures.

Table 1-4.3-1

SRV AND LOCA STRUCTURAL LOADS

LOADS	STRUCTURES						OTHER WETWELL INTERIOR STRUCTURES		
	TORUS SHELL	TORUS SUPPORT SYSTEM	MAIN VENTS	VENT HEADER	DOWNCOMERS	SRV PIPING	ABOVE NORM WATER LEVEL	ABOVE BOTTOM OF DOWNCOMERS AND BELOW NORM WATER LEVEL	BELOW BOTTOM OF DOWNCOMERS
1-4.1.1 CONTAINMENT PRESSURE AND TEMPERATURE RESPONSE	X	X	X	X	X	X	X	X	X
1-4.1.2 VENT SYSTEM DISCHARGE LOADS			X	X	X				
1-4.1.3 POOL SWELL LOADS ON THE TORUS SHELL	X	X							
1-4.1.4 POOL SWELL LOADS ON ELEVATED STRUCTURES									
1-4.1.4.1 IMPACT AND DRAG LOADS ON THE VENT SYSTEM			X	X	X				
1-4.1.4.2 IMPACT AND DRAG LOADS ON OTHER STRUCTURES			X			X	X		
1-4.1.4.3 POOL SWELL FROTH IMPINGEMENT LOADS			X				X		
1-4.1.4.4 POOL FALLBACK LOADS						X	X	X	
1-4.1.5 LOCA WATERJET LOADS ON SUBMERGED STRUCTURES						X			X
1-4.1.6 LOCA BUBBLE-INDUCED LOADS ON SUBMERGED STRUCTURES						X			X
1-4.1.7 CONDENSATION OSCILLATION LOADS									
1-4.1.7.1 CO LOADS ON THE TORUS SHELL	X	X							
1-4.1.7.2 CO LOADS ON THE DOWNCOMERS AND VENT SYSTEM			X	X	X				
1-4.1.7.3 CO LOADS ON SUBMERGED STRUCTURES						X		X	X
1-4.1.8 CHUGGING LOADS									
1-4.1.8.1 CHUGGING LOADS ON THE TORUS SHELL	X	X							
1-4.1.8.2 CHUGGING DOWNCOMER LATERAL LOADS				X	X				
1-4.1.8.3 CHUGGING LOADS ON SUBMERGED STRUCTURES						X		X	X
1-4.2 SAFETY RELIEF VALVE DISCHARGE LOADS									
1-4.2.2 SRV DISCHARGE LINE CLEARING LOADS						X			
1-4.2.3 SRV LOADS ON THE TORUS SHELL	X	X							
1-4.2.4 SRV LOADS ON SUBMERGED STRUCTURES					X	X		X	X

1-4.3.1 Design Basis Accident

The DBA for the Mark I containment design is the instantaneous guillotine rupture of the largest pipe in the primary system (the recirculation line). Figures 1-4.3-1 through 1-4.3-3 present the load combinations for the DBA. Table 1-4.3-2 presents the nomenclature for these figures. The bar charts for the DBA show the loading condition combination for postulated breaks large enough to produce significant pool swell. The length of the bars in the figures indicates the time periods during which the loading conditions may occur. Loads are considered to act simultaneously on a structure at a specific time if the loading condition bars overlap at that time. For SRV discharge, the loads may occur at any time during the indicated time period. The assumption of combining a SRV discharge with the DBA is beyond the design basis of Dresden Units 2 and 3. Therefore, the DBA and SRV load combination is evaluated only to demonstrate containment structural capability. Table 1-4.3-3 shows the SRV discharge loading conditions.

Table 1-4.3-2

EVENT TIMING NOMENCLATURE

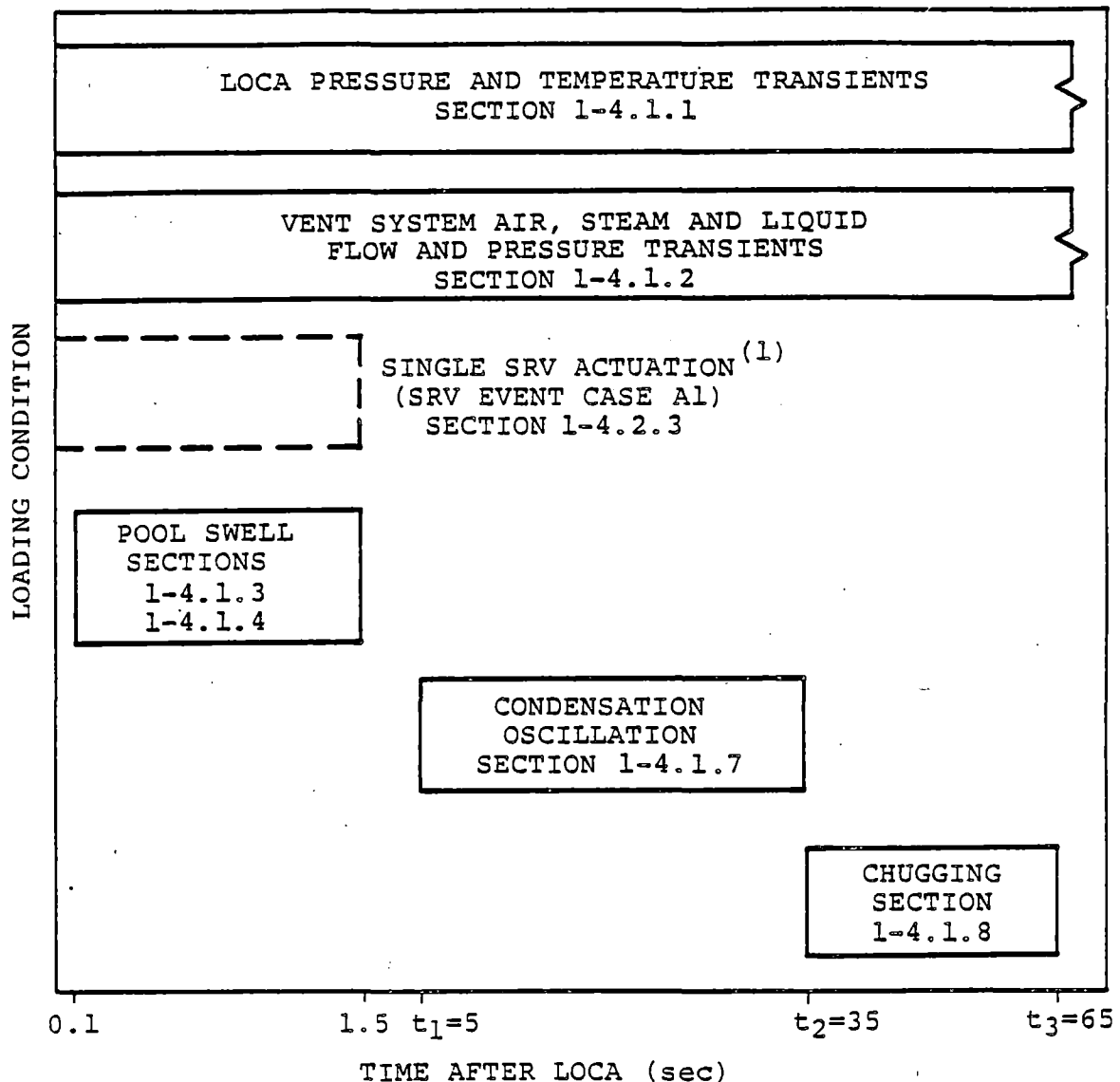
TIME	DESCRIPTION
t_1	THE ONSET OF CONDENSATION OSCILLATION
t_2	THE BEGINNING OF CHUGGING
t_3	THE END OF CHUGGING
t_4	TIME OF COMPLETE REACTOR DEPRESSURIZATION
t_{ADS}	ADS ACTUATION ON HIGH DRYWELL PRESSURE AND LOW REACTOR WATER LEVEL. THE ADS IS ASSUMED TO BE ACTUATED BY THE OPERATOR FOR THE SBA.

Table 1-4.3-3

SRV DISCHARGE LOAD CASE
FOR MARK I STRUCTURAL ANALYSIS

INITIAL CONDITIONS	ANY ONE VALVE	ADS VALVES (3)	MULTIPLE VALVES (1)
FIRST ACTUATION	A 1	A 2	A 3
FIRST ACTUATION, LEAKING SRV (2)			B 3
SUBSEQUENT ACTUATION			C 3

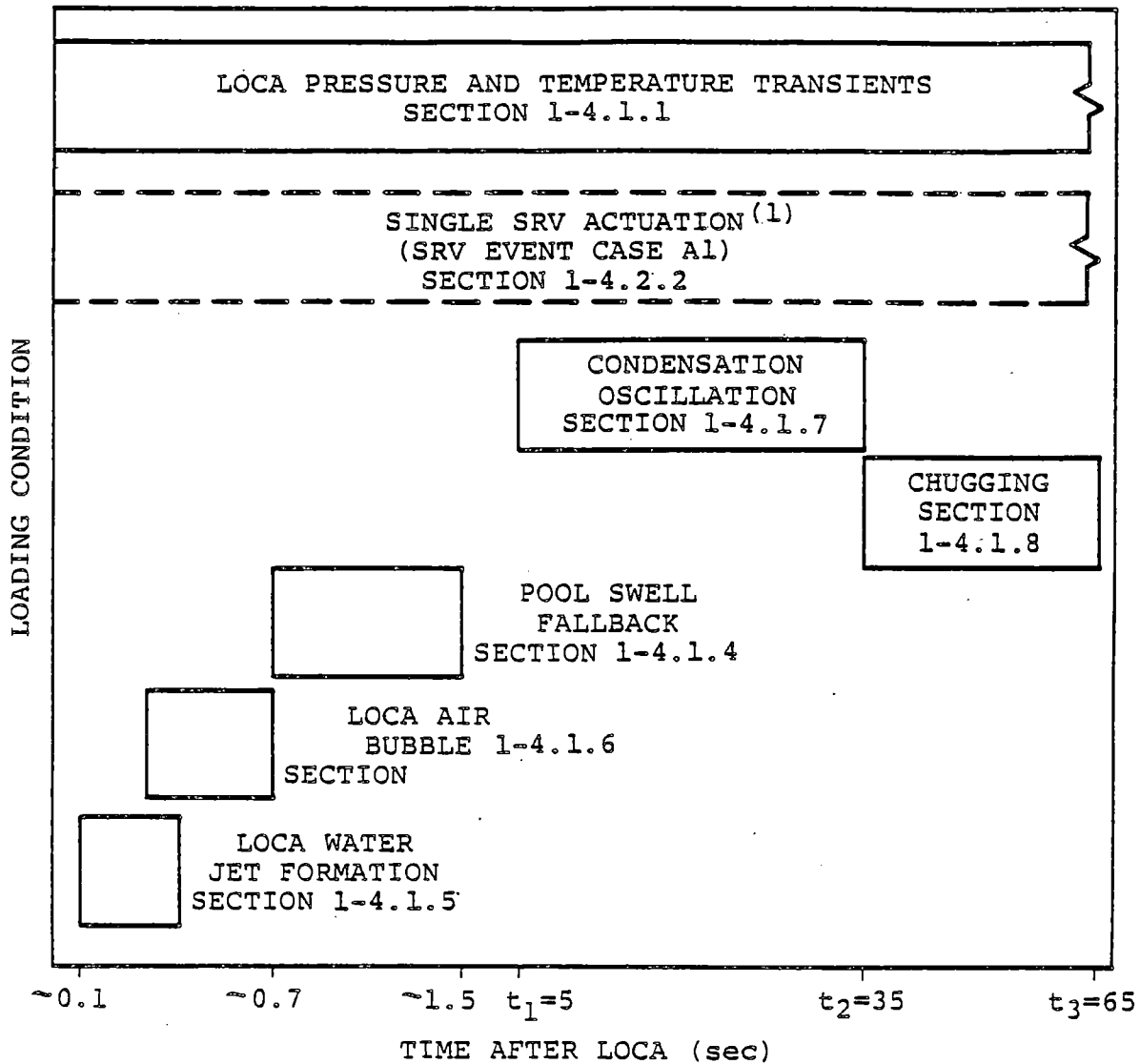
- (1) THE NUMBER (ONE OR MORE) AND LOCATION OF SRV's ASSUMED TO ACTUATE ARE DETERMINED BY PLANT UNIQUE ANALYSIS.
- (2) THE LOADS FOR T-QUENCHER DISCHARGE DEVICES ARE NOT AFFECTED BY LEAKING SRV's. NO SRV's ARE CONSIDERED TO LEAK PRIOR TO A LOCA.
- (3) THE MULTIPLE VALVE CASE AND THE ADS VALVE CASE ARE EQUIVALENT.



- (1) THIS ACTUATION IS ASSUMED TO OCCUR COINCIDENT WITH THE POOL SWELL EVENT. ALTHOUGH SRV ACTUATION CAN OCCUR LATER IN THE DBA, THE RESULTING AIR LOADING ON THE TORUS SHELL IS NEGLIGIBLE, SINCE THE AIR AND WATER INITIALLY IN THE LINE WILL BE CLEARED AS THE DRYWELL-TO-WETWELL ΔP INCREASES DURING THE DBA TRANSIENT.

Figure 1-4.3-1

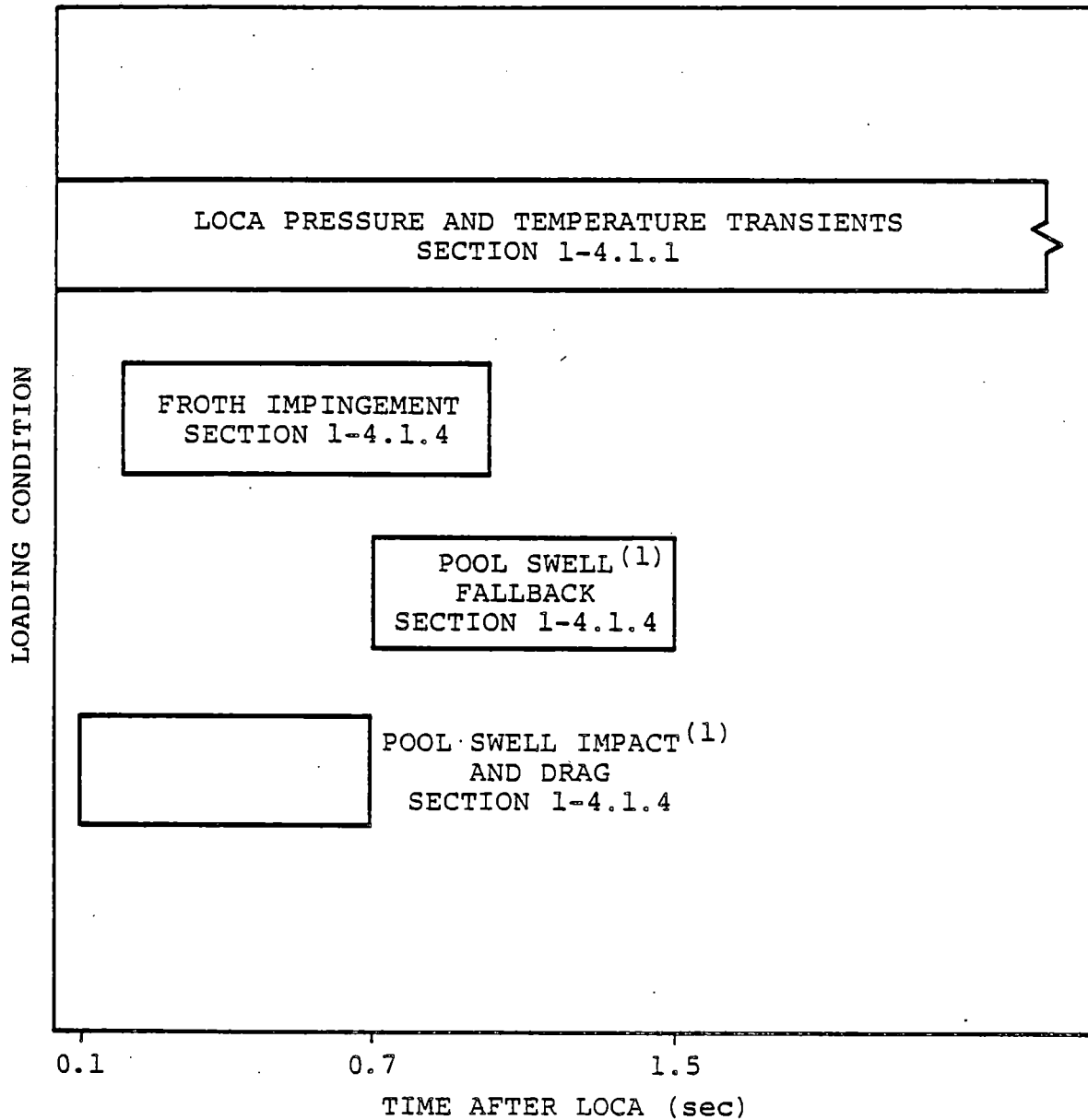
LOADING CONDITION COMBINATIONS FOR THE VENT HEADER,
MAIN VENTS, DOWNCOMERS, AND TORUS SHELL DURING A DBA



- (1) THIS ACTUATION IS ASSUMED TO OCCUR COINCIDENT WITH THE POOL SWELL EVENT. ALTHOUGH SRV ACTUATION CAN OCCUR LATER IN THE DBA, THE RESULTING AIR LOADING ON THE TORUS SHELL IS NEGLIGIBLE, SINCE THE AIR AND WATER INITIALLY IN THE LINE WILL BE CLEARED AS THE DRYWELL-TO-WETWELL ΔP INCREASES DURING THE DBA TRANSIENT.

Figure 1-4.3-2

LOADING CONDITION COMBINATIONS FOR SUBMERGED
STRUCTURES DURING A DBA



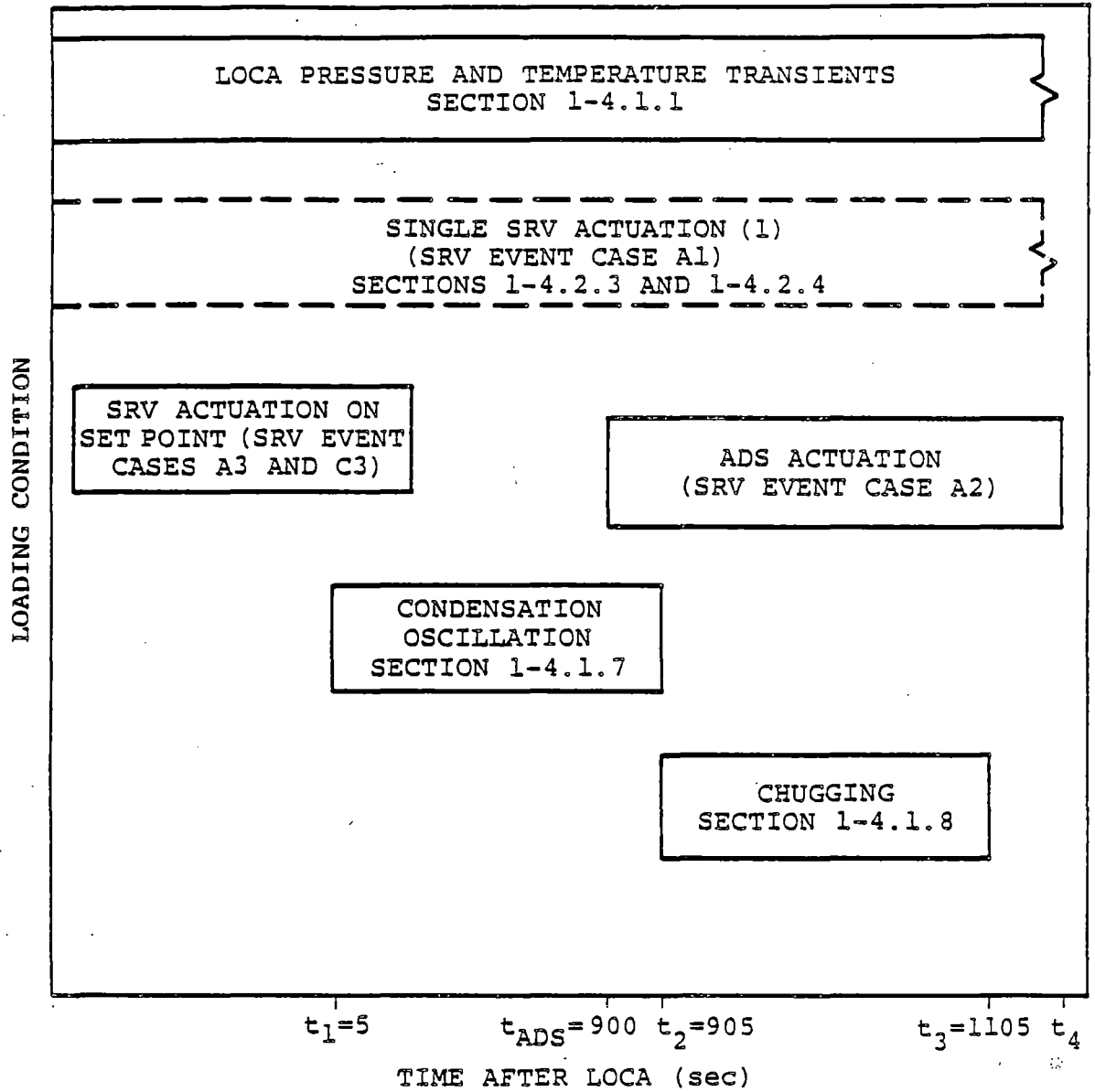
(1) STRUCTURES ARE BELOW MAXIMUM POOL SWELL HEIGHT.

Figure 1-4.3-3

LOADING CONDITION COMBINATIONS FOR SMALL
STRUCTURES ABOVE SUPPRESSION POOL DURING A DBA

1-4.3.2 Intermediate Break Accident

The bar chart in Figure 1-4.3-4 shows conditions for a break size large enough such that the HPCI system cannot prevent ADS actuation on low-water level, but for break sizes smaller than that which would produce significant pool swell loads. A break size of 0.1 ft^2 is assumed for an IBA. Table 1-4.3-3 shows SRV discharge loading conditions. The IBA break is too small to cause significant pool swell.



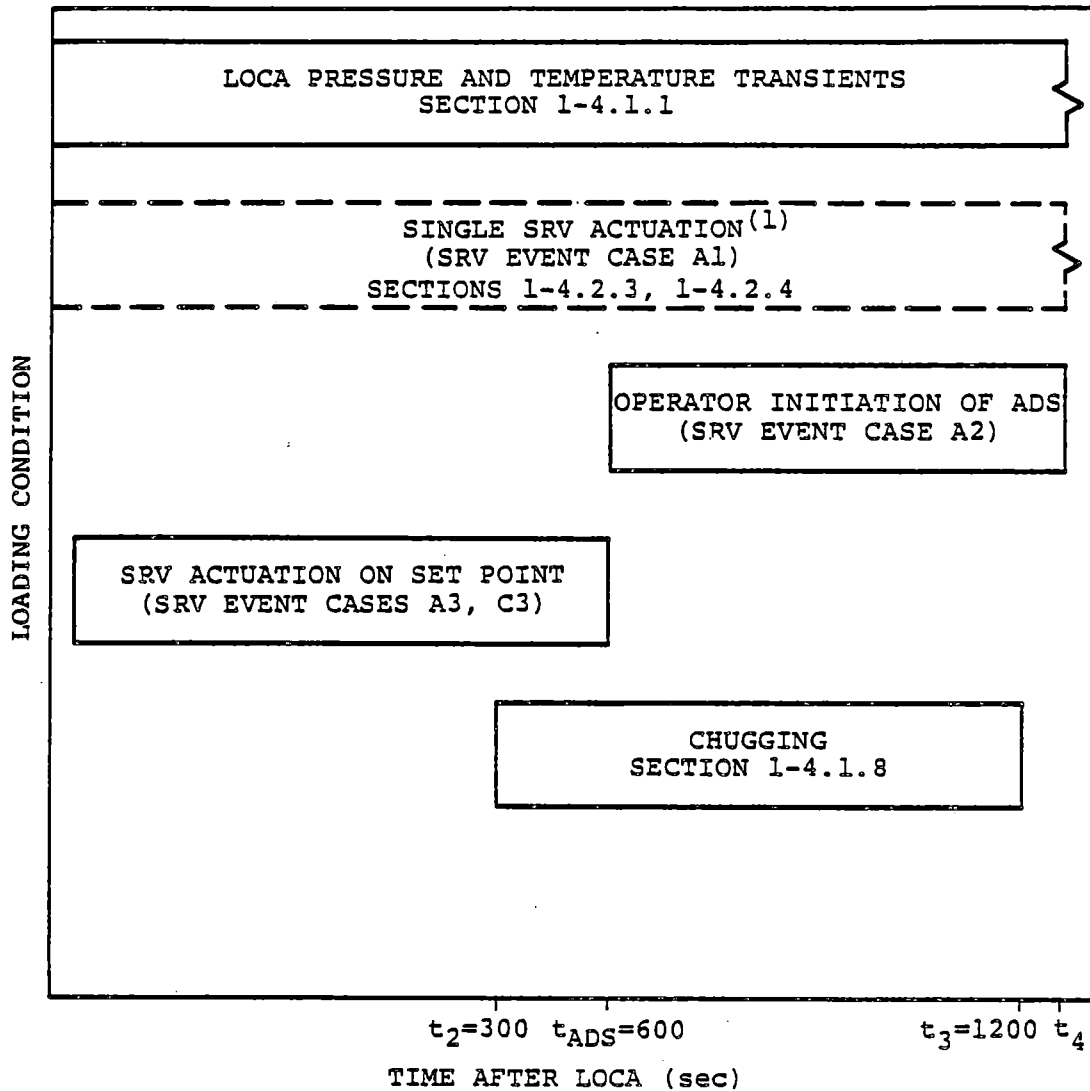
(1) LOADING NOT COMBINED WITH OTHER SRV CASES.

Figure 1-4.3-4

LOADING CONDITION COMBINATIONS FOR THE
VENT HEADER, MAIN VENTS, DOWNCOMERS, TORUS SHELL,
AND SUBMERGED STRUCTURES DURING AN IBA

1-4.3.3 Small Break Accident

The bar chart in Figure 1-4.3-5 shows conditions for a break size equal to 0.01 ft². For a SBA, the HPCI system would be able to maintain the water level and the reactor would be depressurized by means of operator initiation of the automatic depressurization system. Table 1-4.3-3 identifies the SRV discharge loading conditions. The SBA break is too small to cause significant pool swell, and CO does not occur during a SBA. The ADS is assumed to be initiated by the operator 10 minutes after the SBA begins. With the concurrence of the NRC (Reference 17), the procedures which the operator will use to perform this action are being developed as part of the Emergency Procedures Guidelines.



(1) LOADING NOT COMBINED WITH OTHER SRV CASES.

Figure 1-4.3-5

LOADING CONDITION COMBINATIONS FOR THE VENT HEADER,
MAIN VENTS, DOWNCOMERS, TORUS SHELL, AND
SUBMERGED STRUCTURES DURING A SBA

1-5.0

SUPPRESSION POOL TEMPERATURE MONITORING SYSTEM

This section describes the Dresden Units 2 and 3 suppression pool temperature response to SRV transients and the design of the suppression pool temperature monitoring system.

COM-02-041-1
Revision 0

1-5.1

1-5.1

Suppression Pool Temperature Response to SRV
Transients

Dresden Units 2 and 3 take advantage of the large thermal capacitance of the suppression pool during plant transients requiring safety relief valve actuation. Steam is discharged through the SRV's into the suppression pool where it is condensed, resulting in an increase in the temperature of the suppression pool water. Although stable steam condensation is expected at all pool temperatures, Reference 18 imposes a local temperature limit in the vicinity of the T-quencher discharge devices (Figure 1-5.1-1).

To demonstrate that the local pool temperature limit is satisfied, seven limiting transients involving SRV discharges are analyzed (Reference 19). Table 1-5.1-1 presents a summary of the transients analyzed and the corresponding pool temperature results. Three of the transients conservatively assume the failure of one residual heat removal (RHR) loop in addition to the single equipment malfunction or operator error which initiated the event. This conservative assumption exceeds the

current licensing basis for anticipated operational transients.

Each of the SRV discharge transients is analyzed assuming an initial pool temperature of 95°F, which is the Technical Specification pool temperature limit for normal power operation. The notes to Table 1-5.1-1 list other initial conditions and assumptions included in these analyses.

The analysis of Case 2C, normal depressurization at isolated hot shutdown, shows a maximum local pool temperature of 165°F. This demonstrates that with no system failures and in the event of a nonmechanistic scram, depressurizing the reactor pressure vessel (RPV) with SRV's at 100°F/hr results in local pool temperatures well below the condensation stability limit in Figure 1-5.1-1.

Case 3A, a SBA with one RHR loop available, results in a maximum local pool temperature of 177°F, which is below the condensation stability limit of 205°F. High local temperatures are predicted in this case because of reduced mixing when the available RHR pool cooling system is switched to the shutdown cooling mode.

The maximum local pool temperature of all other cases also remains below the condensation stability limit throughout the transient. In general, local-to-bulk temperature differences at the time of maximum temperatures are about 9°F for cases where two RHR loops are assumed available, and about 28°F for cases where one RHR loop is assumed available. Thus, bulk pool circulation induced by the RHR loops leads to good thermal mixing, which effectively lowers the local pool temperatures in the vicinity of quencher devices.

Table 1-5.1-1

SUMMARY OF DRESDEN UNITS 2 AND 3
POOL TEMPERATURE RESPONSE TO SRV TRANSIENTS

CASE NUMBER	EVENT	NUMBER OF SRV's MANUALLY OPENED	MAXIMUM COOLDOWN RATE (°F/hr)	MAXIMUM BULK POOL TEMPERATURE (°F)	MAXIMUM LOCAL POOL TEMPERATURE (°F)
1A	SORV AT POWER, 1 RHR LOOP	0	1919	131	161
1B	SORV AT POWER, SPURIOUS ISOLATION, 2 RHR LOOPS	0	530	129	167
2A	RAPID DEPRESSURIZATION AT ISOLATED HOT SHUTDOWN, 1 RHR LOOP	1	258	113	156
2B	SORV AT ISOLATED HOT SHUTDOWN, 2 RHR LOOPS	1	517	122	160
2C	NORMAL DEPRESSURIZATION AT ISOLATED HOT SHUTDOWN, 2 RHR LOOPS	2	258	115	153
3A	SBA-ACCIDENT MODE, 1 RHR LOOP	5 (ADS) *	2100	154	180
3B	SBA-FAILURE OF SHUTDOWN COOLING MODE, 2 RHR LOOPS	5	100	147	156

* ADS - AUTOMATIC DEPRESSURIZATION SYSTEM

NOTES TO TABLE 1-5.1-1

1. REACTOR OPERATION AT 102% OF RATED THERMAL POWER (2578 MWt).
2. MINIMUM TECHNICAL SPECIFICATION SUPPRESSION POOL WATER VOLUME (112,203 FT³).
3. THE SUPPRESSION POOL HAS NO INITIAL VELOCITY.
4. WETWELL AND DRYWELL AIRSPACES ARE AT NORMAL OPERATING CONDITIONS.
5. NORMAL AUXILIARY POWER IS AVAILABLE.
6. OFFSITE POWER IS ASSUMED AVAILABLE FOR ALL CASES.
7. NORMAL AUTOMATIC OPERATION OF THE PLANT AUXILIARY SYSTEM (HIGH PRESSURE COOLANT INJECTION (HPCI), ADS).
8. THE CORE SPRAY PUMPS HAVE A MANUAL SHUTOFF AT VESSEL HIGH WATER LEVEL (LEVEL 8 ELEVATION). THEY ARE REACTIVATED WHEN THE LEVEL DROPS AS NEEDED TO MAINTAIN WATER LEVEL AND MAY BE SHUT OFF AGAIN.
9. CONTROL ROD DRIVE (CRD) FLOW IS MAINTAINED CONSTANT AT 11.111 BM/SEC.
10. SRV (MANUAL, AUTOMATIC, ADS) CAPACITIES ARE AT 122.5% OF ASME-RATED FLOW TO CONSERVATIVELY CALCULATE MAXIMUM POOL TEMPERATURES.
11. THE LICENSED DECAY-HEAT CURVE (MAY-WITT) FOR CONTAINMENT ANALYSIS IS USED.
12. NO HEAT TRANSFER IS CONSIDERED IN THE DRYWELL AND WETWELL AIRSPACE.
13. THE MSIV'S CLOSE THREE SECONDS AFTER A ONE-HALF SECOND DELAY FOR THE ISOLATION SIGNAL.
14. OPERATOR ACTIONS ARE BASED ON NORMAL OPERATOR ACTION TIMES AND LICENSING BASIS DELAYS DURING THE GIVEN EVENT.
15. THE SHUTDOWN COOLING SYSTEM AND THE POOL COOLING MODE OF THE RHR-LPCI SYSTEM ARE TWO INDEPENDENT SYSTEMS. THE ACTUATION OF ONE SYSTEM IS NOT DEPENDENT ON TURNING-OFF THE OTHER SYSTEM. THE OPERATOR ACTION TIME TO TURN ON THE SHUTDOWN COOLING SYSTEM IS ASSUMED TO BE 16 MINUTES.

CCM-02-041-1
Revision 0

1-5.6

NOTES TO TABLE 1-5.1-1
(Concluded)

16. ONCE IT IS TURNED ON, THE POOL COOLING FUNCTION STAYS ON AND IS NOT AFFECTED BY THE ACTUATION OF THE SHUTDOWN COOLING SYSTEM. THERE ARE TWO LOOPS OF POOL COOLING AND ONE LOOP CAN BE ASSUMED FAILED, AS DEMONSTRATED IN EVENT CASES 1A, 2A, AND 3A.
17. DRYWELL FAN COOLERS ARE INITIALLY AVAILABLE IN SORV EVENTS AND ISOLATION EVENTS TO KEEP THE DRYWELL PRESSURE BELOW THE HIGH DRYWELL PRESSURE TRIP SET POINT (~2 PSIG).
18. THE ADS SYSTEM IS MODELED BY FULLY OPENING FIVE SRV'S IN THE ADS MODE. THE ADS SYSTEM MAY BE ACTUATED MANUALLY AT A HIGH SUPPRESSION POOL TEMPERATURE OF 120°F.
19. ALL RHR AND ECCS PUMPS HAVE 100% OF THEIR HORSEPOWER RATING CONVERTED TO A PUMP HEAT INPUT (BTU/SEC) AND ADDED DIRECTLY TO THE POOL AS AN ENTHALPY RISE OVER THE TIME OF PUMP OPERATION. THIS ASSUMPTION ADDS CONSERVATISM TO THE POOL TEMPERATURE RESULTS.
20. THE FEEDWATER TEMPERATURE IS TAKEN AS THE ACTUAL TEMPERATURE IN THE FEEDWATER SYSTEM. HOWEVER, FOR THAT PORTION OF FEEDWATER WHICH IS LOWER THAN 170°F, THE TEMPERATURE IS CONSERVATIVELY ASSUMED TO BE 170°F.
21. THE SERVICE WATER TEMPERATURE FOR THE RHR HEAT EXCHANGERS IS ASSUMED CONSTANT AT 93°F, GIVING A HEAT TRANSFER CAPACITY OF 127.4 BTU/SEC-°F PER LOOP SHUTDOWN COOLING FUNCTION, AND 416.7 BTU/SEC-°F PER LOOP FOR POOL COOLING FUNCTION.
22. THE 10" RHR-LPCI DISCHARGE LINE IS DIRECTED PARALLEL TO FLOW IN THE DISCHARGE BAY.
23. THE BREAK FLOW MASS AND ENERGY ARE ADDED TO FLOW THROUGH THE QUENCHERS FOR SBA CASES. THIS APPROACH MAKES THE RESULTS OF SBA CASES MORE CONSERVATIVE BECAUSE IT MAINTAINS A "HOT SPOT" AROUND THE QUENCHERS AT ALL TIMES.
24. THE ANALYSES ARE TERMINATED WHEN THE POOL TEMPERATURE REACHES A MAXIMUM AND TURNS AROUND, OR WHEN THE STEAM DISCHARGING ACTIVITIES OF THE SRV'S ARE OVER.
25. THE OPERATOR WILL ATTEMPT TO RECLOSE AN SORV. BASED ON AVAILABLE OPERATING PLANT DATA PRIOR TO THE IMPLEMENTATION OF THE REQUIREMENTS OF IE BULLETIN 80-25 (REFERENCE 20), SORV'S HAVE BEEN SHOWN TO RECLOSE AT AN AVERAGE PRESSURE OF 260 PSIG. THE LOWEST RECLOSURE PRESSURE RECORDED WAS 50 PSIG, AND THIS VALUE IS CONSERVATIVELY ASSUMED FOR THIS ANALYSIS.
26. THE ISOLATION CONDENSER CAN BE ACTUATED BY A HIGH-REACTOR-PRESSURE SIGNAL OF 1085 PSIA SUSTAINED FOR 15 SECONDS. HOWEVER, AN ADDITIONAL 60 SECOND DELAY FOR ITS TUBE SIDE OUTLET VALVE OPENING IS ASSUMED TO LINE UP THE CONDENSER FOR FULL OPERATION. A TOTAL OF 90,000 GALLONS IS AVAILABLE FROM THE CONDENSATE STORAGE TANK TO SUPPLY THE SHELL SIDE WATER INVENTORY WHENEVER NEEDED. THE ISOLATION CONDENSER HAS A DESIGNED COOLING RATE OF 252.5×10^6 BTU/HR.

COM-02-041-1
Revision 0

1-5.7

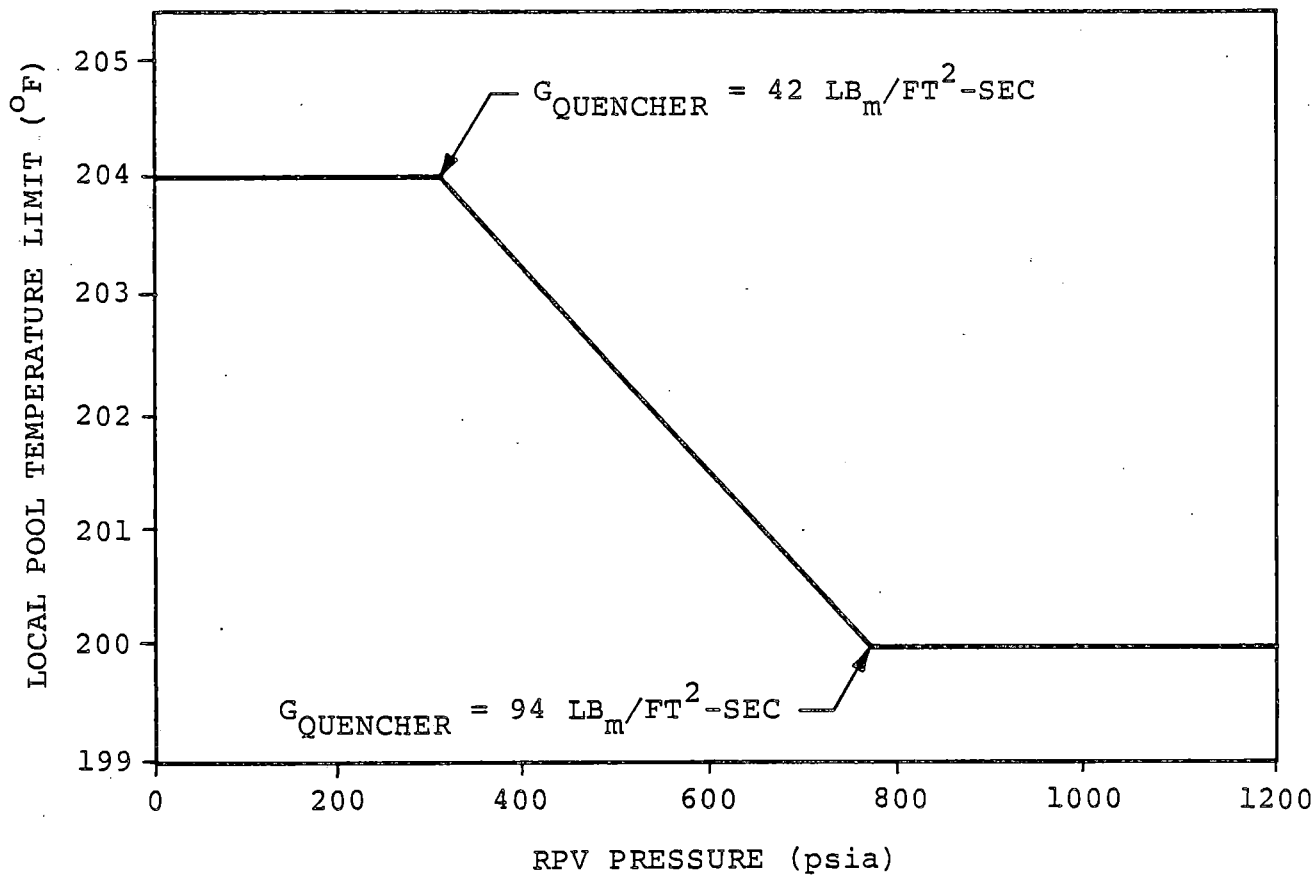


Figure 1-5.1-1

LOCAL POOL TEMPERATURE LIMIT FOR DRESDEN UNITS 2&3

COM-02-041-1
Revision 0

1-5.8

Suppression Pool Temperature Monitoring System
Design

The Dresden SPTMS has been designed by Bechtel Power Corporation (Reference 21) in conjunction with NUTECH Engineers for Commonwealth Edison Company.

The SPTMS is used to provide a measure of the suppression pool water temperature (bulk pool temperature). The SPTMS has eight thermocouples which are placed inside thermowells around the torus. Four thermowells at the main vent bays are located on the inner circumference and four thermowells at the non-main vent bays are on the outer circumference (Figure 1-5.2-1). The inputs from the eight sensors are averaged to provide a bulk pool temperature measurement. The sensors are placed on a horizontal plane 5.88' below the minimum torus water level, near the centroid of the water mass to assure an accurate measurement of the bulk pool temperature.

The bulk suppression pool temperature and the individual sensor readings will be continuously recorded in the control room. The SPTMS is designed to operate continuously during all modes of reactor

operation. It is also designed to operate in both post-LOCA and post-ATWS (Anticipated Transients Without Scram) environments and after a safe shutdown earthquake.

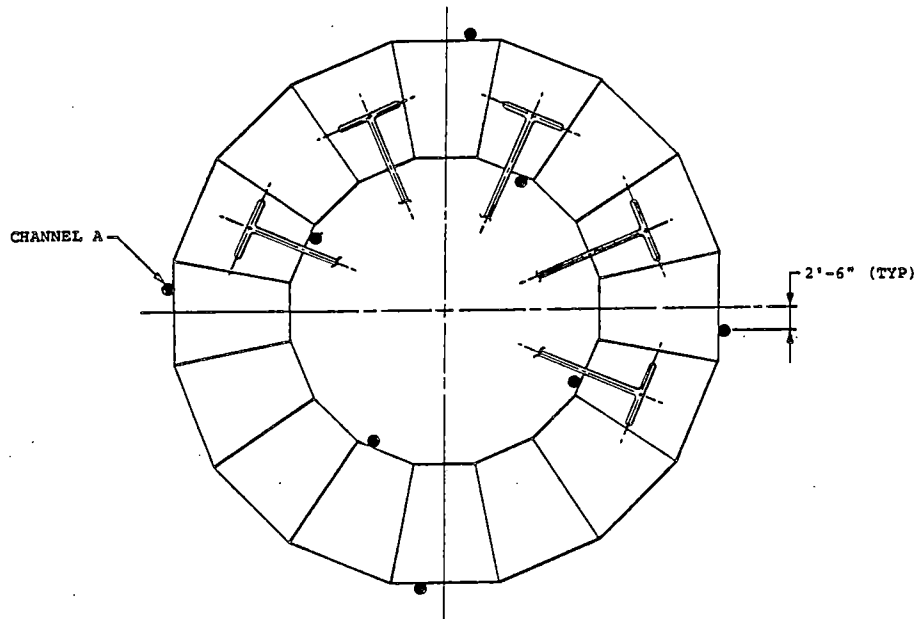
The SPTMS is classified as safety-related and is designed in accordance with the Institute of Electrical and Electronics Engineers (IEEE) Standard 279-1971. The equipment is qualified to IEEE Standards 323-1974, 344-1971, or 344-1975. The sensors are designed to meet Seismic Category I and Quality Group B requirements.

Reference 22 assesses the bulk temperature accuracy of the SPTMS to be installed at the Dresden Units 2 and 3. The SPTMS bulk temperature is least accurate when a stuck-open relief valve (SORV) causes steam discharge into a torus bay without a SPTMS thermowell. When this occurs, the SPTMS may underestimate the actual bulk temperature by as much as 5.2°F.

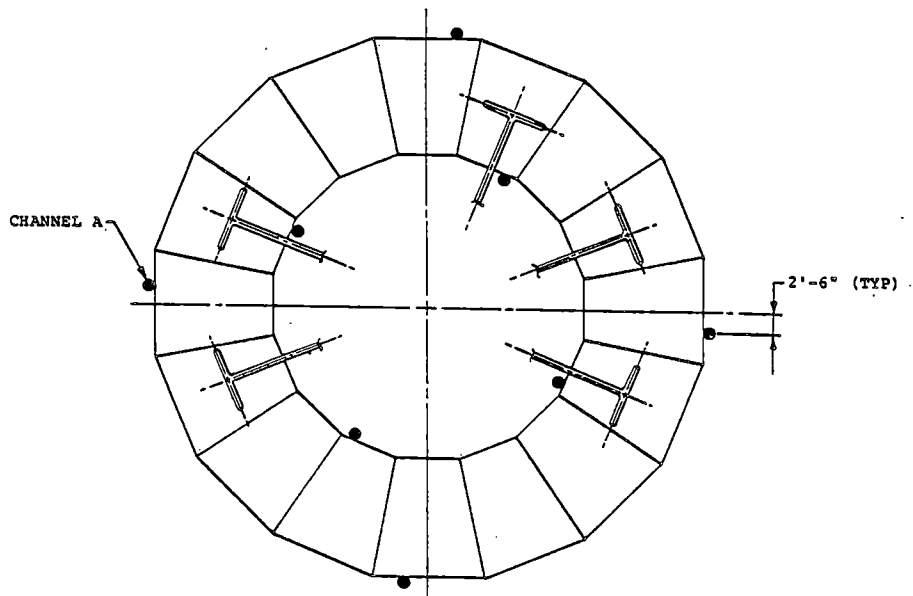
When the operator actions required by the Technical Specification are taken based on the SPTMS reading, the timing of the actions can be later than those assumed in Reference 19 (i.e., at a higher

temperature than required by the Technical Specification). A separate analysis will be performed to demonstrate that the delayed action will not cause the suppression pool temperature to exceed the limit specified in Reference 18.

Reference 23 provides specific recommendations for changes to the plant operating procedures in order to continue operation until the new SPTMS is installed during the next refueling outages. Table 1-1.0-1 shows the scheduled installation dates for the SPTMS.



DRESDEN UNIT 2



DRESDEN UNIT 3

1. EACH MONITOR IS PLACED BELOW THE NORMAL TORUS WATER LEVEL, NEAR THE NORMAL CENTER OF GRAVITY OF THE WATER MASS.

Figure 1-5.2-1

SUPPRESSION POOL TEMPERATURE MONITOR LOCATIONS
FOR DRESDEN UNITS 2 AND 3

LIST OF REFERENCES

1. "Mark I Containment Program Load Definition Report," General Electric Company, NEDO-21888, Revision 2, November 1981.
2. "Mark I Containment Program Structural Acceptance Criteria Plant-Unique Analysis Applications Guide," Task Number 3.1.3, Mark I Owners Group, General Electric Company, NEDO-24583, Revision 1, July 1979.
3. "Mark I Containment Long-Term Program," Safety Evaluation Report, USNRC, NUREG-0661, July 1980; Supplement 1, August 1982.
4. "Final Report In-Plant SRV Discharge Test," Dresden Unit 2, NUTECH Engineers, Inc., COM-19-142, Revision 0, June 30, 1982.
5. "Safety Analysis Report (SAR)," Dresden Station Units 2 and 3, Commonwealth Edison Company, July 20, 1982.
6. "Containment Data," Dresden 2, General Electric Company, 22A5743, Revision 1, April 1979.
7. "Containment Data," Dresden 3, General Electric Company, 22A5744, Revision 1, April 1979.
8. "The General Electric Pressure Suppression Containment Analytical Model," General Electric Company, NEDO-10320, April 1971; Supplement 1, May 1971; Supplement 2, January 1973.
9. "Mark I Containment Program Plant Unique Load Definition," Dresden Station: Units 2 and 3, General Electric Company, NEDO-24566, Revision 1, November 1981.
10. "Mark I Containment Program Quarter-Scale Plant Unique Tests, Task Number 5.5.3, Series 2," General Electric Company, NEDE-21944-P, Volumes 1-4, April 1979.
11. Patton, K.T., "Tables of Hydrodynamic Mass Factors for Translational Motion," ASME Manuscript, Chicago, November 7-11, 1965.

12. Miller, R.R., "The Effects of Frequency and Amplitude of Oscillation on the Hydrodynamic Masses of Irregularly-Shaped Bodies," MS Thesis, University of Rhode Island, Kingston, R.I., 1965.
13. Fitzsimmons, G. W. et al., "Mark I Containment Program Full-Scale Test Program Final Report, Task Number 5.11," General Electric Company, NEDE-24539-P, April 1979.
14. "Mark I Containment Program Letter Reports MI-LR-81-01 and MI-LR-81-01-P, Supplemental Full-Scale Condensation Test Results and Load Confirmation-Proprietary and Nonproprietary Information," General Electric Company, May 6, 1981.
15. "Mark I Containment Program - Full-Scale Test Program - Evaluation of Supplemental Tests," General Electric Company, NEDO-24539, Supplement 1, July 1981.
16. Hsiao, W. T. and Valandani, P., "Mark I Containment Program Analytical Model for Computing Air Bubble and Boundary Pressures Resulting from an SRV Discharge Through a T-Quencher Device," General Electric Company, NEDE-21878-P, August 1979.
17. Letter from T. A. Ippolito (NRC) to J. F. Quirk (GE) dated October 16, 1981.
18. "Suppression Pool Temperature Limits for BWR Containment," USNRC, NUREG-0783, November 1981.
19. "Suppression Pool Temperature Response, Dresden Units 2 and 3," General Electric Company, NEDC-22170, July 1982.
20. "Operating Problems with Target Rock Safety-Relief Valves at BWR's," USNRC, Office of Inspection and Enforcement, IE Bulletin No. 80-25, December 19, 1980.
21. Letter and Attachment from L. R. Basinski (Bechtel) to W. H. Koester (CECo), G35-N-010, dated September 29, 1980. (Attachment to letter is the SPTMS design criteria.)

22. "Suppression Pool Temperature Monitoring System (SPTMS) Bulk Temperature Accuracy Assessment for the Dresden 2 and 3 and Quad Cities 1 and 2 Stations," NUTECH, COM-27-210, Revision 0, April 1983.
23. Letter report from H. W. Massie (NUTECH) to R. H. Mirochna (CECo), COM-27-171, dated November 19, 1982.